91602
new 82-10

ontario hydro
research division

COMPLIMENTARY COPY
Please Credit Ontario Hydro Research if
Reproduced in Whole or in Part

DARLINGTON LEAK BEFORE BREAK MATERIAL TEST PROGRAM J-RESISTANCE CURVES VOLUME 1 – GENERAL SUMMARY, DISCUSSION OF RESULTS AND CONCLUSIONS

Report No. 87-232-K

B. Mukherjee and D. Carpenter
Nondestructive and Fracture Evaluation Section
Metallurgical Research Department

ABSTRACT

The Darlington Leak Before Break (LBB) approach has been developed for large diameter (21, 22, 24 inch) SA106B heat transport (HT) piping and A105 fittings as a design alternative to pipewhip restraints and in recognition of the questionable benefits of providing such restraints. Ontario Hydro's LBB approach is based on the elastic plastic fracture mechanics (EPFM) method.

In order to assess the stability of HT piping in the presence of hypothetical flaws, the material value of the J-integral associated with crack extension, which is also known as a material resistance curve or a J-R curve, must be known. In this test program, J-R curves were determined from actual pipe heats that were used in the construction of the Darlington heat transport systems (Units 1 and 2). Test blocks were prepared using four different welding procedures for nuclear Class I piping. Two SA105 vesselet forgings were also tested.

job	file	date	report no.
83-153-451	826.2	October 20, 1987	87-232-K

The test program was designed to take into account the effect of various factors such as test temperature, crack plane orientation, welding effects, etc, which have influence on fracture properties. The objective was to identify those factors which tend to lower the resistance curves and apply the appropriate lower bound resistance curves that were obtained from this program, for structural analyses. A total of 91 tests were conducted. An acceptable lower bound J-resistance curve for the piping steels was obtained by machining maximum thickness specimens from the pipes and by testing side grooved compact tension specimens.

Due to the size of the material test program, results have been reported in two volumes. The first volume of this report includes a brief introduction to the elastic plastic fracture mechanics methods and the test procedure, summary of test results, discussion and major conclusions. The second volume of this report describes the test method, calculations and interpretation of results, specimen configuration, dimension and preparation and documents all experimental test data for archival purposes. The entire data set is stored in a data base in the Mechanical Design Department's VAX computer for quick access and for application to the Darlington LBB project.

Test results showed that all product forms utilized in the construction of Darlington heat transport piping and all welds and heat affected zone materials within the scope of the Darlington Leak Before Break (DLBB) program exhibit uppershelf toughness behaviour. All specimens showed high crack initiation toughness J_{Ic}, rising J-resistance curve and stable and ductile crack extension. Toughness of product forms depends on the direction of crack extension (circumferential versus axial crack orientation).

Toughness of DLBB welds and parent materials at 250°C was lower than that at 20°C. This behaviour is characteristic of low strength high toughness carbon manganese steels and welds and is possibly due to a drop in yield strength with temperature.

All welds within the scope of the DLBB program were subject to suitable post weld heat treatment. Non post weld heat treated welds remained tough and ductile at 250°C, but showed comparatively lower J_{Ic} and J-resistance curves than those observed in post weld heat treated welds. However, toughness of non post-weld heat treated welds increased significantly after a post-weld heat treatment.

The test method for J-resistance curves was validated by comparing six test results against tests conducted by Material Engineering Associates (MEA) of Lanham, Maryland. The J_{Ic} and J-resistance curves obtained by Ontario Hydro and MEA were comparable.

91602
new 82-10

ontario hydro
research division

EXECUTIVE SUMMARY

DARLINGTON LEAK BEFORE BREAK MATERIAL TEST PROGRAM J-RESISTANCE CURVES VOLUME 1 - GENERAL SUMMARY, DISCUSSION OF RESULTS AND CONCLUSIONS

B. Mukherjee and D.W. Carpenter
Nondestructive and Fracture Evaluation Section
Metallurgical Research Department

The Darlington Leak Before Break (LBB) approach has been developed for large diameter (21, 22, 24 inch) SA106B heat transport (HT) piping and A105 fittings as a design alternative to pipewhip restraints and in recognition of the questionable benefits of providing such restraints. Ontario Hydro's LBB approach is based on elastic plastic fracture mechanics (EPFM) method.

In order to assess the stability of HT piping in the presence of hypothetical flaws, the material value of the J-integral associated with crack extension, which is also known as a material resistance curve or a J-R curve, must be known. In this test program, J-R curves were determined from actual pipe heats that were used in the construction of the Darlington heat transport systems (Units 1 and 2). Test blocks were prepared using four different welding procedures for nuclear Class I piping. Two SA105 vesselet forgings were also tested.

The test program was designed to take into account the effect of various factors such as test temperature, crack plane orientation, welding effects, etc, which have influence on fracture properties. The objective was to identify those factors which tend to lower the resistance curves and apply the appropriate lower bound resistance curves that were obtained from this program, for structural analyses. A total of 91 tests were conducted. An acceptable lower bound J-resistance curve for the piping steels was obtained by machining maximum thickness specimens from the pipes and by testing side grooved compact tension specimens.

JAB
9/8

job	file	date	report no.
83-153-451	826.2	October 20, 1987	87-232-K

Due to the size of the material test program, results have been reported in two volumes. Volume I of this report includes a brief introduction to the elastic plastic fracture mechanics methods and the test procedure, summary of test results, discussion and major conclusions. Volume II of this report describes the test method, calculations and interpretation of results, specimen configuration, dimension and preparation and documents all experimental test data for archival purposes. The entire data set is stored in a data base in the Mechanical Design Department's VAX computer for quick access and for application to the Darlington LBB project.

Test results showed that all product forms utilized in the construction of Darlington heat transport piping and all welds and heat affected zone materials within the scope of the Darlington Leak Before Break (DLBB) program exhibit uppershelf toughness behaviour. All specimens showed high crack initiation toughness J_{Ic}, rising J-resistance curve and stable and ductile crack extension. Toughness of product forms depends on the direction of crack extension (circumferential versus axial crack orientation).

Toughness of DLBB welds and parent materials at 250°C was lower than that at 20°C. This behaviour is characteristic of low strength high toughness carbon manganese steels and welds and is possibly due to a drop in yield strength with temperature.

All welds within the scope of the DLBB program were subject to suitable post weld heat treatment. Non post weld heat treated welds remained tough and ductile at 250°C, but showed comparatively lower J_{Ic} and J-resistance curves than those observed in post weld heat treated welds. Toughness of non post-weld heat treated welds increased significantly after a suitable heat treatment.

The test method for J-resistance curves was validated by comparing six test results against tests conducted by Material Engineering Associates (MEA) of Lanham, Maryland. The J_{Ic} and J-resistance curves obtained by Ontario Hydro and MEA were comparable.

TABLE OF CONTENTS

		Page
1.0	INTRODUCTION	1
2.0	EXPERIMENTAL PROGRAM	2
3.0	TEST METHOD	4
4.0	RESULTS	6
	4.1 Pipe Size	6
	4.2 Crack Plane Orientation	7
	4.3 Effect of Temperature	7
	4.4 Welding Effects	8
	4.5 Validation of Test Results	9
5.0	DISCUSSION OF RESULTS	10
6.0	CONCLUSIONS	12
7.0	ACKNOWLEDGEMENTS	13
REFERENCES		14
TABLES		17
DISTRIBUTION		last page

LIST OF TABLES

Table I	Large Diameter Piping Heats Darlington NGS A Heat Transport Piping Units 1 and 2
Table II	Ontario Hydro Nuclear Weld Procedures
Table III	Darlington LBB Material Test Matrix and Summary of Test Data (six page table, Lotus File JTTABLE3)

LIST OF FIGURES

Figure 1	Specimen Orientation with Respect to a Pipe Geometry
Figure 2 (File TD13-18)	Comparison of J-Resistance Curves at Three Temperatures
Figure 3 (File JC13-18)	Variation of J_{Ic} Between 200°C and 300°C
Figure 4	J-R Curve
Figure 5 (File JC01.47.ENG)	Comparison of J_{Ic} for Various Product Forms, 12", 22" and 24" NPS Sch 100 at 250°C
Figure 6 (File J01-47)	J-Resistance Curves for Three Pipe Sizes, 12", 22" and 24" NPS Sch 100 Parent at 250°C, (L-C)
Figure 7 (File JT01-47)	J-T Curves for Three Pipe Sizes, 12", 22" and 24" NPS Sch 100 Parent at 250°C, (L-C)
Figure 8 (File J59-70)	J-Resistance Curves for Three Pipe Sizes, 12", 22" and 24" NPS Sch 100 Parent at 250°C, (C-L)
Figure 9 (File JT59-70)	J-T Curves for Three Pipe Sizes, 12", 22" and 24" NPS Sch 100 Parent at 250°C, (C-L)
Figure 10 (File J01-03)	Effect of Orientation on J-Resistance Curves, 24" NPS Sch 100 Parent at 250°C, (L-C) vs (C-L)
Figure 11 (File JT01-03)	Effect of Orientation on J-T Curves, 24" NPS Sch 100 Parent at 250°C, (L-C) vs (C-L)
Figure 12 (File J65-67)	Effect of Orientation on J-Resistance Curves, 22" NPS Sch 100 Parent at 250°C, (L-C) vs (C-L)
Figure 13 (File JT65-67)	Effect of Orientation on J-T Curves, 22" NPS Sch 100 Parent at 250°C, (L-C) vs (C-L)
Figure 14 (File J45-47)	Effect of Orientation on J-Resistance Curves, 12" NPS Sch 100 Parent at 250°C, (L-C) vs (C-L)
Figure 15 (File JT45-47)	Effect of Orientation on J-T Curves, 12" NPS Sch 100 Parent at 250°C, (L-C) vs (C-L)
Figure 16 (File J56-58)	Effect of Orientation on J-Resistance Curves, 22" x 12" Vesselet at 250°C, (L-C) vs (C-L)
Figure 17 (File J56-58)	Effect of Orientation on J-T Curves, 22" x 12" Vesselet at 250°C, (L-C) vs (C-L)

Figure 18 (File JCPARENT.ENG)	Variation of J_{Ic} with Temperature for Two Product Forms, at 250°C and 20°C 12" NPS Sch 100 and 22" x 12" Vesselet
Figure 19 (File J14-19)	Effect of Temperature on J-Resistance Curves, 22" NPS Sch 100 Parent at 250°C and 20°C, Orientation (L-C)
Figure 20 (File JT14-19)	Effect of Temperature on J-T Curves, 22" NPS Sch 100 Parent at 250°C and 20°C, Orientation (L-C)
Figure 21 (File J62-67)	Effect of Temperature on J-Resistance Curves, 22" NPS Sch 100 Parent at 250°C and 20°C, Orientation (C-L)
Figure 22 (File JT62-67)	Effect of Test Temperature on J-T Curves, 22" NPS Sch 100 Parent at 250°C and 20°C, Orientation (C-L)
Figure 23 (File J53-58)	Effect of Test Temperature on J-Resistance Curves, 22" x 12" Vesselet at 250°C and 20°C, Orientation (L-C)
Figure 24 (File JT53-58)	Effect of Test Temperature on J-T Curves, 22" x 12" Vesselet at 250°C and 20°C, Orientation (L-C)
Figure 25 (File J71-79)	Effect of Test Temperature on J-Resistance Curves, 22" x 12" Vesselet at 250°C and 20°C, Orientation (C-L)
Figure 26 (File JT71-79)	Effect of Test Temperature on J-T Curves, 22" x 12" Vesselet at 250°C and 20°C, Orientation (C-L)
Figure 27 (File JCWELD.ENG)	Variation of J_{Ic} with Temperature for Three Weld Procedures at 250°C and 20°C, PN-232, PN-107 Weld and HAZ, PN-229 Weld and HAZ
Figure 28 (File J80-82)	Effect of Test Temperature on J-Resistance Curves, 24" NPS Sch 100 - PN 232 Weld at 250°C and 20°C, Orientation (L-C)
Figure 29 (File JT80-82)	Effect of Test Temperature on J-T Curves, 24" NPS Sch 100 - PN 232 Weld at 250°C and 20°C, Orientation (L-C)
Figure 30 (File J20-25)	Effect of Test Temperature on J-Resistance Curves, 22" NPS Sch 100 - PN 107 Weld at 250°C and 20°C, Orientation (L-C)

Figure 31 (File JT20-25)	Effect of Test Temperature on J-T Curves, 22" NPS Sch 100 - PN-107 Weld at 250°C and 20°C, Orientation (L-C)
Figure 32 (File J26-29)	Effect of Test Temperature on J-Resistance Curves, 22" NPS Sch 100 - PN-107 HAZ at 250°C and 20°C, Orientation (L-C)
Figure 33 (File JT26-29)	Effect of Test Temperature on J-T Curves, 22" NPS Sch 100 - PN-107 HAZ at 250°C and 20°C, Orientation (L-C)
Figure 34 (File J30-35)	Effect of Test Temperature on J-Resistance Curves, 22" NPS Sch 100 - PN-229 Weld at 250°C and 20°C, Orientation (L-C)
Figure 35 (File JT30-35)	Effect of Test Temperature on J-T Curves, 22" NPS Sch 100 - PN-229 Weld at 250°C and 20°C, Orientation (L-C)
Figure 36 (File J36-39)	Effect of Test Temperature on J-Resistance Curves, 22" NPS Sch 100 - PN-229 HAZ at 250°C and 20°C, Orientation (L-C)
Figure 37 (File JT36-39)	Effect of Test Temperature on J-T Curves, 22" NPS Sch 100 - PN-229 HAZ at 250°C and 20°C, Orientation (L-C)
Figure 38 (File JCHAZ1.ENG)	Weld and HAZ J_{Ic} Values for Post Weld Heat Treated Welds at 250°C, 24" - PN-108, 22" - PN-108, 24" - PN 232 and Parent Material
Figure 39 (File JCHAZ2.ENG)	Weld and HAZ J_{Ic} Values for Non Post Weld Heat Treated Welds at 250°C, 24" - PN-108, 22" - PN-108, 24" - PN-232 and Parent Material
Figure 40 (File JCHAZ3.ENG)	Weld and HAZ J_{Ic} Values for Non Post Weld Heat Treated Welds at 250°C, 22" - PN-107, 22" - PN-229, Parent Material
Figure 41 (File J04-08)	Comparison of J-Resistance Curves for Weld and HAZ, 24" NPS Sch 100 - PN-108 Weld and HAZ at 250°, Orientation (L-C)
Figure 42 (File JT04-08)	Comparison of J-T Curves for Weld and HAZ, 24" NPS Sch 100 - PN-108 Weld and HAZ at 250°, Orientation (L-C)
Figure 43 (File J40-44)	Comparison of J-Resistance Curves for Weld and HAZ, 22" NPS Sch 100 - PN-108 Weld and HAZ at 250°, Orientation (L-C)

Figure 44 (File JT40-44)	Comparison of J-T Curves for Weld and HAZ, 22" NPS Sch 100 - PN-108 Weld and HAZ at 250°, Orientation (L-C)
Figure 45 (File J09-13)	Comparison of J-Resistance Curves for Weld and HAZ, 24" NPS Sch 100 - PN-232 Weld and HAZ at 250°, Orientation (L-C)
Figure 46 (File JT09-13)	Comparison of J-T Curves for Weld and HAZ, 24" NPS Sch 100 - PN-232 Weld and HAZ at 250°, Orientation (L-C)
Figure 47 (File J20-22)	Comparison of J-Resistance Curves for Weld and HAZ, 22" NPS Sch 100 - PN-107 Weld and HAZ at 20°, Orientation (L-C)
Figure 48 (File JT20-22)	Comparison of J-T Curves for Weld and HAZ, 22" NPS Sch 100 - PN-107 Weld and HAZ at 20°, Orientation (L-C)
Figure 49 (File J23-25)	Comparison of J-Resistance Curves for Weld and HAZ, 22" NPS Sch 100 - PN-107 Weld and HAZ at 250°, Orientation (L-C)
Figure 50 (File JT23-25)	Comparison of J-T Curves for Weld and HAZ, 22" NPS Sch 100 - PN-107 Weld and HAZ at 250°, Orientation (L-C)
Figure 51 (File J48-52)	Comparison of J-Resistance Curves for Weld and HAZ, 12" NPS Sch 100 - PN-107 Weld and HAZ at 250°, Orientation (L-C)
Figure 52 (File JT48-52)	Comparison of J-T Curves for Weld and HAZ, 12" NPS Sch 100 - PN-107 Weld and HAZ at 250°, Orientation (L-C)
Figure 53 (File J30-32)	Comparison of J-Resistance Curves for Weld and HAZ, 22" NPS Sch 100 - PN-229 Weld and HAZ at 20°, Orientation (L-C)
Figure 54 (File JT30-32)	Comparison of J-T Curves for Weld and HAZ, 22" NPS Sch 100 - PN-229 Weld and HAZ at 20°, Orientation (L-C)
Figure 55 (File J33-35)	Comparison of J-Resistance Curves for Weld and HAZ, 22" NPS Sch 100 - PN-229 Weld and HAZ at 250°, Orientation (L-C)
Figure 56 (File JT33-35)	Comparison of J-T Curves for Weld and HAZ, 22" NPS Sch 100 - PN-229 Weld and HAZ at 250°, Orientation (L-C)

Figure 57 (File JCPWHT.ENG)	J_{Ic} Values of Post Weld Heat Treated (PWHT) Versus Non PWHT Welds at 250°C
Figure 58 (File J40–42)	Comparison of J-Resistance Curves for PWHT vs Non PWHT Welds, 22" NPS Sch 100 – PN-107 vs PN-108 Weld at 250°C, Orientation (L-C)
Figure 59 (File JT40–42)	Comparison of J-T Curves for PWHT vs Non PWHT Welds, 22" NPS Sch 100 – PN-107 vs PN-108 Weld at 250°C, Orientation (L-C)
Figure 60 (File J43–44)	Comparison of J-Resistance Curves for PWHT vs Non PWHT, HAZ Material, 22" NPS Sch 100 – PN-107 vs PN-108 HAZ at 250°C, Orientation (L-C)
Figure 61 (File JT43–44)	Comparison of J-T Curves for PWHT vs Non PWHT, HAZ Material, 22" NPS Sch 100 – PN-107 vs PN-108 HAZ at 250°C, Orientation (L-C)
Figure 62 (File J09–11)	Comparison of J-Resistance Curves for PWHT vs Non PWHT Welds, 24" NPS Sch 100 – PN 232 vs 22" NPS Sch 100 – PN-229 Weld at 250°C, Orientation (L-C)
Figure 63 (File JT09–11)	Comparison of J-T Curves for PWHT vs Non PWHT Welds, 24" NPS Sch 100 – PN-232 vs 22" NPS Sch 100 – PN-229 Weld at 250°C, Orientation (L-C)
Figure 64 (File J83–00)	Effect of Stress Relieving on J-Resistance Curves of Welds, 22" NPS Sch 100 – PN-229 Weld at 20°C, Orientation (L-C)
Figure 65 (File JT83–00)	Effect of Stress Relieving on J-T Curves of Welds, 22" NPS Sch 100 – PN-229 Weld at 20°C, Orientation (L-C)
Figure 66 (File J84–85)	Effect of Stress Relieving on J-Resistance Curves of Welds, 22" NPS Sch 100 – PN-229 Weld at 250° Orientation (L-C)
Figure 67 (File JT84–85)	Effect of Stress Relieving on J-T Curves of Welds, 22" NPS Sch 100 – PN-229 Weld at 250°C, Orientation (L-C)
Figure 68 (File JCMEA.ENG)	Comparison of J_{Ic} Values Between OH and MEA Tests, 22" NPS Sch 100 Parent and PN-107 Weld Material, Orientation (L-C)
Figure 69 (File J86–88ME)	Comparison of J-Resistance Curves Between OH and MEA Tests, 22" NPS Sch 100 at 250°C, Orientation (L-C)
Figure 70 (File JT86–88M)	Comparison of J-T Curves Between OH and MEA Tests, 22" NPS Sch 100 at 250°C, Orientation (L-C)

Figure 71
(File J89-91ME) Comparison of J-Resistance Curves Between OH and MEA Tests, 22" NPS Sch 100 - PN-107 Weld at 250°C, Orientation (L-C)

Figure 72
(File JT89-91M) Comparison of J-T Curves Between OH and MEA Tests, 22" NPS Sch 100 - PN-107 Weld at 250°, Orientation (L-C)

ontario hydro
research division

To

Mr. M.A. Machacek
Manager of Engineering – Darlington GS
Design and Construction

DARLINGTON LEAK BEFORE BREAK MATERIAL TEST PROGRAM J-RESISTANCE CURVE VOLUME 1 – GENERAL SUMMARY, DISCUSSION OF RESULTS AND CONCLUSIONS

1.0 INTRODUCTION

Ontario Hydro has developed a leak-before-break (LBB) methodology for application to the large diameter heat transport piping for Darlington NGS A because of the difficulties encountered in attempting to provide pipewhip restraints and in recognition of the questionable benefits of providing such restraints. This approach has been developed for pipe sizes which are equal to or greater than 21" nominal diameter (21" NPS). However, the basic approach and underlying theories are applicable to smaller pipe sizes equally well.

Piping steels are expected to exhibit a stable crack extension behaviour with rising load up to the point of instability in the ductile uppershelf regime. Under these conditions, the application of structural integrity concepts that are based on crack initiation alone will be overly conservative. Thus the margin against failure must be determined under elastic-plastic conditions by taking into account both crack initiation and stable crack growth. Several methods are currently available to analyze and evaluate leak-before-break conditions in ductile piping with postulated flaws under elastic-plastic conditions. These methods include but are not limited to limit load analysis (net section collapse), the J integral/tearing modulus (J/T) approach, the R-6 approach and its derivative the failure assessment diagram (FAD).

The Ontario Hydro leak-before-break approach is based on the J/T method/1/. A brief history of the development of J-integral approach is also given in /1/. In 1968, Hutchinson/2/ and Rice and Rosengren/3/ showed that for elastic-plastic fracture mechanics (EPFM) there is a unique crack tip stress-strain field with a crack tip singularity. McClintock/4/ showed that the singular field could be written with a single characterizing parameter, the J-integral of Rice/5/. This formed the basis for a set of experiments showing that this J-integral would work as a fracture parameter. The work of Begley and Landes/6,7/ labelled the point of fracture initiation, J_{Ic} and offered proof of its applicability with two steels. Rice, Paris and Merkle/8/ developed a simple formula which allowed J to be calculated from the area under a load versus load-point displacement record.

Development of single-specimen J-integral test methodology/9,10/ has reduced the cost of these tests compared to the multiple specimen test that is given in ASTM "Standard Test Method for J_{Ic}, a Measure of Fracture Toughness" (E813-81). The single specimen method also establishes a resistance curve well beyond the point of crack initiation. The theoretical foundation for the use of J-integral beyond crack initiation was discussed by Hutchinson and Paris/11/ and conditions for J-controlled crack growth were defined. Subsequently, analyses of the stability of crack growth in the J-controlled regime were conducted by Paris and co-workers/12,13/ and the tearing modulus parameter which incorporates the slope of the J-Resistance curve was introduced.

The J/T approach has been selected by Ontario Hydro because it is a general procedure that incorporates a rational crack tip parameter, can discriminate between materials of different toughness and tensile properties, and can incorporate various boundary conditions (e.g., load vs displacement control) and pipe system characteristics (e.g., system configuration and support characteristics)/14/. There are two critical steps in a leak-before-break analysis, which are initiation or first extension of a hypothetical flaw and stability of a growing flaw subsequent to initiation. The material value of J associated with initiation is J_{Ic}. If the applied value of J is less than J_{Ic} then initiation or extension of a crack will not occur and the stability of an existing crack is ensured automatically. When crack extension is predicted, the amount of extension must be evaluated to determine if this extension would occur in a stable manner. The material value of J associated with crack extension which is also known as material resistance curve or a J-R curve is required for stability assessment. The nondimensionalised slope of a J-R curve at a given value of J is defined as the tearing modulus (T). The margin against instability is determined from a J-T plot where J is plotted against T for the material and the structure.

In this Darlington leak-before-break material test program J-R and J-T curves were determined from actual Darlington NGS A large diameter heat transport piping, forgings, associated welds and heat affected zones. Volume I of this report includes a summary of the test results and major conclusions. Volume II of this report describes the test method, specimen selection and configuration, procedure, calculation and interpretation of results and documents all experimental test data for archival purposes.

2.0 EXPERIMENTAL PROGRAM

A comprehensive description of the test program is given in /15/. The test program was designed to take into account the effect of various factors which influence fracture properties. The objective was to identify those factors which tend to lower resistance curves and apply the appropriate lower bound resistance curves that were obtained from this program, for structural analyses. Variables that were considered to be of significance and were therefore included in this project were:

Pipe size and Product Form;
Heat of Piping Material;
Crack Plane Orientation;
Temperature;
Welding Effects.

Three different pipe sizes of SA-106 Grade B were used (12, 22 and 24 inch NPS). Two SA-105 vesselet forgings were also tested. "Vesselet" is a trade name for a weld-in contour fitting. The test program utilized piping material from piping heats used in the construction of the Darlington heat transport system (Units 1 and 2). Table I lists all heats of large diameter piping employed in Darlington NGS A Units 1 and 2. Refer to Volume II - Appendix A to see how various heats were incorporated. It describes the procedure for preparing the test coupons and identifies the weld procedure and the heats that were used in preparing the weld samples. It also identifies the coupon numbers and their locations for all weld and parent material samples.

In the stability assessment of through wall circumferential and longitudinal flaws, J-Resistance curves in L-C and C-L crack plane orientations, respectively, are required. Figure 1 shows the orientation of the specimens with respect to the product geometry. Specimens from SA106B and SA105 forgings were machined from both L-C and C-L orientation. Since the welds are circumferential, the weld samples and the heat affected zone samples can only be machined in the L-C orientation.

NUREG-1061, Volume 3, "Evaluation of Potential Pipe Breaks"/14/ recommends that J-resistance tests should be conducted at a temperature near the upper range of normal plant operation. The maximum normal operating temperature of the heat transport system occurs in the reactor outlet header and is 310°C. It is known that ductility of SA106B steel, as measured by the lateral contraction during a tensile test, shows a minimum value between 200°C and 300°C. Tensile tests were conducted in this temperature range and it was established that the lateral contraction of this material is minimum in the neighbourhood of 250°C/16/. Single specimen J_{Ic} tests were conducted at 200°C. 250°C and 300°C to confirm that the toughness of the material, when characterized by J_{Ic} and R-curve, also goes through a minimum near 250°C. Figure 2 shows the J-resistance curves from 6 specimens from 24" NPS Sch 100 SA106B Parent Material. Two specimens were tested at each temperature. Although specimens from either C-L or L-C orientation could have been used to confirm the temperature effect, C-L orientation was selected for this program since pipes exhibit lower toughness in the C-L direction. The J_{Ic} values for these specimens are shown in Figure 3. These figures show that temperature effects on J_{Ic} and R curves are not very strong between 200°C to 300°C. Nevertheless, the lowest J_{Ic} and R curves were obtained at 250°C. Therefore, 250°C was confirmed as the appropriate test temperature for measuring, conservatively, the material response at 310°C. In order to determine if there is any significant dependence of toughness on temperature over the temperature range of an operating plant, a temperature of 20°C was selected arbitrarily, as a lower bound of the lowest service temperature for the heat transport system.

Two Ontario Hydro welding procedures (PN-107 and PN-229) were used at Darlington NGS-A for girth-butt welds on 12" and 22" NPS pipes. Two different Ontario Hydro welding procedures (PN-108 and PN-232) were used for the 24" pipe. All four of these welding procedures for nuclear Class I piping were included in the test program. These welding procedures are listed in Table II. Tests were conducted on the weld material and the heat affected zone (HAZ) material. The specimen orientation in the weld and HAZ was in the L-C direction. Due to the V-shape of the weld preparation surface, the crack front in a HAZ specimen

straddled the HAZ, parent and weld material. The measured HAZ toughness is therefore an average toughness.

The ASME Boiler and Pressure Vessel Code/17/ Table NB-4622.7(b)-1 requires post weld heat treatment (PWHT) for welds to pipes with nominal wall thickness greater than 38 mm (1.5 inches). Therefore, the only large diameter pipe that did not require post weld heat treatment at Darlington NGS was the 22" NPS Schedule 100 pipe. In order to assess the effect of post-weld heat treatment on the J-R curves, 22" NPS girth-butt welds were tested with post-weld heat treatment (22" NPS with PN-108 weld procedure) and without post-weld heat treatment (22" NPS with PN-107 weld procedure). The PN-229 weld procedure applied to the 22" NPS pipe was also tested with and without post-weld heat treatment.

The entire test matrix is shown in Table III. Altogether 91 tests were conducted in this test program.

3.0 TEST METHOD

This section describes briefly, a single specimen compliance procedure that was used to determine the J-Resistance curves. A detailed description of the test method and calculation procedures is given in the second volume of this report/18/.

Three different sizes of compact tension (CT) specimens, 1-1/4T, 1T and 3/4T, conforming to the geometry of the ASTM test procedure E813, Standard Test Method for J_{Ic}, a Measure of Fracture Toughness, were used. The sizes of the specimens were determined by the largest CT specimens that could be machined from the 24", 22" and 12" NPS Schedule 100 pipe, respectively. All specimens were precracked and sidegrooved after precracking to ensure a straight crack front. The R-curves produced with a straight crack front extension exhibit slopes (dJ/da) lower than those produced with a non sidegrooved specimen. Sidegrooving also appears to produce a slightly lower (more conservative) value of crack initiation toughness.

Regarding specimen geometry, existing data indicate that fracture toughness specimens having approximately the same thickness as the pipe wall and without sidegrooves tend to model actual pipe behaviour most accurately. However, sidegrooved specimens will provide an acceptable lower bound J-resistance curve/14/. Also note that CT specimens are bend type specimens. J-R curves from bend type specimens defines the lower bound estimate of the measuring capacity of J as a function of crack extension, and have been observed to be conservative in comparison with those obtained with tensile loading specimen configuration/19/. In this test program sidegrooved CT specimens were utilized. The specimen thicknesses were approximately 80% of the respective pipe wall thicknesses from which they were machined. Therefore, this test program provides an acceptable lower bound J-resistance curve.

A single specimen technique documented in /19/ was utilized to determine the J-R curves. In this test method, crack length and crack extension were determined from elastic compliance measurements. These measurements were taken on a series of unloading/reloading segments spaced along the load versus load-line displacement record. The unload/reload segments were conducted under elastic conditions, even when the specimen has undergone extensive plastic deformation. Therefore, the change in the crack length from one unloading to the next can be in-

ferred through a change in compliance/18/. J values were calculated at the end of the test from the area under the load versus load-line deflection curves using equations given in /18/ and /19/. The extent of the slow stable crack extension at the end of the test was highlighted by heat tinting. The initial crack size after precracking and the final physical crack size were then measured on the fracture surface using a nine point average method as per the ASTM test specification E813.

A personal computer was used for test control and data acquisition. A computer program was developed to control the loading and unloading sequence. A separate computer program was used to analyze the acquired data and plot final graphs shown in /18/.

A typical R-curve produced with the single specimen compliance technique is shown in Figure 4. The proposed ASTM test method indicates that the R curves should be limited to a small crack extension given by:

$$a_{max} = 0.1 \times \text{remaining ligament (b)}$$

to maintain a region of J controlled growth at the crack tip. The requirement of J controlled growth has been formulated by Hutchinson and Paris/11/ as

$$\omega \gg 1$$

where

$$\omega = (b/J)(dJ/da)$$

The limits of applicability of J-R curves are associated with the assumptions and conditions of J-integral computation. Within the limits of the ω restriction and the plane strain condition

$$J_{max} \leq (b \times \text{Flow Stress})/20$$

J-integral computations are rigorous.

However, R-curves associated with longer crack extension, which would violate the ω -criteria may be necessary for application to a given structural analysis. The proposed ASTM validity criteria, including that of ω are still being researched and may be altered in the future. Therefore, in this program R-curves have been recorded which exceed the current ASTM crack extension, (ω) and plane strain J_{max} limitation. When a J-R curve exceeds the plane strain limitation, it simply means that the crack extends under non-plane strain condition. Since sidegrooved and approximately full thickness specimens were utilized, this data will still be applicable for piping analysis beyond the plane strain limitation on J-integral.

Where valid data cannot be generated for large crack extensions, some method of estimating the ductile fracture resistance at large crack extension is necessary. A procedure for making such an extrapolation is recommended in /14/. In this method a J-resistance curve is extrapolated up to a J level twice the highest J where valid data are available using a straight line tangent to the specimen J-resistance curve at its point of maximum valid J. A modified version of J called

J_M has also been formulated where calculated J values exceed the ASTM validation limits/20/. J_M values have been calculated for all tests in /18/.

The calculation of J_{Ic} in Figure 4 is according to ASTM E813. J_{Ic} is defined by the intersection of a linear regression fit to the data, that fall within the 0.15 and 1.5 mm exclusion lines, with the blunting line

$$J = 2 \sigma_y \Delta a$$

A J-R curve is established by fitting a curve through the experimental data points using a power law equation in the form

$$J = C_1 (\Delta a)^{C_2}$$

This equation has been used extensively to establish J-R curves for ferritic steels/21/. An examination of the data in /18/ will show that this equation provides an excellent fit through the experimental J-Δa data points for each experiment in this test program. The J-R curves shown in the Volume 1 of this report, for comparison between groups of tests, are the fitted curves. Symbols have been used in these figures to differentiate between groups of tests. They do not represent experimental points.

4.0 RESULTS

All individual test results are reported in /18/. In this section test results are grouped and summarized to show the effect of various factors which may have an influence on the fracture properties of SA106B piping steel, associated welds and SA105 forgings.

4.1 Pipe Size

Initiation toughness values J_{Ic} are plotted for the 24", 22" and 12" NPS Sch 100 pipes and SA105 forgings (vesselet) at 250°C in Figure 5. The results are grouped by orientation, L-C and C-L. This figure shows that the J_{Ic} values within each orientation are comparable between pipe sizes except for one 24" NPS Sch 100 test sample which showed a high value. Average J_{Ic} values after eliminating the outliers (maximum and minimum value in each orientation) are 148.3 kn/m and 99.6 kn/m in the (L-C) and (C-L) orientation, respectively.

J-resistance curves at 250°C and (L-C) orientation are plotted in Figure 6 for three pipe sizes. A 24" NPS Sch 100 specimen (J3) which exhibited the highest J_{Ic} in Figure 5 also gives the highest R curve in Figure 6. This may be a material variability since J3 was machined from a different heat of pipe than its companion specimens J1 and J2. The R-curves for the remaining specimens from all three product forms lie within a narrow scatterband. The lower bound of the scatterband is delineated by a 12" NPS Sch 100 test result.

The J-T curves corresponding to the J-R curves of Figure 6 are plotted in Figure 7. These curves start at J values approximately equal to J_{Ic} and extend to the maximum measured J values. Unlike the J-R curves, the J-T curves show a layering effect. All 22" and 24" NPS Sch 100 specimens, except J3, lie in a narrow

band. The 12" NPS Sch 100 specimen results lie below this band. Closely clustered J-R curves will show up as layers in the J-T domain since the slope change of J-R curves between J_{Ic} and J_{max} is much larger than the actual change of J values.

J-resistance curves at 250°C and (C-L) orientation are plotted in Figure 8 for three pipe sizes. In this orientation the R-curves from 12" NPS Sch 100 specimens are higher than those obtained from 22" and 24" NPS Sch 100 specimens. The J-T curves corresponding to Figure 8 are shown in Figure 9.

4.2 Crack Plane Orientation

In order to determine stability assessment of longitudinal (C-L) and circumferential (L-C) cracks, J-R and J-T curves are required for both orientations. Specimens were machined from both orientations (Figure 1). The effect of orientation on J-R curves is shown in Figures 10, 12, 14 and 16 for 24", 22", 12" NPS Sch 100 pipes and 22" x 12" vesselet respectively. The corresponding J-T curves are shown in Figures 11, 13, 15 and 17. Crack initiation toughness, J_{Ic}, values for all product forms are shown in Figure 5. All product forms have higher J_{Ic} and higher J-resistance curves in (L-C) direction compared to those of (C-L) orientation. At 250°C, average J_{Ic} value for all product forms is 148.3 kn/m in (L-C) orientation and 99.6 kn/m in (C-L) orientation. The variation of toughness with orientation is related to the principal direction of mechanical working or grain flow in pipes and forgings. Similar material behaviour in pipes has been observed by other investigators through conventional Charpy tests/22/.

4.3 Effect of Temperature

In order to determine the effect of temperature on the J-resistance curves of SA106B piping, SA105 forging and associated welds, tests were conducted at 250°C and 20°C. In principle J-resistance curves are needed for the operating temperature of 310°C. However, tests were conducted at 250°C as these provide a slightly conservative J-resistance curve, see Figures 2 and 3. Toughness behaviour of high toughness - low strength C-Mn steels such as A106B shows a transition with temperature. An examination of the load displacement curves indicated that at 20°C all SA106B pipes, SA105 forging and welds exhibited ductile, high toughness upper shelf behaviour. Two PN-229 weld samples at 20°C were the only exception. After significant ductile and stable crack extension their final fracture surface showed some areas of cleavage.

The effect of test temperature on crack initiation toughness, J_{Ic}, values for a 22" NPS Sch 100 pipe and a vesselet is shown in Figure 18. Temperature effects are shown for L-C and C-L orientations. The average J_{Ic} values at 250°C were lower than those at 20°C but the degree of reduction is dependent on product form and specimen orientation. For 22" NPS Sch 100 pipe the average J_{Ic} value in the L-C orientation was reduced by 39%, but the reduction in the C-L orientation was only 22%. The average J_{Ic} values for forged vesselet material were not influenced by temperature to the same degree. Its average J_{Ic} value was reduced by only 6% in the L-C orientation and by 15% in the C-L orientation.

The J-resistance curves and the corresponding J-T curves at two test temperatures for a 22" NPS Sch 100 parent material and a vesselet are shown in Figures 19 to

26. These figures show that the J-resistance curves for parent materials at 250°C are lower than those at 20°C. A comparison of Figures 19 and 21 and Figures 23 and 25 will show that the lowering of the J-resistance curves in the C-L orientation with temperature is not as large as that observed for L-C orientation.

The effect of test temperature on J_{Ic} and J-resistance curves of weld materials and heat affected zones is similar to that observed for parent material. Specifically, J_{Ic} values and J-resistance curves for PN-232 weld, PN-107 weld and heat affected zone (HAZ) and PN-229 weld and HAZ material at 250°C are lower than those at 20°C. J_{Ic} values of the above welds and heat affected zones are shown in Figure 27. Figures 28 to 37 show the J-resistance curves and the J-T curves for these welds and HAZ material. All weld and HAZ specimens were machined from C-L orientation.

Average J_{Ic} values of PN-107 and PN-229 weld and HAZ at 250°C were approximately 50% lower than those at 20°C. These procedures do not require a post weld heat treatment. In comparison, J_{Ic} values of PN-232 weld procedure, which requires a post weld treatment, were lowered by only 25% between two test temperatures (Figure 27). Similarly, change in J-resistance curves with temperature for PN-232 weld (Figure 28) is not as large as that observed for PN-107 and PN-229 weld and HAZ.

The observation that J_{Ic} and J-R curves are lowered with increasing temperature in the upper shelf temperature range, is characteristic of low-strength high toughness structural steels/23,24/. Reduction of material tensile stress with temperature will promote this behaviour. Other factors such as strain aging will also reduce J_{Ic} and J-resistance curves. The presence of a strain aging phenomenon was identified in some of the weld samples through serrated load-displacement traces and from load peaks during an unload-reload sequence/25/.

4.4 Welding Effects

Two Ontario Hydro welding procedures (PN-108 and PN-232) were used for the 24" pipe. J_{Ic} values for the weld and HAZ material for these welds procedures are shown in Figure 38. Two different Ontario Hydro welding procedures (PN-107 and PN-229) were used for girth-butt welds on 12" and 22" NPS pipes. J_{Ic} values for the weld and HAZ for these procedures are shown in Figures 39 and 40. Average parent metal J_{Ic} (average of 3 tests) are also shown in these figures. J-resistance curves and the corresponding J-T curves for these welds and HAZ are shown in Figures 41 to 46 (PN-108 and PN-232) and Figures 47 to 56 (PN-107 and PN-229). An examination of these figures show that there is no significant mismatch between weld-HAZ material toughness properties.

The weld material J-resistance curves of PN-108 and PN-232 procedures applied to 24" NPS Sch 100 pipes were slightly higher than the corresponding HAZ J-resistance curves. In comparison, the J-resistance curves of PN-107 and PN-229 weld materials were slightly lower than the corresponding HAZ J-resistance curves.

Several tests were conducted to determine the effect of post-weld-heat treatment (PWHT) on various weld procedures. Test results show that an application of PWHT increases toughness of welds significantly.

The PN-107 weld procedure does not require a PWHT. The PN-108 weld procedure is identical to PN-107 except that it requires a PWHT. In the test program, PN-107 and PN-108 weld procedures were applied to a 22" NPS girth weld to study the effect of PWHT. J_{Ic} values of these tests are shown in Figure 57. J-resistance curves for the weld and HAZ are shown in Figures 58 and 60 respectively. J_{Ic} values and J-resistance curves for PN-108 procedure are significantly higher than those of PN-107.

The PN-229 weld procedure which was developed for 22" NPS pipes, also does not require a PWHT. Test coupons from PN-229 were stress relieved at 620°C for 2 hours and specimens were tested at 20°C and 250°C for comparison (see Figures 57 and 64 to 67). Again the J_{Ic} values and J-resistance curves were enhanced due to the stress relieving treatment.

4.5 Validation of Test Results

Considerable care was exercised in checking transducer calibration and computer programs that were developed for data analysis of single specimen J_{Ic} tests. Since the material test program is pivotal to the Darlington LBB program, it was decided to validate the material test program by comparing six test results against tests conducted by an independent laboratory. Materials Engineering Associate of Lanham, Maryland was selected for conducting the validation tests because of their experience in conducting single specimen J-resistance curve tests for U.S. Nuclear Regulatory Commission/26/ and Electric Power Research Institute/24/.

A section of a 22" NPS Sch 100 parent material and two coupons of PN-107 weld were shipped to MEA. Six 2.5 cm thick compact tension specimens were machined by MEA and were tested at 250°C. All specimens were machined in the L-C orientation. Yield and UTS values were provided to MEA by Ontario Hydro.

A comparison of J_{Ic} values between the OH and MEA tests are shown in Figure 68. J-resistance and J-T curves are compared in Figures 69 to 72. With the exception of one MEA test, which produced a high J_{Ic}, all OH and MEA J_{Ic} values of 22" NPS Sch 100 parent material were comparable (Figure 68). The MEA J-resistance curves for the parent material (Figure 69) were slightly higher than the OH J-resistance curves. A comparison of Figure 69 with all parent material tests in Figure 6 suggests that both OH and MEA data lie within the observed scatterband of all parent material tests.

J_{Ic} values obtained by OH and MEA on PN-107 weld at 250°C were also comparable (Figure 68). Three OH J-resistance curve tests on PN-107 weld lie within the band created by 3 MEA tests (Figure 71). The lower bound of this band is delineated by two tests, one each from MEA and OH.

In summary, the J_{Ic} and J-resistance curves obtained by OH and MEA on parent and weld materials were comparable. There was no systematic variation or discrepancy between the tests conducted by two independent laboratories. This comparison provides an independent but indirect validation of transducer calibration, test method, crack length and J calculation procedures.

5.0 DISCUSSION OF RESULTS

The objective of this test program was to develop a comprehensive material data base for product forms, heats of steel and weld procedures that have been used in the construction of large diameter Darlington heat transport piping. At the end of the test program, it can be stated with confidence that this objective has been achieved. In order to facilitate use of this data, test results have been grouped and summarized in this report. All test results are available in print medium as well as in a computerized data base.

Specimens from four product forms were tested. These were 24", 22" and 12" NPS Sch 100 pipes and SA105 forgings. Toughness values and J-resistance curves of these product forms depend on temperature and orientation. However, at a fixed temperature and at a fixed orientation, toughness values (Figure 5) and J-resistance curves (Figures 6, 8, 16) are dependent on product forms to a lesser degree. At 250°C and L-C orientation (circumferential crack), J-resistance curves from all product forms (Figures 6 and 16) lie in a narrow scatterband. The lower bound of this band is delineated by the 12" NPS Sch 100 and vesselet test results. At 250°C and C-L orientation (longitudinal crack) the observed scatter band is comparatively wider (Figures 8 and 16). The lower bound of this band is delineated by 24" NPS Sch 100 and vesselet test results. The upper bound of this band is formed by 12" NPS Sch 100 test results.

A general observation from all parent material results is that all precracked parent material specimens showed stable and ductile crack extension with rising load. Toughness values of pipes depend on the direction of crack extension relative to the pipe geometry. Tests using conventional Charpy specimens have shown that the toughness of SA106B steel, (as indicated by total energy absorbed at high strain rate) depends on specimen orientation/22/. A literature search was conducted to identify papers which had investigated the effect of specimen orientation on J_{Ic} and J-resistance curves but none were found in this particular search. Stability assessments of longitudinal and circumferential cracks require that J_{Ic} and J-resistance curves be known for both orientations. Therefore, tests were conducted on all product forms to quantify the effect of orientation on toughness.

At 250°C, J_{Ic} and J-resistance curves in the circumferential direction were higher than those in the axial direction for all product forms. Changes in J_{Ic} values and J-resistance curves were comparable for the 24" and 22" NPS Sch 100 pipes and SA105 forgings (Figures 5, 10, 12 and 16). The 12" NPS Sch 100 pipe specimens showed the least reduction of toughness with orientation.

Toughness behaviour of high toughness - low strength C-Mn steels such as SA106B and SA105 forgings shows a transition with temperature. An examination of load displacement curves and Charpy energy values indicated that these steels show an uppershelf toughness behaviour at 20°C. Specifically, load versus displacement behaviour of all parent material specimens was highly ductile. All specimens exhibited high crack initiation toughness, stable crack extension and steeply rising resistance curves beyond J_{Ic}.

J_{Ic} and J-resistance curves at 250°C were lower than those at 20°C, which is characteristic of lower strength, high toughness structural steels. Reduction of material tensile stress and reduction in lateral contraction with temperature will promote this behaviour.

Ontario Hydro has developed various welding procedures to satisfy ASME Code requirements. The PN-108 and PN-232 weld procedures were used for all welds within the scope of the Darlington LBB project (Units 1 and 2). Post weld heat treatment is required for these weld procedures. All tests on PN-108 and PN-232 weld and HAZ material at both test temperatures showed high J_{Ic} values, stable crack extension and rising resistance curves; that is, uppershelf toughness behaviour.

J_{Ic} values (Figure 38) and J-resistance curves (Figures 41, 43, 45) for the weld and HAZ material of PN-108 and PN-232 procedures were higher than the corresponding parent material properties. Due to the geometry of weld preparation and the given thickness of pipes, the crack front in a HAZ specimen straddled the weld, HAZ and parent material. The measured HAZ J-resistance curves, therefore, lie between the weld and parent material J-resistance curves. Effect of test temperature on the toughness of PN-232 weld was similar to that observed in parent material tests in that J_{Ic} and J-resistance curves at 250°C were lower than those at 20°C. Upper-shelf toughness behaviour was observed at both test temperatures.

Two other welding procedures PN-107 and PN-229 were developed by Ontario Hydro for 12" and 22" diameter pipes. These procedures satisfied the ASME Code requirements, which are based on lateral expansion and Charpy energy values, without a post weld heat treatment. These welds were also included in this test program. At 20°C, PN 107 (Figures 40, 47) and PN-229 (Figures 40, 53) weld and HAZ specimens showed ductile fracture behaviour as evidenced by high J_{Ic}, rising resistance curves and stable crack extension. However, two 22" PN-229 weld samples showed cleavage fracture after significant ductile deformation and approximately 2 mm of stable crack growth. It should be emphasized that the observed ductile specimen instability does not imply a similar structural response. For structural analysis, an accurate model of the applied loading must be available and analyzed in conjunction with the material resistance curve in order to determine the point where instability will occur.

At 250°C all PN-107 and PN-229 weld and HAZ specimens showed rising J-resistance curves and stable crack growth. However, for the weld material, the reduction of J_{Ic} and the lowering of J-resistance curves with temperature were larger than those observed in post weld heat treated weld samples. It is clear that non post weld heat treated welds have a lower resistance to ductile tearing than the post weld heat treated welds. This does not mean that these welds are unfit for that purpose. A structural analysis is required to determine the safety margins of these welds in the presence of hypothetical flaws. Also note that J_{Ic} is a more sensitive measure of material fracture toughness than Charpy tests, since Charpy tests did not identify large difference in toughness between post weld heat treated and non post weld heat treated welds.

There appears to be three mechanisms that contribute to the drop in fracture toughness with temperature in PN-107 and PN-229 welds/21/. The first mechanism is a drop in the J-resistance curve properties because of a drop in the tensile properties of the material. The second mechanism is a drop in toughness caused by

static strain aging. This causes reloading peaks in the load displacement curve. The third mechanism is dynamic strain aging, which occurs during the loading of the specimen. When this mechanism is active, serrations can be observed in the load displacement curves/27/.

All three mechanisms were active in non post weld heat treated PN-107 and PN-229 welds at 250°C which caused the large drop in J-resistance curve properties. The first two mechanisms were present in the post weld heat treated welds and caused a much smaller drop in toughness with temperature.

It was observed that J_{Ic} and J-resistance curves of PN-107 and PN-229 weld improved dramatically when a suitable post weld heat treatment (Figure 57) was applied to these welds. The load displacement curves of post-weld heat treated PN-107 and PN-229 welds were free of serrations. This behaviour is possibly due to the presence of a higher concentration of soluble carbon and nitrogen in the weld material in non-post-weld heat treated condition.

6.0 CONCLUSIONS

1. All product forms utilized in the construction of Darlington primary heat transport piping (24", 22" and 12" SA106B NPS Sch 100 pipes and SA105 forging) exhibited uppershelf toughness behaviour at 20°C and 250°C. All specimens from the above product forms showed high crack initiation toughness J_{Ic}, increasing resistance to crack extension and stable and ductile crack growth.

2. Toughness (J_{Ic} and J-Resistance curve) of parent materials depends on specimen orientations. Toughness of a pipe in the circumferential orientation (L-C) was higher than the corresponding toughness in the axial direction (C-L). The effect of orientation on toughness was quantified.

3. For a given temperature and specimen orientation toughness was also a function of various product forms, although to a lesser extent.

4. All welds and heat affected zone materials within the scope of the Darlington Leak Before Break project exhibited uppershelf toughness behaviour at 20°C and 250°C. All specimens from weld and HAZ material showed high crack initiation toughness, J_{Ic}, increasing resistance to crack extension and stable and ductile crack growth.

5. Weld and heat affected zone toughness values of post weld heat treated welds were higher than the parent material toughness values.

6. Non-post weld heat treated welds remained tough and ductile at 250°C, but showed comparatively lower J_{Ic} and J-resistance curves than those observed in post weld heat treated welds. Toughness (J_{Ic} and J-resistance curve) of non post weld heat treated welds increased significantly after a suitable heat treatment.

7. Two non-post weld heat treated weld specimens (PN-229 weld procedure) showed cleavage failure at 20°C after significant stable and ductile crack extension.

8. The material test method for J-resistance curves was validated by comparing six test results against tests conducted by Materials Engineering Associates of Lanham, Maryland. The J_{Ic} and J-resistance curves obtained by Ontario Hydro and MEA were comparable.

7.0 ACKNOWLEDGEMENTS

The fracture mechanics leak before break material test program was compiled with the collaboration of the Leak Before Break (LBB) Task Group B5 (Material Testing Task Group) members and other Ontario Hydro staff listed below as well as Dr. A. Zahoor of Novetech Corporation.

Material Testing Task Group Members:

M.L. Lau (Chairman)
B.L. Kee
B.W. Manning
N.D. Martin
J.S. Nathwani
M.L. Vanderglas

Other Ontario Hydro staff:

M.J. Kozluk
M.L. Aggarwal
M.A. Clark
D.A. Scarth
O.E. Lepik
E.T. Ho

Their help with this project is greatly appreciated.

Prepared:

B. Mukherjee
Unit Head – Fracture Mechanics
Nondestructive and Fracture
Evaluation Section
Metallurgical Research Dept

D.W. Carpenter
Technologist
Nondestructive and Fracture
Evaluation Section
Metallurgical Research Dept

Reviewed:

J.A. Baron
Section Head
Nondestructive and Fracture
Evaluation Section

Approved:

J. Brown
Manager
Metallurgical Research Dept

BM/DWC:SEH

REFERENCES

1. Kee, B.L. and Nathwani, J.S., "Darlington NGS A Leak-Before-Break Approach for Large Diameter Heat Transport (HT) Piping", Ontario Hydro Design and Development Division Report No. 85371, December, 1985.

2. Hutchinson, J.W., "Singular Behaviour at the End of Tensile Crack in a Hardening Material", Journal of the Mechanics and Physics of Solids, Vol. 16, No. 1, 1968, pp 13–31.

3. Rice, J.R. and Rosengren, C.F., "Plane Strain Deformation Near a Crack Tip in a Power Law Hardening Material", Journal of Mechanics and Physics of Solids, Vol. 16, No. 1, 1968, pp 1–12.

4. McClintock, F.A., in Fracture, H. Liebowitz, ed., Vol. 3, Academic Press, New York, 1971, pp 47–225.

5. Rice, J.R., Journal of Applied Mechanics, Transactions, American Society of Mechanical Engineers, Vol. 35, June 1968, pp 329–386.

6. Begley, J.A. and Landes, J.D., "The J-Integral as a Fracture Criterion", in Fracture Toughness, ASTM STP 514, American Society for Testing and Materials, 1972, pp 1–23.

7. Landes, J.D. and Begley, J.A., "The Effect of Specimen Geometry on J_{Ic}", in Fracture Toughness, ASTM STP 514, American Society for Testing and Materials, 1972, pp 24–39.

8. Rice. J.R., Paris, P.C. and Merkle, J.G., "Some Further Results of J-Integral Analysis and Estimates", in progress in Flaw Growth and Fracture Toughness Testing, ASTM STP 536, American Society for Testing and Materials", 1973, pp 231–245.

9. Landes, J.D. and Begley, J.A., "Test Results from J-Integral Studies: An Attempt to Establish a J_{Ic} Testing Procedure", in Fracture Analysis, ASTM STP 560, American Society for Testing and Materials", 1974, pp 170–186.

10. Clarke, G.A., Andrews, W.R., Paris, P.C. and Schmidt, D.W., "Single Specimen Tests for J_{Ic} Determination", in Mechanics of Crack Growth, ASTM STP 590, American Society for Testing and Materials, 1976, pp 27–42.

11. Hutchinson, J.W. and Paris, P.C., "Stability Analysis of J-Controlled Crack Growth", in Elastic-Plastic Fracture, ASTM STP 668, American Society for Testing and Materials, Philadelphia, 1979, pp. 37–64.

12. Paris, P.C., Tada, H., Zahoor, A., and Ernst, H., "The Theory of Instability of the Tearing Mode of Elastic-Plastic Crack Growth", in Elastic-Plastic Fracture, ASTM STP 668, American Society for Testing and Materials, Philadelphia, 1979, 5–36.

13. Paris, P.C., Tada, H., Zahoor A., and Ernst, H., "Initial Experimental Investigation of Tearing Instability Theory", in Elastic-Plastic Fracture, ASTM STP 668, American Society for Testing and Materials, Philadelphia, 1979, pp. 251–265.

14. Report of the U.S. Nuclear Regulatory Commission Piping Review Committee, Nureg-1061, Volume 3.

15. Manning, B.W., "Fracture Mechanics Leak-Before-Break Material Test Program", Ontario Hydro Design and Development Division – Generation, report No. 85120, September 1986 (Rev. 2).

16. Ho. E.T.C. and McGraw, M.J., "Tensile Properties of ASME SA106 Grade B and SA105 Darlington Primary Heat Transport Piping Material at 293 and 523 K", Ontario Hydro Research Division Report No. 86-11-K, July 1986.

17. ASME Boiler and Pressure Vessel Code, Section III, Division 1, "Nuclear Power Plant Components", 1980 with Summer 1980 Addenda.

18. Mukherjee, B. and Carpenter, D.W., "Darlington Leak Before Break Material Test Program J-Resistance Curves, Volume 2, Test Method and Results", Ontario Hydro Research Division Report No. 87-103-K, 1987.

19. Standard Test Method for Determining J-R Curves, 12th Draft. A proposed test method developed by the ASTM E24.08 Subcommittee.

20. Ernst, H.A., "Materials Resistance and Instability Beyond J-Controlled Crack Growth", ASTM STP 803, Ed. C.F. Shih, and J.P. Gudas, Eds., 1983, pp. I 191-213.

21. Loss, F.J. et al, "J-R Curve Characterization of Irradiated Low-Shelf Nuclear Vessel Steels", Elastic-Plastic Fracture: Second Symposium, Volume II - Fracture Resistance Curves and Engineering Applications, ASTM STP 803, C.F. Shih and J.P. Gudas, Eds., ASTM, 1983, pp. II-771-795.

22. "PVRC Recommendations on Toughness Requirements for Ferritic Materials", Welding Research Council Bulletin No. 175.

23. Carlsoon, A.J., "Fracture Mechanics in Scandinavia", Fracture Mechanics, Editors N. Perrone, H. Liebowitz, D. Mulville and W. Pilkey, University Press of Virginia.

24. Menke, B.H. et al, "R Curve Characteristics of Low-Strength Structural Steels", EPRI Report No. NP-2715, October 1982.

25. Miglin, M.T. et al, "Effect of Strain Aging in the Unloading Compliance J Test", Elastic-Plastic Fracture Test Methods. The User's Experience, ASTM STP 856, E.T. Wessel and F.J. Loss, Eds., American Society for Testing and Materials, 1985, pp. 150-165.

26. "Structural Integrity of Water Reactor Pressure Boundary Components", Annual Report for 1984. Edited by F.J. Loss, Materials Engineering Associate, NUREG/CR-3228, MEA-2051, Vol. 3.

27. Van Der Sluys, W.A. Emanuelson, R.H. and Futato, R.J., "Elastic-Plastic Properties of Submerged Arc Weld Metal", Elastic-Plastic Toughness Test Methods: The User's Experience, ASTM STP 856, E.T. Wessel and F.J. Loss, Eds., American Society for Testing and Materials, 1985, pp. 68-83.

TABLE I

Large Diameter Piping Heats Darlington NGS A
Heat Transport Piping Units 1 and 2

Pipe Size (NPS)	Heat Numbers
21	J1136
	J1157
	J9980
22	J9968
	J9969
	L7204
24	J1136
	J1157
	J9980
	J9982
	L7204
	L7205

TABLE II

Ontario Hydro Nuclear Weld Procedures

NPS (Inches)	Ontario Hydro Weld Procedure	Weld Process
12 22	PN 107	- GTAW root pass - SMAW fill up - field and shop welding - no PWHT
	PN 229	- GTAW root pass - SMAW 2nd pass - SAW fill up - for shop welding only - no PWHT
24	PN 108	- GTAW root pass - SMAW fill up - for field and shop welding - PHWT performed
	PN 232	- GTAW root pass - SMAW 2nd pass - SAW fill up - for shop welding only - PWHT performed

Notes: (1) PN 108 weld procedure applied to 22" NPS pipe also for comparison of effect of PHWT.

DARLINGTON LBB A106B MATERIAL DATA SUMMARY TABLE

	TEST NO	MATERIAL	DIRECTION OF TEST	COUPON NO	DESCRIPTION	TEST TEMP C	DATE	YIELD STRESS MPa	ULTIMATE STRESS MPa	THICKNESS B cm	SIDE GROOVE %	Bn cm	WIDTH W cm	YOUNGS MODULUS Pa
J	1	PARENT	L-C	M1	24" NPS Sch 100	250	23-May-86	228.0	510.8	3.175	19.8	2.547	6.365	1.828E+11
J	2	PARENT	L-C	M1	24" NPS Sch 100	250	17-Sep-85	228.0	510.8	3.174	19.8	2.547	6.361	1.828E+11
J	3	PARENT	L-C	S1	24" NPS Sch 100	250	18-Sep-85	228.0	510.8	3.175	19.6	2.552	6.364	1.828E+11
J	4	WELD PN-108	L-C	A1	24" NPS Sch 100	250	20-Sep-85	275.3	482.0	3.047	21.2	2.400	6.360	1.828E+11
J	5	WELD PN-108	L-C	A1	24" NPS Sch 100	250	19-Sep-85	275.3	482.0	3.046	21.2	2.400	6.365	1.828E+11
J	6	WELD PN-108	L-C	A3	24" NPS Sch 100	250	23-Sep-85	275.3	482.0	3.048	21.0	2.409	6.361	1.828E+11
J	7	HAZ PN-108	L-C	A2	24" NPS Sch 100	250	21-Jan-86	275.3	482.0	3.053	21.4	2.400	6.360	1.828E+11
J	8	HAZ PN-108	L-C	A2	24" NPS Sch 100	250	20-Jan-86	275.3	482.0	2.901	21.3	2.284	6.297	1.828E+11
J	9	WELD PN-232	L-C	B1	24" NPS Sch 100	250	24-Sep-85	249.3	423.4	3.047	21.1	2.403	6.359	1.828E+11
J	10	WELD PN-232	L-C	B1	24" NPS Sch 100	250	25-Sep-85	249.3	423.4	3.046	20.9	2.410	6.361	1.828E+11
J	11	WELD PN-232	L-C	B3	24" NPS Sch 100	250	26-Sep-85	249.3	423.4	3.051	21.4	2.398	6.360	1.828E+11
J	12	HAZ PN-232	L-C	B2	24" NPS Sch 100	250	23-Jan-86	249.3	423.4	3.040	20.5	2.418	6.351	1.828E+11
J	13	HAZ PN-232	L-C	B2	24" NPS Sch 100	250	22-Jan-86	249.3	423.4	3.055	20.3	2.434	6.300	1.828E+11
J	14	PARENT	L-C	N1	22" NPS Sch 100	20	26-Nov-85	320.3	532.6	3.048	19.4	2.458	6.349	1.923E+11
J	15	PARENT	L-C	N1	22" NPS Sch 100	20	25-Nov-85	320.3	532.6	3.050	19.3	2.461	6.349	1.923E+11
J	16	PARENT	L-C	N2	22" NPS Sch 100	20	29-Nov-85	320.3	532.6	3.050	19.3	2.461	6.349	1.923E+11
J	17	PARENT	L-C	N1	22" NPS Sch 100	250	28-Nov-85	220.7	508.5	3.049	19.3	2.460	6.347	1.828E+11
J	18	PARENT	L-C	N2	22" NPS Sch 100	250	28-Nov-85	220.7	508.5	3.049	19.4	2.459	6.344	1.828E+11
J	19	PARENT	L-C	N2	22" NPS Sch 100	250	27-Nov-85	220.7	508.5	3.049	19.5	2.455	6.345	1.828E+11
J	20	WELD PN-107	L-C	C1	22" NPS Sch 100	20	23-Oct-85	347.7	547.2	2.541	20.1	2.030	5.095	1.923E+11
J	21	WELD PN-107	L-C	C1	22" NPS Sch 100	20	24-Oct-85	347.7	547.2	2.542	21.5	1.995	5.090	1.923E+11
J	22	WELD PN-107	L-C	C2	22" NPS Sch 100	20	25-Oct-85	347.7	547.2	2.540	20.9	2.008	5.093	1.923E+11
J	23	WELD PN-107	L-C	C4	22" NPS Sch 100	250	18-Oct-85	353.7	542.3	2.540	20.8	2.012	5.092	1.828E+11
J	24	WELD PN-107	L-C	C2	22" NPS Sch 100	250	21-Oct-85	353.7	542.3	2.541	20.7	2.015	5.091	1.828E+11
J	25	WELD PN-107	L-C	C4	22" NPS Sch 100	250	22-Oct-85	353.7	542.3	2.540	20.5	2.020	5.090	1.828E+11
J	26	HAZ PN-107	L-C	C3	22" NPS Sch 100	20	03-Dec-85	347.7	547.2	2.537	21.0	2.005	5.082	1.923E+11
J	27	HAZ PN-107	L-C	C3	22" NPS Sch 100	20	04-Dec-85	347.7	547.2	2.540	20.6	2.017	5.082	1.923E+11
J	28	HAZ PN-107	L-C	C6	22" NPS Sch 100	250	14-Nov-85	353.7	542.3	2.538	21.0	2.006	5.084	1.828E+11
J	29	HAZ PN-107	L-C	C6	22" NPS Sch 100	250	13-Nov-85	353.7	542.3	2.540	21.0	2.007	5.084	1.828E+11
J	30	WELD PN-229	L-C	D1	22" NPS Sch 100	20	28-Oct-85	367.0	516.1	2.540	20.8	2.011	5.095	1.923E+11
J	31	WELD PN-229	L-C	D1	22" NPS Sch 100	20	29-Oct-85	367.0	516.1	2.540	20.5	2.019	5.091	1.923E+11
J	32	WELD PN-229	L-C	D2	22" NPS Sch 100	20	30-Oct-85	367.0	516.1	2.540	20.8	2.012	5.095	1.923E+11
J	33	WELD PN-229	L-C	D4	22" NPS Sch 100	250	27-Sep-85	364.0	553.1	2.540	20.7	2.014	5.093	1.828E+11
J	34	WELD PN-229	L-C	D2	22" NPS Sch 100	250	30-Sep-85	364.0	553.1	2.540	20.5	2.020	5.091	1.828E+11
J	35	WELD PN-229	L-C	D4	22" NPS Sch 100	250	01-Oct-85	364.0	553.1	2.541	20.4	2.022	5.093	1.828E+11
J	36	HAZ PN-229	L-C	D3	22" NPS Sch 100	20	11-Nov-85	367.0	516.1	2.540	21.1	2.003	5.084	1.923E+11
J	37	HAZ PN-229	L-C	D3	22" NPS Sch 100	20	12-Nov-85	367.0	516.1	2.540	21.4	1.996	5.083	1.923E+11
J	38	HAZ PN-229	L-C	D6	22" NPS Sch 100	250	08-Nov-85	364.0	553.7	2.539	21.4	1.996	5.082	1.828E+11
J	39	HAZ PN-229	L-C	D6	22" NPS Sch 100	250	07-Nov-85	364.0	553.7	2.540	20.9	2.009	5.085	1.828E+11
J	40	WELD PN-108	L-C	E1	22" NPS Sch 100	250	02-Oct-85	273.0	479.8	2.538	21.1	2.002	5.091	1.828E+11
J	41	WELD PN-108	L-C	E1	22" NPS Sch 100	250	03-Oct-85	273.0	479.8	2.544	21.2	2.004	5.091	1.828E+11
J	42	WELD PN-108	L-C	E2	22" NPS Sch 100	250	04-Oct-85	273.0	479.8	2.540	21.2	2.001	5.093	1.828E+11
J	43	HAZ PN-108	L-C	E2	22" NPS Sch 100	250	05-Nov-85	273.0	479.8	2.540	21.2	2.002	5.083	1.828E+11
J	44	HAZ PN-108	L-C	E2	22" NPS Sch 100	250	06-Nov-85	273.0	479.8	2.539	20.3	2.024	5.082	1.828E+11
J	45	PARENT	L-C	P1	12" NPS Sch100	250	17-Jan-86	267.3	559.3	1.908	20.3	1.521	3.810	1.828E+11
J	46	PARENT	L-C	P1	12" NPS Sch100	250	16-Jan-86	267.3	559.3	1.906	21.0	1.505	3.809	1.828E+11

DARLINGTON LBB A106B MATERIAL DATA SUMMARY TABLE

	TEST NO	MATERIAL	DIRECTION OF TEST	COUPON NO	DESCRIPTION	TEST TEMP C	DATE	YIELD STRESS MPa	ULTIMATE STRESS MPa	THICKNESS B cm	SIDE GROOVE %	Bn cm	WIDTH W cm	YOUNGS MODULUS Pa
J	47	PARENT	L-C	P2	12" NPS Sch100	250	15-Jan-86	267.3	559.3	1.905	20.2	1.520	3.809	1.828E+11
J	48	WELD PN-107	L-C	F1	12" NPS Sch100	250	14-Jan-86	324.0	548.2	1.589	20.8	1.259	3.810	1.828E+11
J	49	WELD PN-107	L-C	F1	12" NPS Sch100	250	13-Jan-86	324.0	548.2	1.637	20.4	1.303	3.809	1.828E+11
J	50	WELD PN-107	L-C	F2	12" NPS Sch100	250	09-Jan-86	324.0	548.2	1.637	19.3	1.321	3.808	1.828E+11
J	51	HAZ PN-107	L-C	F3	12" NPS Sch100	250	08-Jan-86	324.0	548.2	1.637	18.6	1.333	3.804	1.828E+11
J	52	HAZ PN-107	L-C	F3	12" NPS Sch100	250	07-Jan-86	324.0	548.2	1.637	18.9	1.328	3.813	1.828E+11
J	53	PARENT	L-C	R1	22"*12" VESSELET	20	29-Nov-85	322.7	560.6	2.540	21.1	2.005	5.079	1.923E+11
J	54	PARENT	L-C	R1	22"*12" VESSELET	20	02-Dec-85	322.7	560.6	2.540	21.6	1.991	5.083	1.923E+11
J	55	PARENT	L-C	R2	22"*12" VESSELET	20	02-Dec-85	322.7	560.6	2.541	21.2	2.003	5.084	1.923E+11
J	56	PARENT	L-C	R1	22"*12" VESSELET	250	28-Oct-85	231.0	528.8	2.540	20.8	2.012	5.083	1.828E+11
J	57	PARENT	L-C	R2	22"*12" VESSELET	250	30-Oct-85	231.0	528.8	2.542	21.5	1.995	5.080	1.828E+11
J	58	PARENT	L-C	R2	22"*12" VESSELET	250	31-Oct-85	231.0	528.8	2.540	21.1	2.005	5.081	1.828E+11
J	59	PARENT	C-L	M2	24" NPS Sch 100	250	07-Oct-85	268.3	525.5	3.180	20.0	2.544	6.362	1.828E+11
J	60	PARENT	C-L	M2	24" NPS Sch 100	250	08-Oct-85	268.3	525.5	3.177	20.0	2.541	6.365	1.828E+11
J	61	PARENT	C-L	S1	24" NPS Sch 100	250	09-Oct-85	268.3	525.5	3.175	19.7	2.551	6.366	1.828E+11
J	62	PARENT	C-L	N3	22" NPS Sch 100	20	10-Oct-85	324.0	529.5	3.160	19.0	2.560	6.370	1.923E+11
J	63	PARENT	C-L	N3	22" NPS Sch 100	20	11-Oct-85	324.0	529.5	3.150	18.2	2.576	6.360	1.923E+11
J	64	PARENT	C-L	N4	22" NPS Sch 100	20	15-Oct-85	324.0	529.5	3.175	19.5	2.555	6.360	1.923E+11
J	65	PARENT	C-L	N3	22" NPS Sch 100	250	16-Oct-85	224.0	506.1	3.160	18.9	2.563	6.360	1.828E+11
J	66	PARENT	C-L	N4	22" NPS Sch 100	250	16-Oct-85	224.0	506.1	3.176	19.8	2.546	6.358	1.828E+11
J	67	PARENT	C-L	N4	22" NPS Sch 100	250	17-Oct-85	224.0	506.1	3.177	20.1	2.540	6.367	1.828E+11
J	68	PARENT	C-L	P2	12" NPS Sch100	250	06-Jan-86	218.0	554.9	1.905	20.4	1.517	3.807	1.828E+11
J	69	PARENT	C-L	P3	12" NPS Sch100	250	03-Jan-86	218.0	554.9	1.906	20.6	1.513	3.812	1.828E+11
J	70	PARENT	C-L	P3	12" NPS Sch100	250	02-Jan-86	218.0	554.9	1.906	20.7	1.511	3.808	1.828E+11
J	71	PARENT	C-L	R3	22"*12" VESSELET	20	01-Nov-85	311.0	561.7	2.540	20.9	2.009	5.083	1.923E+11
J	72	PARENT	C-L	R3	22"*12" VESSELET	20	03-Nov-85	311.0	561.7	2.540	21.1	2.004	5.079	1.923E+11
J	73	PARENT	C-L	R4	22"*12" VESSELET	20	02-Nov-85	311.0	561.7	2.540	21.2	2.001	5.077	1.923E+11
J	74	PARENT	C-L	R3	22"*12" VESSELET	20	02-Nov-85	311.0	561.7	2.542	21.9	1.986	5.079	1.923E+11
J	75	PARENT	C-L	R4	22"*12" VESSELET	20	03-Nov-85	311.0	561.7	2.540	21.1	2.004	5.084	1.923E+11
J	76	PARENT	C-L	R4	22"*12" VESSELET	20	04-Nov-85	311.0	561.7	2.540	21.1	2.004	5.085	1.923E+11
J	77	PARENT	C-L	R5	22"*12" VESSELET	250	14-Apr-86	228.3	526.4	2.541	20.0	2.032	5.081	1.828E+11
J	78	PARENT	C-L	R5	22"*12" VESSELET	250	10-Apr-86	228.3	526.4	2.540	19.9	2.034	5.093	1.828E+11
J	79	PARENT	C-L	F6	22"*12" VESSELET	250	11-Apr-86	228.3	526.4	2.541	19.7	2.042	5.079	1.828E+11
J	80	WELD PN-232	L-C	B3	24" NPS Sch 100	20	07-Apr-86	309.0	512.0	2.539	20.2	2.026	5.082	1.923E+11
J	81	WELD PN-232	L-C	B8	24" NPS Sch 100	20	08-Apr-86	309.0	512.0	3.032	20.9	2.397	6.352	1.923E+11
J	82	WELD PN-232	L-C	B8	24" NPS Sch 100	20	09-Apr-86	309.0	512.0	2.541	20.3	2.024	5.081	1.923E+11
J	83	W PN229 SR	L-C	D5	22" NPS Sch 100	20	24-Feb-86	367.0	516.0	2.541	21.6	1.991	5.089	1.923E+11
J	84	W PN229 SR	L-C	D5	22" NPS Sch 100	250	25-Feb-86	364.0	553.1	2.539	21.1	2.003	5.090	1.828E+11
J	85	W PN229 SR	L-C	D8	22" NPS Sch 100	250	26-Feb-86	364.0	553.1	2.540	21.2	2.001	5.087	1.828E+11
TD	13	PARENT	C-L	M5	24" NPS Sch 100	200	15-Sep-85	248.5	482.0	3.177	20.3	2.531	6.365	1.864E+11
TD	14	PARENT	C-L	M5	24" NPS Sch 100	200	14-Sep-85	248.5	482.0	3.174	19.9	2.543	6.363	1.864E+11
TD	15	PARENT	C-L	M5	24" NPS Sch 100	250	13-Sep-85	228.0	510.8	3.175	19.7	2.551	6.360	1.828E+11
TD	16	PARENT	C-L	M2	24" NPS Sch 100	300	28-May-86	223.0	513.8	3.174	19.6	2.552	6.366	1.785E+11
TD	17	PARENT	C-L	M6	24" NPS Sch 100	300	11-Sep-85	223.0	513.8	3.175	20.0	2.541	6.359	1.785E+11
TD	18	PARENT	C-L	M6	24" NPS Sch 100	250	10-Sep-85	228.0	510.8	3.176	20.2	2.535	6.362	1.828E+11

TEST NO	FATIGUE CRACK MEASURED cm	FATIGUE CRACK COMPLIANCE cm	CRACK EXTENSION MEASURED cm	FINAL CRACK COMPLIANCE cm	CRACK EXTENSION COMPLIANCE cm	REMAINING LIGAMENT cm	Jic kN/m	SLOPE MPa	INTERCEPT kN/m	AV. T AT Jic	APPROX. w AT Jic
J 1	3.715	3.620	0.613	4.185	0.565	2.037	185	94	161	125.9	13.4
J 2	3.818	3.723	0.401	4.137	0.414	2.142	160	93	140	124.6	14.7
J 3	3.743	3.655	0.394	4.009	0.354	2.227	265	101	229	135.3	9.9
J 4	3.681	3.554	0.407	3.939	0.385	2.272	419	129	347	164.4	8.2
J 5	3.697	3.560	0.282	3.806	0.246	2.386	495	148	397	188.7	7.9
J 6	3.720	3.630	0.697	4.287	0.657	1.944	378	134	311	170.8	9.3
J 7	3.716	3.618	0.548	4.016	0.398	2.096	274	109	234	139.0	10.4
J 8	3.717	3.593	0.315	3.881	0.288	2.265	355	107	305	136.4	7.7
J 9	3.715	3.618	0.570	4.156	0.538	2.074	246	99	209	159.9	10.6
J 10	3.753	3.664	0.637	4.253	0.589	1.971	243	96	208	155.1	10.2
J 11	3.745	3.643	0.545	4.152	0.509	2.070	223	119	183	192.3	13.8
J 12	3.736	3.630	0.529	4.091	0.461	2.086	214	75	189	121.2	9.1
J 13	3.767	3.662	0.444	4.080	0.418	2.089	179	118	147	190.6	16.6
J 14	3.965	3.872	0.168	4.032	0.160	2.216	235	261	163	276.0	26.3
J 15	3.952	3.848	0.430	4.232	0.384	1.967	219	227	161	240.1	24.6
J 16	3.968	3.864	0.435	4.266	0.402	1.946	255	224	188	236.9	20.7
J 17	3.944	3.814	0.466	4.281	0.467	1.937	131	118	109	162.2	21.5
J 18	3.934	3.830	0.446	4.255	0.425	1.964	160	106	137	145.7	15.8
J 19	3.959	3.870	0.437	4.310	0.440	1.949	138	113	117	155.4	19.4
J 20	3.103	2.985	0.189	3.157	0.172	1.803	281	327	178	314.2	22.9
J 21	3.064	2.966	0.359	3.328	0.362	1.667	281	240	205	230.6	17.1
J 22	3.034	2.928	0.366	3.277	0.349	1.694	335	241	244	231.5	14.7
J 23	3.015	2.940	0.552	3.483	0.543	1.525	134	89	121	81.1	13.7
J 24	3.090	3.020	0.623	3.652	0.632	1.378	110	72	101	65.6	13.0
J 25	3.037	2.924	0.564	3.515	0.591	1.489	135	87	122	79.2	13.1
J 26	3.013	2.925	0.273	3.202	0.277	1.796	421	201	326	193.1	9.8
J 27	3.022	2.942	0.353	3.287	0.345	1.707	385	235	283	225.8	12.5
J 28	3.111	3.025	0.425	3.395	0.370	1.548	187	82	170	74.7	8.6
J 29	3.047	2.970	0.455	3.387	0.417	1.582	196	85	178	77.4	8.7
J 30	3.130	3.036	0.207	3.796	0.760	1.758	175	188	137	185.5	20.9
J 31	3.100	3.021	0.216	3.217	0.196	1.775	172	185	136	182.5	21.2
J 32	3.191	3.107	0.260	3.833	0.726	1.644	178	155	147	152.9	16.4
J 33	3.039	2.963	0.476	3.447	0.484	1.578	86	59	80	51.3	14.0
J 34	3.201	3.106	0.488	3.627	0.521	1.402	63	62	58	53.9	18.4
J 35	3.227	3.126	0.495	3.646	0.520	1.371	74	63	69	54.8	15.7
J 36	3.215	3.123	0.385	3.549	0.375	1.484	214	231	158	227.9	20.0
J 37	3.228	3.132	0.246	3.344	0.212	1.609	275	236	201	232.8	15.7
J 38	3.221	3.148	0.534	3.661	0.513	1.327	113	98	101	85.1	16.0
J 39	3.063	3.006	0.568	3.547	0.541	1.454	101	106	89	92.0	21.0
J 40	3.035	2.952	0.420	3.343	0.391	1.636	346	137	283	176.7	8.1
J 41	3.237	3.194	0.508	3.660	0.466	1.346	236	111	201	143.2	8.6
J 42	3.423	3.364	0.312	3.633	0.269	1.358	323	141	262	181.9	7.2
J 43	3.217	3.117	0.355	3.428	0.311	1.511	189	156	150	201.3	15.2
J 44	3.156	3.074	0.333	3.357	0.283	1.593	361	115	306	148.4	6.1
J 45	2.309	2.226	0.384	2.601	0.375	1.117	131	114	106	122.0	12.9
J 46	2.304	2.227	0.412	2.627	0.400	1.093	158	98	139	104.9	9.2

TEST NO	FATIGUE CRACK MEASURED cm	FATIGUE CRACK COMPLIANCE cm	CRACK EXTENSION MEASURED cm	FINAL CRACK COMPLIANCE cm	CRACK EXTENSION COMPLIANCE cm	REMAINING LIGAMENT cm	Jic kN/m	SLOPE MPa	INTERCEPT kN/m	AV. T AT Jic	APPROX. w AT Jic
J 47	2.307	2.222	0.377	2.614	0.392	1.125	112	112	96	119.8	14.8
J 48	2.386	2.320	0.342	2.680	0.360	1.082	104	78	95	75.0	10.5
J 49	2.279	2.204	0.366	2.579	0.375	1.164	121	79	110	75.9	9.9
J 50	2.317	2.239	0.368	2.590	0.351	1.123	95	104	84	99.9	16.1
J 51	2.449	2.400	0.357	2.750	0.350	0.998	88	98	78	94.2	14.9
J 52	2.306	2.250	0.311	2.538	0.288	1.196	191	136	161	130.7	10.6
J 53	3.146	3.047	0.420	3.473	0.426	1.513	133	192	104	189.3	27.6
J 54	3.193	3.090	0.358	3.434	0.344	1.532	140	204	107	201.2	27.2
J 55	3.179	3.091	0.325	3.413	0.322	1.580	174	179	138	176.5	19.4
J 56	3.181	3.087	0.538	3.584	0.497	1.364	139	69	127	87.4	9.3
J 57	3.158	3.094	0.504	3.547	0.453	1.418	131	111	111	140.6	16.1
J 58	3.156	3.067	0.460	3.505	0.438	1.465	150	103	130	130.4	13.1
J 59	3.701	3.627	0.563	4.173	0.546	2.098	81	53	76	61.5	17.3
J 60	3.729	3.643	0.684	4.309	0.666	1.952	108	43	102	49.9	10.4
J 61	3.898	3.805	0.612	4.417	0.612	1.856	100	59	93	68.5	14.4
J 62	3.934	3.845	0.604	4.424	0.579	1.832	111	75	102	79.2	16.3
J 63	3.688	3.606	0.595	4.172	0.566	2.077	190	58	177	61.3	8.1
J 64	3.832	3.723	0.556	4.268	0.545	1.972	71	105	63	110.9	37.1
J 65	3.730	3.637	0.553	4.140	0.503	2.077	111	34	105	46.6	8.0
J 66	3.759	3.674	0.652	4.302	0.628	1.947	94	38	89	52.1	10.4
J 67	3.743	3.649	0.679	4.312	0.663	1.945	86	52	80	71.3	15.7
J 68	2.345	2.283	0.392	2.660	0.377	1.070	102	71	93	86.9	10.0
J 69	2.292	2.225	0.356	2.574	0.349	1.164	147	90	136	110.1	9.2
J 70	2.317	2.237	0.357	2.603	0.366	1.134	133	85	118	104.0	9.4
J 71	3.159	3.099	0.467	3.513	0.414	1.457	110	93	98	93.9	16.1
J 72	3.122	3.058	0.538	3.573	0.515	1.419	104	113	91	114.2	21.0
J 73	3.139	3.078	0.466	3.506	0.428	1.472	104	90	93	90.9	16.6
J 74	3.192	3.126	0.477	3.580	0.454	1.410	97	97	86	98.0	18.7
J 75	3.192	3.122	0.610	3.730	0.608	1.282	89	77	81	77.8	16.2
J 76	3.158	3.087	0.599	3.650	0.563	1.328	88	80	80	80.8	17.3
J 77	3.079	2.989	0.419	3.366	0.377	1.583	74	69	67	88.6	18.5
J 78	3.079	3.024	0.506	3.498	0.474	1.508	81	51	76	65.5	12.6
J 79	3.059	2.966	0.697	3.592	0.626	1.323	96	42	90	53.9	8.7
J 80	3.109	2.997	0.414	3.387	0.390	1.559	267	220	195	251.1	16.1
J 81	3.802	3.671	0.408	4.034	0.363	2.142	302	237	215	270.5	19.9
J 82	3.099	2.984	0.335	3.292	0.308	1.647	389	266	263	303.6	13.4
J 83	3.093	3.026	0.176	3.195	0.169	1.820	240	256	170	252.6	21.1
J 84	3.079	2.992	0.361	3.358	0.366	1.650	162	138	138	120.0	17.0
J 85	3.088	3.004	0.359	3.334	0.330	1.640	132	142	112	123.4	21.3
TD 13	3.742	3.658	0.891	4.527	0.869	1.732	113	47	105	65.7	10.8
TD 14	3.791	3.679	0.898	4.577	0.898	1.674	100	50	93	69.8	12.8
TD 15	3.728	3.609	0.468	4.053	0.444	2.164	98	37	93	49.6	9.9
TD 16	3.702	3.581	0.572	4.134	0.553	2.092	106	49	99	64.5	12.2
TD 17	3.731	3.618	0.614	4.248	0.630	2.014	104	46	98	60.5	11.5
TD 18	3.709	3.599	0.702	4.310	0.711	1.951	79	62	72	83.0	20.7

YES = ++++++ ; NO = .
(1) Bn > 25Jic/FLOW STRESS
(2) LIGAMENT > 25Jic/FLOW STRESS
(3) DJ/DA < FLOW STRESS

(4) Bn*FLOW STRESS /20
(5) LIGAMENT*FLOW STRESS /20
(6) ABS(La-Lc) < 0.15* CRACK EXTENSION
(7) 0.1* ORIGINAL LIGAMENT

QUALIFICATION OF R-CURVE DATA

J IN kN/m, DA IN mm
CURVE FIT TO THE FORM J=C1*(da)^C2

TEST NO	Jic VALIDITY (1)	Jic VALIDITY (2)	J VALIDITY (3)	25*Jic/F.S. cm	CRACK EXTENSION ALLOWED (7) cm	J(MAX) ALLOWED (4) kN/m	J(MAX) ALLOWED (5) kN/m	CRACK SIZE VALIDITY (6)	FIRST POINT	LAST POINT	CONSTANT C1	EXPONENT C2
J 1	++++++	++++++	++++++	1.252	0.275	470.4	402.6	++++++	19	36	259.280	0.4025
J 2	++++++	++++++	++++++	1.083	0.264	470.4	410.8	++++++	17	31	242.430	0.4292
J 3	++++++	++++++	++++++	1.793	0.271	471.4	435.0	++++++	22	34	336.520	0.3387
J 4	.	.	++++++	2.766	0.281	454.4	458.4	++++++	31	43	482.700	0.2979
J 5	.	.	++++++	3.268	0.281	454.4	484.5	++++++	34	44	544.580	0.3582
J 6	.	.	++++++	2.496	0.273	456.1	392.7	++++++	22	41	450.010	0.3831
J 7	++++++	++++++	++++++	1.809	0.274	454.4	443.8	.	22	32	347.440	0.3047
J 8	.	.	++++++	2.344	0.270	432.5	457.4	++++++	25	33	408.320	0.3654
J 9	++++++	++++++	++++++	1.828	0.274	404.1	370.5	++++++	18	34	309.700	0.4183
J 10	++++++	++++++	++++++	1.806	0.270	405.3	354.5	++++++	19	35	298.680	0.4382
J 11	++++++	++++++	++++++	1.657	0.272	403.3	371.3	++++++	17	34	309.720	0.4398
J 12	++++++	++++++	++++++	1.591	0.272	406.6	380.1	++++++	19	32	266.410	0.3938
J 13	++++++	++++++	++++++	1.330	0.264	409.3	373.3	++++++	18	32	269.190	0.3991
J 14	++++++	++++++	++++++	1.378	0.248	524.1	494.0	++++++	18	28	429.650	0.6130
J 15	++++++	++++++	++++++	1.284	0.250	524.8	451.4	++++++	17	44	400.400	0.6575
J 16	++++++	++++++	++++++	1.495	0.249	524.8	444.1	++++++	19	43	419.940	0.5806
J 17	++++++	++++++	++++++	0.898	0.253	448.5	376.6	++++++	12	28	232.330	0.4819
J 18	++++++	++++++	++++++	1.097	0.251	448.3	380.8	++++++	14	28	250.200	0.4432
J 19	++++++	++++++	++++++	0.946	0.247	447.6	371.0	++++++	13	28	235.480	0.4554
J 20	++++++	++++++	++++++	1.570	0.211	454.2	433.6	++++++	21	32	511.490	0.6540
J 21	++++++	++++++	++++++	1.570	0.212	446.3	394.2	++++++	16	34	452.450	0.5991
J 22	++++++	.	++++++	1.872	0.217	449.2	406.3	++++++	17	34	490.080	0.5476
J 23	++++++	++++++	++++++	0.748	0.215	450.7	360.4	++++++	13	25	219.640	0.4056
J 24	++++++	++++++	++++++	0.614	0.207	451.4	322.3	++++++	12	24	180.000	0.4152
J 25	++++++	++++++	++++++	0.753	0.217	452.5	352.8	++++++	13	25	216.800	0.3831
J 26	.	.	++++++	2.352	0.216	448.6	420.6	++++++	19	30	527.560	0.4569
J 27	.	.	++++++	2.151	0.214	451.3	401.6	++++++	19	34	521.420	0.5036
J 28	++++++	++++++	++++++	1.044	0.206	449.4	378.3	++++++	15	24	258.450	0.3283
J 29	++++++	++++++	++++++	1.094	0.211	449.6	380.1	++++++	15	26	271.000	0.3463
J 30	++++++	++++++	++++++	0.991	0.206	444.0	286.8	.	15	25	333.030	0.5903
J 31	++++++	++++++	++++++	0.974	0.207	445.8	413.7	++++++	15	25	328.230	0.5830
J 32	++++++	++++++	++++++	1.008	0.199	444.2	278.6	.	14	26	310.800	0.5352
J 33	++++++	++++++	++++++	0.469	0.213	461.8	377.4	++++++	9	16	147.000	0.4018
J 34	++++++	++++++	++++++	0.343	0.199	463.1	335.7	++++++	9	19	126.060	0.4397
J 35	++++++	++++++	++++++	0.403	0.197	463.6	331.8	++++++	9	19	135.370	0.4226
J 36	++++++	++++++	++++++	1.212	0.196	442.2	339.0	++++++	14	33	397.580	0.5665
J 37	++++++	++++++	++++++	1.557	0.195	440.7	383.9	++++++	16	33	450.310	0.5830
J 38	++++++	++++++	++++++	0.616	0.193	458.0	326.0	++++++	11	27	204.710	0.4554
J 39	++++++	++++++	++++++	0.550	0.208	460.9	352.9	++++++	11	23	190.140	0.3753
J 40	.	.	++++++	2.298	0.214	376.8	329.0	++++++	18	29	426.660	0.3462
J 41	++++++	.	++++++	1.567	0.190	377.2	269.3	++++++	14	29	319.130	0.3886
J 42	.	.	++++++	2.145	0.173	376.6	274.8	++++++	18	29	408.320	0.3968
J 43	++++++	++++++	++++++	1.255	0.197	376.8	311.5	++++++	15	33	318.030	0.5294
J 44	.	.	++++++	2.398	0.201	380.8	324.6	.	23	33	424.150	0.3301
J 45	++++++	++++++	++++++	0.792	0.158	314.3	249.8	++++++	12	26	227.200	0.4703
J 46	++++++	++++++	++++++	0.956	0.158	311.0	244.3	++++++	13	28	247.040	0.4010

YES = ++++++ ; NO = .
(1) Bn > 25Jic/FLOW STRESS
(2) LIGAMENT > 25Jic/FLOW STRESS
(3) DJ/DA < FLOW STRESS

(4) Bn*FLOW STRESS /20
(5) LIGAMENT*FLOW STRESS /20
(6) ABS(Lm-Lc) < 0.15* CRACK EXTENSION
(7) 0.1* ORIGINAL LIGAMENT

QUALIFICATION OF R-CURVE DATA

J IN kN/m, DA IN mm

TEST NO	Jic VALIDITY (1)	VALIDITY (2)	VALIDITY (3)	25*Jic/F.S. cm	CRACK EXTENSION ALLOWED (7) cm	J(MAX) ALLOWED (4) kN/m	J(MAX) ALLOWED (5) kN/m	CRACK SIZE VALIDITY (6)	CURVE FIT TO THE FORM J=C1*(da)^C2 FIRST POINT	LAST POINT	CONSTANT C1	EXPONENT C2
J 47	++++++	++++++	++++++	0.677	0.159	314.1	246.9	++++++	11	25	212.390	0.4507
J 48	++++++	++++++	++++++	0.596	0.149	274.6	246.4	++++++	7	16	179.360	0.4280
J 49	++++++	++++++	++++++	0.694	0.161	284.1	268.2	++++++	11	19	194.360	0.3720
J 50	++++++	++++++	++++++	0.545	0.157	288.1	265.6	++++++	10	20	191.950	0.4730
J 51	++++++	++++++	++++++	0.504	0.140	290.7	229.8	++++++	9	20	181.630	0.4862
J 52	++++++	++++++	++++++	1.095	0.156	289.6	278.0	++++++	14	27	307.030	0.4739
J 53	++++++	++++++	++++++	0.753	0.203	442.8	354.6	++++++	12	31	301.100	0.5934
J 54	++++++	++++++	++++++	0.792	0.199	439.7	364.1	++++++	11	30	316.070	0.6381
J 55	++++++	++++++	++++++	0.985	0.199	442.3	369.0	++++++	12	30	327.420	0.5957
J 56	++++++	++++++	++++++	0.915	0.200	382.2	284.7	++++++	14	29	200.500	0.4308
J 57	++++++	++++++	++++++	0.862	0.199	379.0	291.2	++++++	12	30	228.220	0.4299
J 58	++++++	++++++	++++++	0.987	0.201	380.9	299.4	++++++	15	30	237.190	0.4283
J 59	++++++	++++++	++++++	0.510	0.274	504.9	434.4	++++++	13	21	130.580	0.3527
J 60	++++++	++++++	++++++	0.680	0.272	504.3	408.0	++++++	15	26	152.670	0.2956
J 61	++++++	++++++	++++++	0.630	0.256	506.2	386.8	++++++	15	28	156.360	0.3465
J 62	++++++	++++++	++++++	0.650	0.253	546.3	415.2	++++++	13	30	188.320	0.4485
J 63	++++++	++++++	++++++	1.113	0.275	549.7	466.9	++++++	16	30	253.770	0.3032
J 64	++++++	++++++	++++++	0.416	0.264	545.2	446.4	++++++	11	29	174.760	0.5418
J 65	++++++	++++++	++++++	0.760	0.272	467.8	405.2	++++++	16	24	142.400	0.3038
J 66	++++++	++++++	++++++	0.644	0.268	464.7	375.3	++++++	15	24	131.470	0.3078
J 67	++++++	++++++	++++++	0.589	0.272	463.6	375.1	++++++	14	25	134.660	0.3269
J 68	++++++	++++++	++++++	0.660	0.152	293.1	221.6	++++++	10	21	169.070	0.3877
J 69	++++++	++++++	++++++	0.951	0.159	292.4	239.2	++++++	14	24	224.250	0.3567
J 70	++++++	++++++	++++++	0.860	0.157	292.0	232.8	++++++	13	25	209.540	0.4340
J 71	++++++	++++++	++++++	0.630	0.198	438.3	342.5	++++++	11	25	198.790	0.4529
J 72	++++++	++++++	++++++	0.596	0.202	437.2	328.6	++++++	11	27	204.200	0.4405
J 73	++++++	++++++	++++++	0.596	0.200	436.6	342.8	++++++	10	23	187.410	0.4006
J 74	++++++	++++++	++++++	0.556	0.195	433.3	327.0	++++++	10	24	187.840	0.4592
J 75	++++++	++++++	++++++	0.510	0.196	437.2	295.4	++++++	10	28	163.830	0.4762
J 76	++++++	++++++	++++++	0.504	0.200	437.2	313.1	++++++	10	25	162.760	0.4575
J 77	++++++	++++++	++++++	0.490	0.209	383.4	323.6	++++++	9	17	132.970	0.3435
J 78	++++++	++++++	++++++	0.537	0.207	383.8	300.9	++++++	11	22	130.800	0.3595
J 79	++++++	++++++	++++++	0.636	0.211	385.2	280.6	++++++	12	23	137.960	0.2881
J 80	++++++	.	++++++	1.626	0.209	415.9	347.9	++++++	19	45	423.800	0.5837
J 81	++++++	++++++	++++++	1.839	0.268	492.0	475.8	++++++	21	42	455.770	0.6135
J 82	.	.	++++++	2.369	0.210	415.4	367.2	++++++	23	45	526.780	0.6024
J 83	++++++	++++++	++++++	1.359	0.206	439.5	418.1	++++++	19	32	433.930	0.5969
J 84	++++++	++++++	++++++	0.883	0.210	459.3	397.1	++++++	14	31	283.000	0.4601
J 85	++++++	++++++	++++++	0.720	0.208	458.8	401.9	++++++	11	31	266.940	0.5390
TD 13	++++++	++++++	++++++	0.773	0.271	462.2	335.7	++++++	7	16	167.800	0.3487
TD 14	++++++	++++++	++++++	0.684	0.268	464.4	326.2	++++++	13	29	152.790	0.3752
TD 15	++++++	++++++	++++++	0.663	0.275	471.2	426.1	++++++	14	22	133.850	0.3650
TD 16	++++++	++++++	++++++	0.719	0.278	470.1	411.1	++++++	14	22	154.050	0.2854
TD 17	++++++	++++++	++++++	0.706	0.274	468.0	388.8	++++++	13	25	154.010	0.3507
TD 18	++++++	++++++	++++++	0.535	0.276	468.2	379.0	++++++	11	24	140.310	0.3425

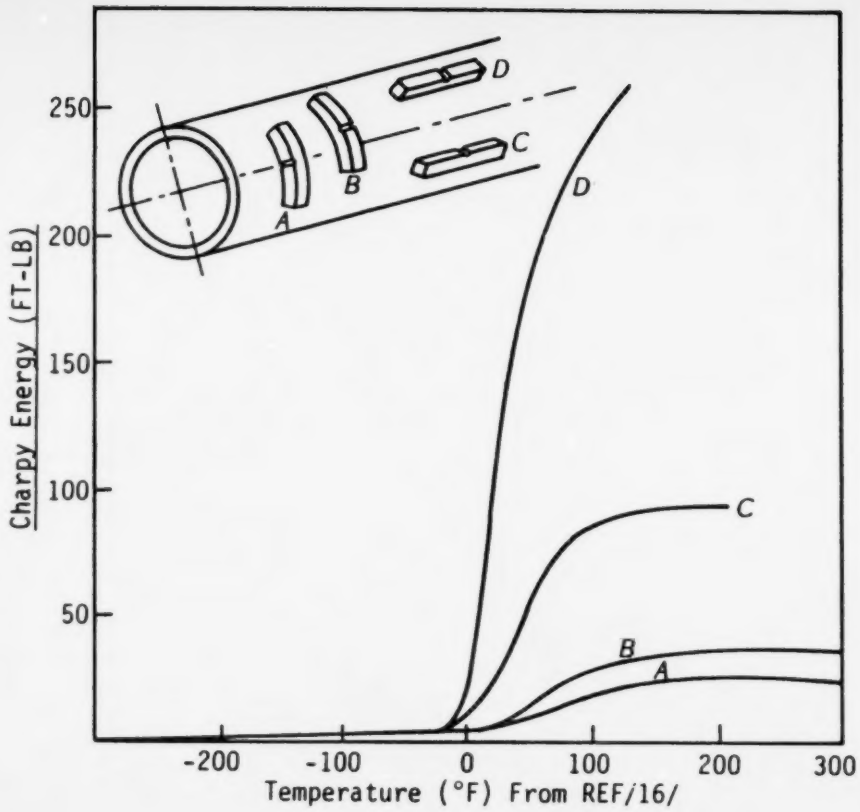

Legend	Crack Plane Orientation
A	(C-L)
B	(C-R)
C	(L-C)
D	(L-R)

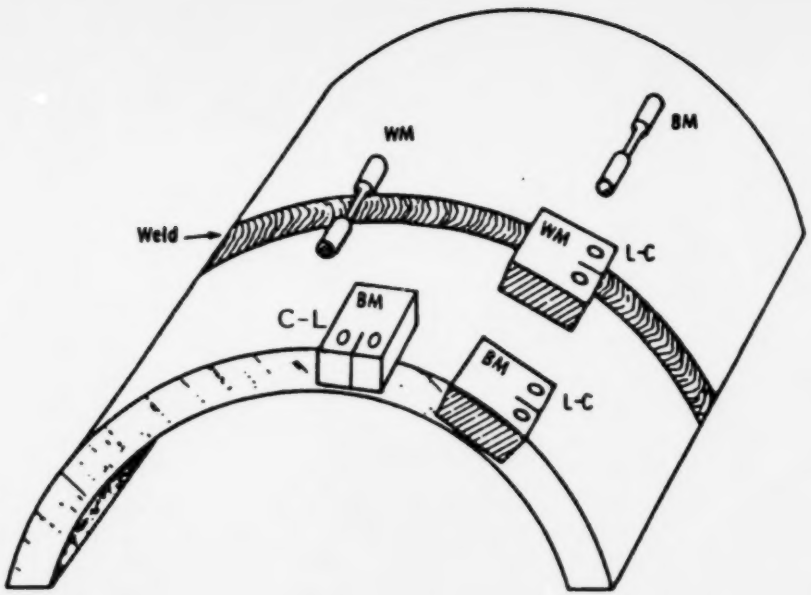

FIGURE 1

SPECIMEN ORIENTATION WITH RESPECT TO A PIPE GEOMETRY

17457-RD

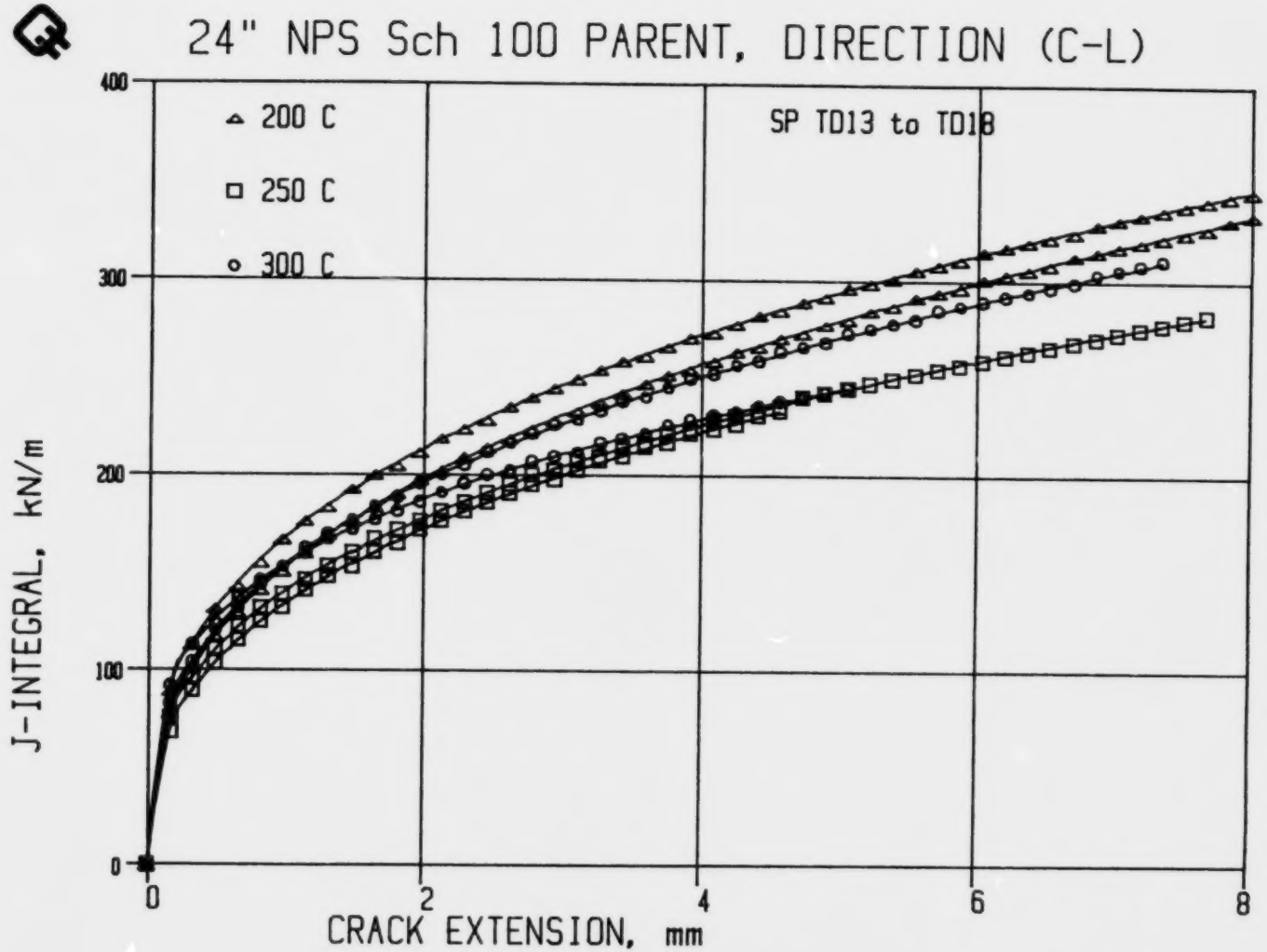

FIGURE 2
COMPARISON OF J-RESISTANCE CURVES AT 3 TEMPERATURES

File TD 13-18
174366-RD

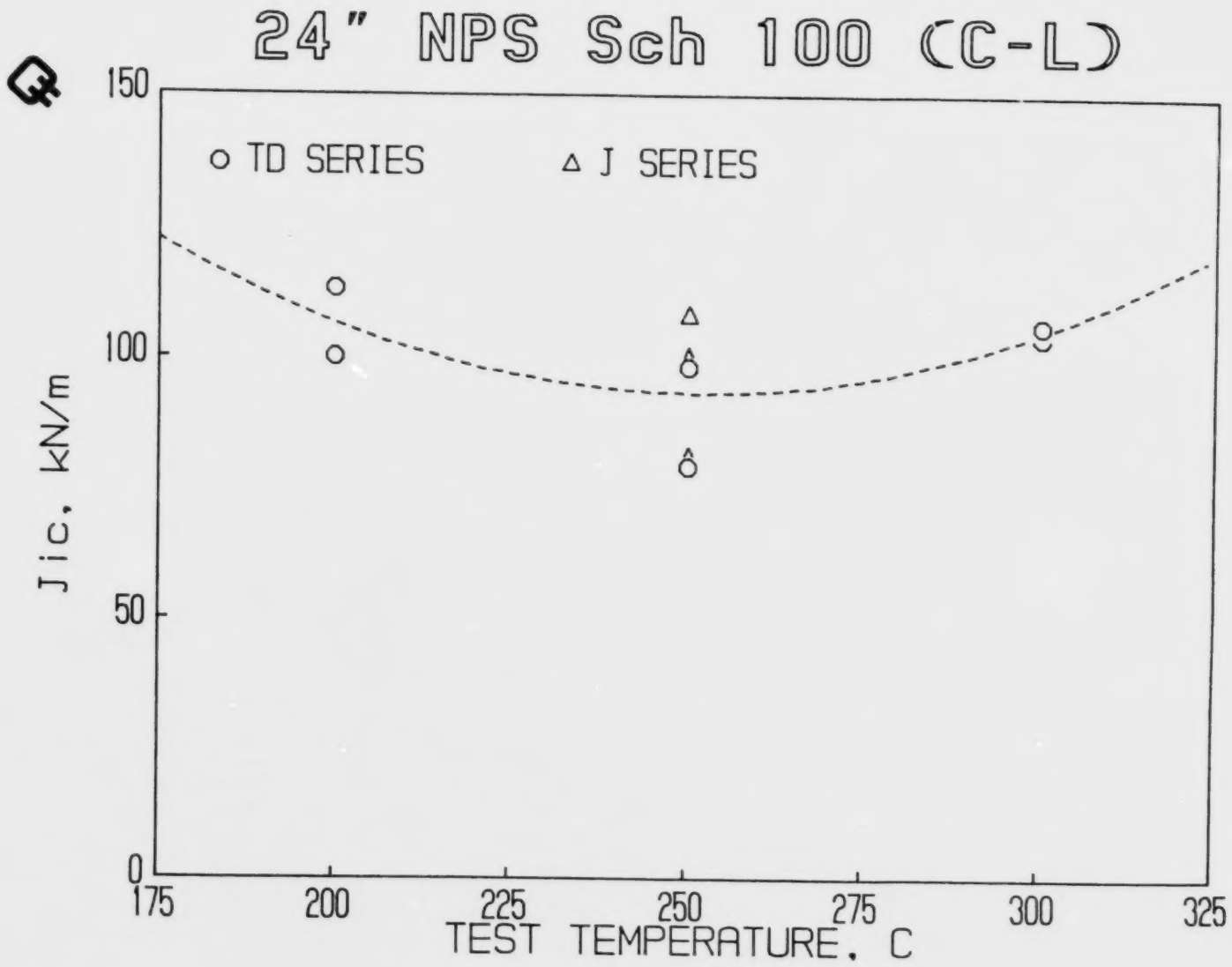

FIGURE 3

VARIATION OF J_{IC} BETWEEN 200°C AND 300°C

File JC 13-18 ENG
174367-RD

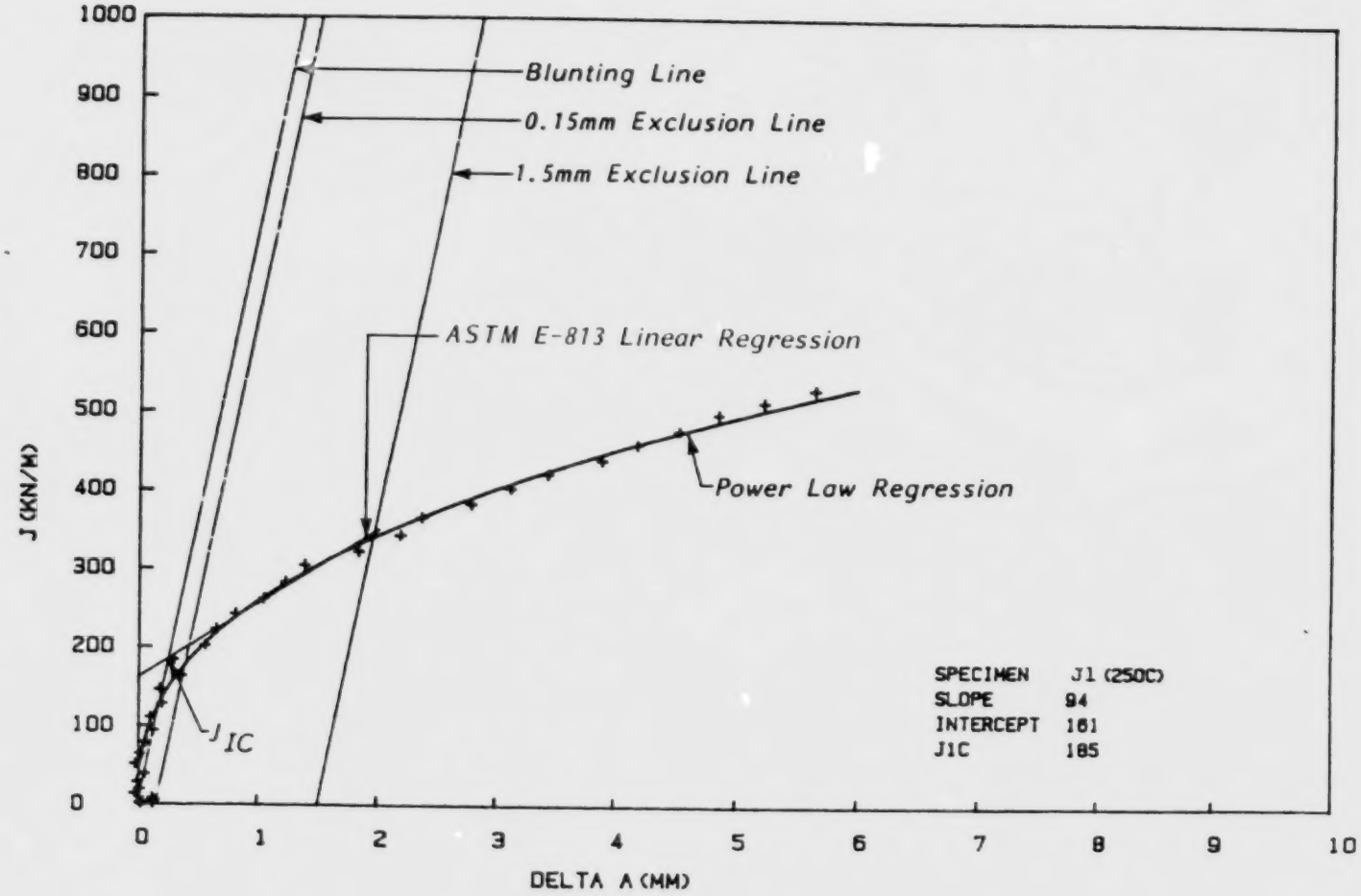

FIGURE 4
J-R CURVE

174576-RD

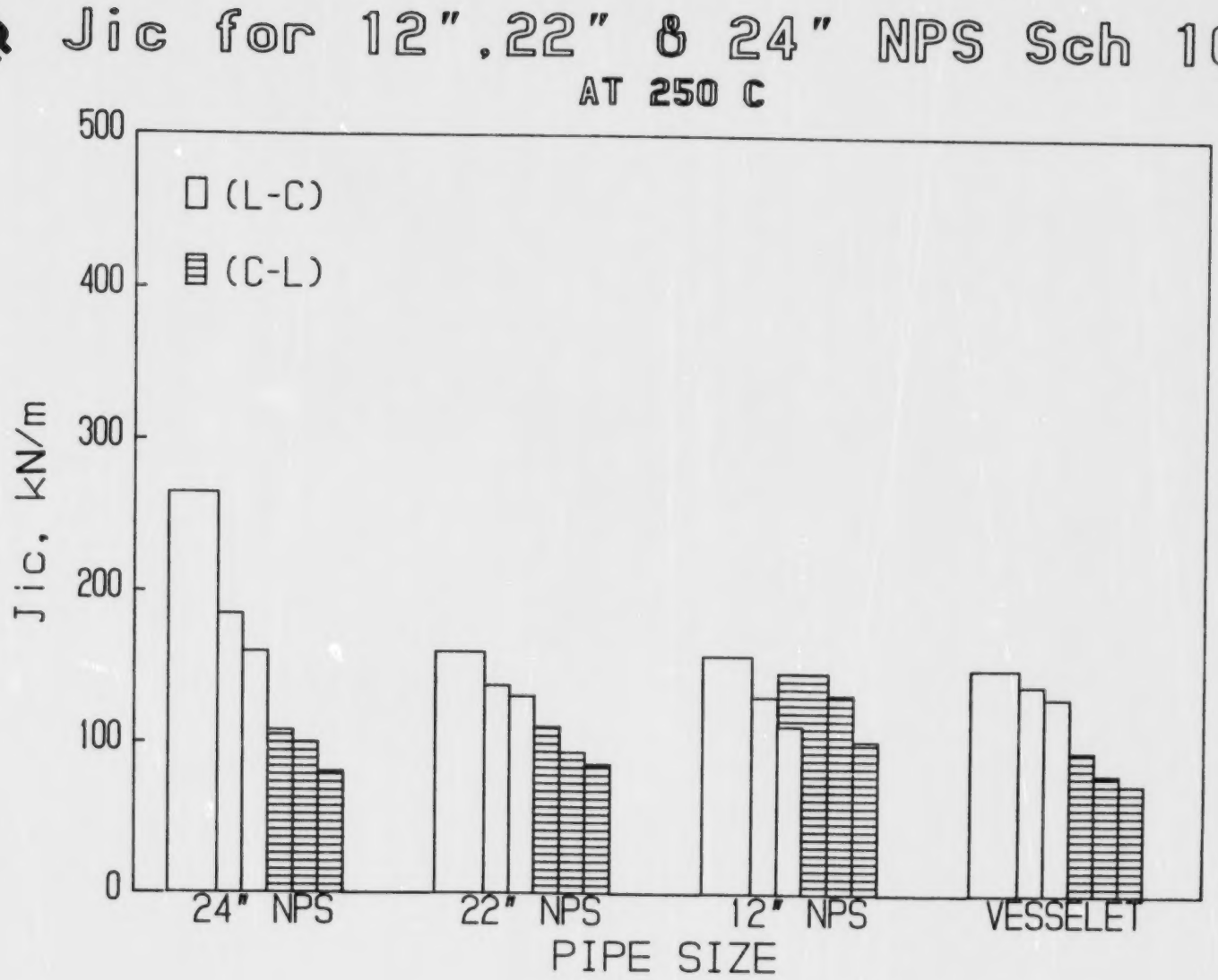

FIGURE 5

COMPARISON OF J_{IC} FOR VARIOUS PRODUCT FORMS

File JC 01-47 ENG
174311-RD

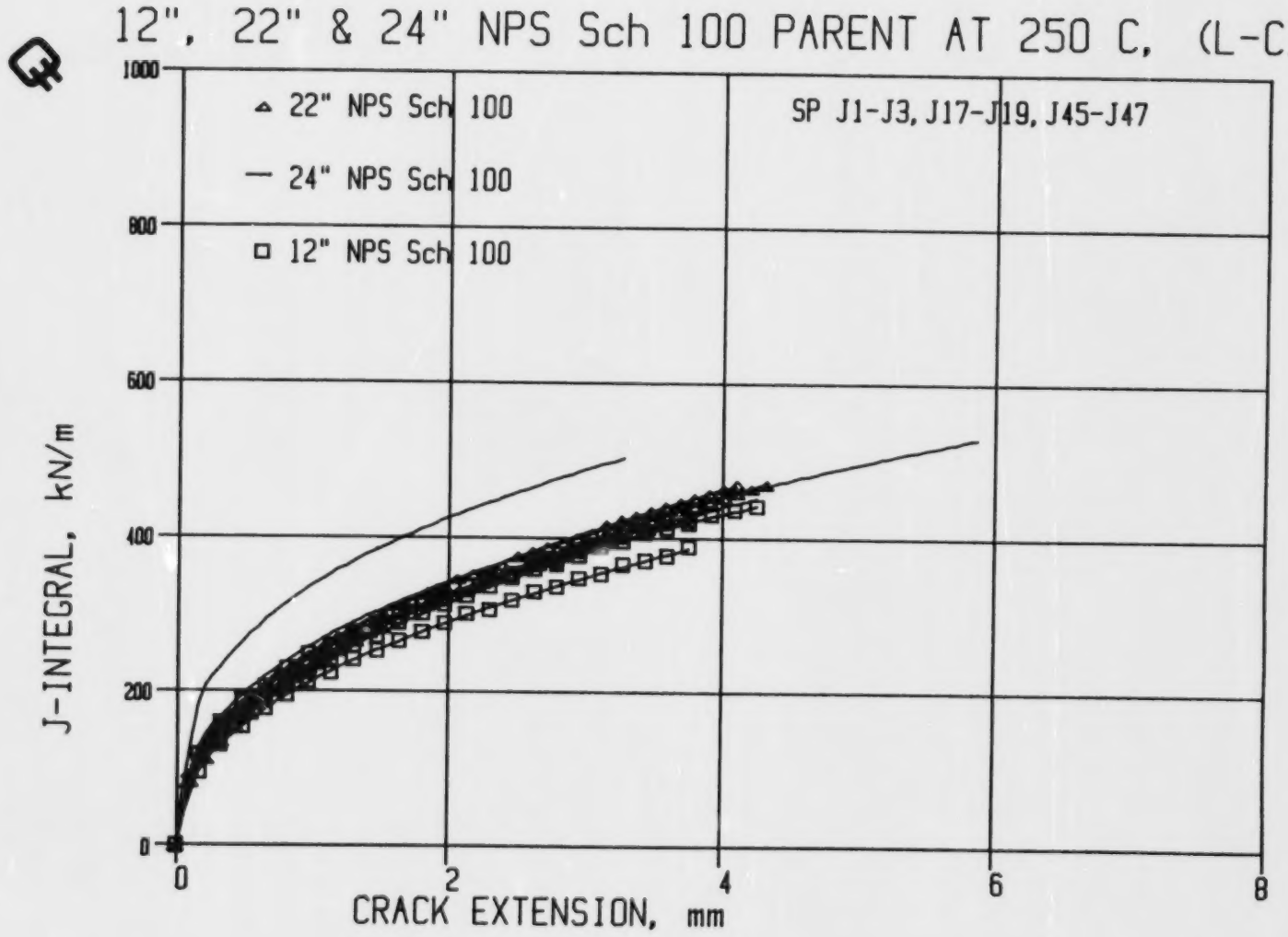

FIGURE 6

J-RESISTANCE CURVES FOR THREE PIPE SIZES

File J 01-47
174365-RD

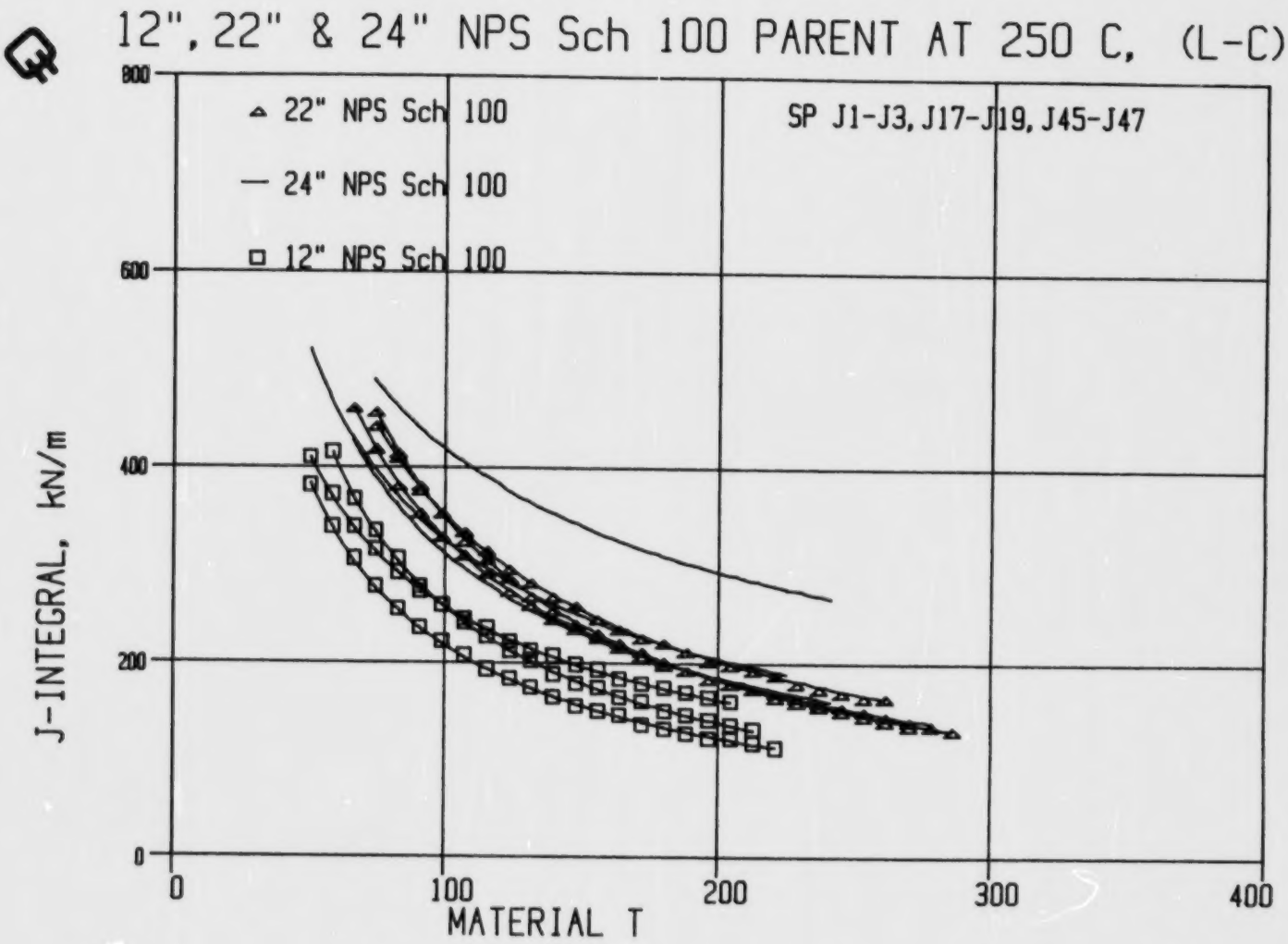

FIGURE 7
J-T CURVES FOR THREE PIPE SIZES

File JT 01-47
174364-RD

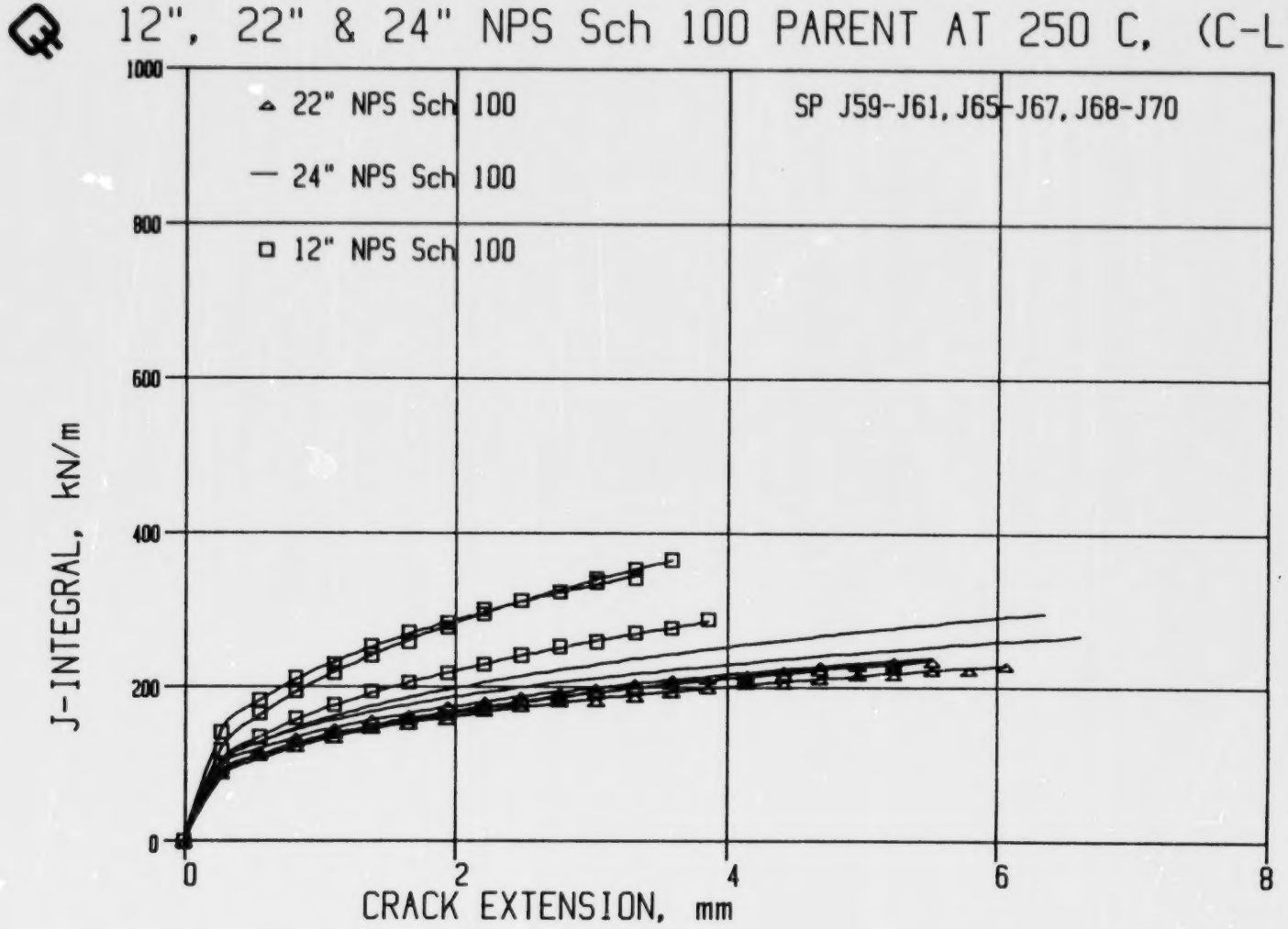

FIGURE 8

J-RESISTANCE CURVES FOR THREE PIPE SIZES

File J 59-70
174363-RD

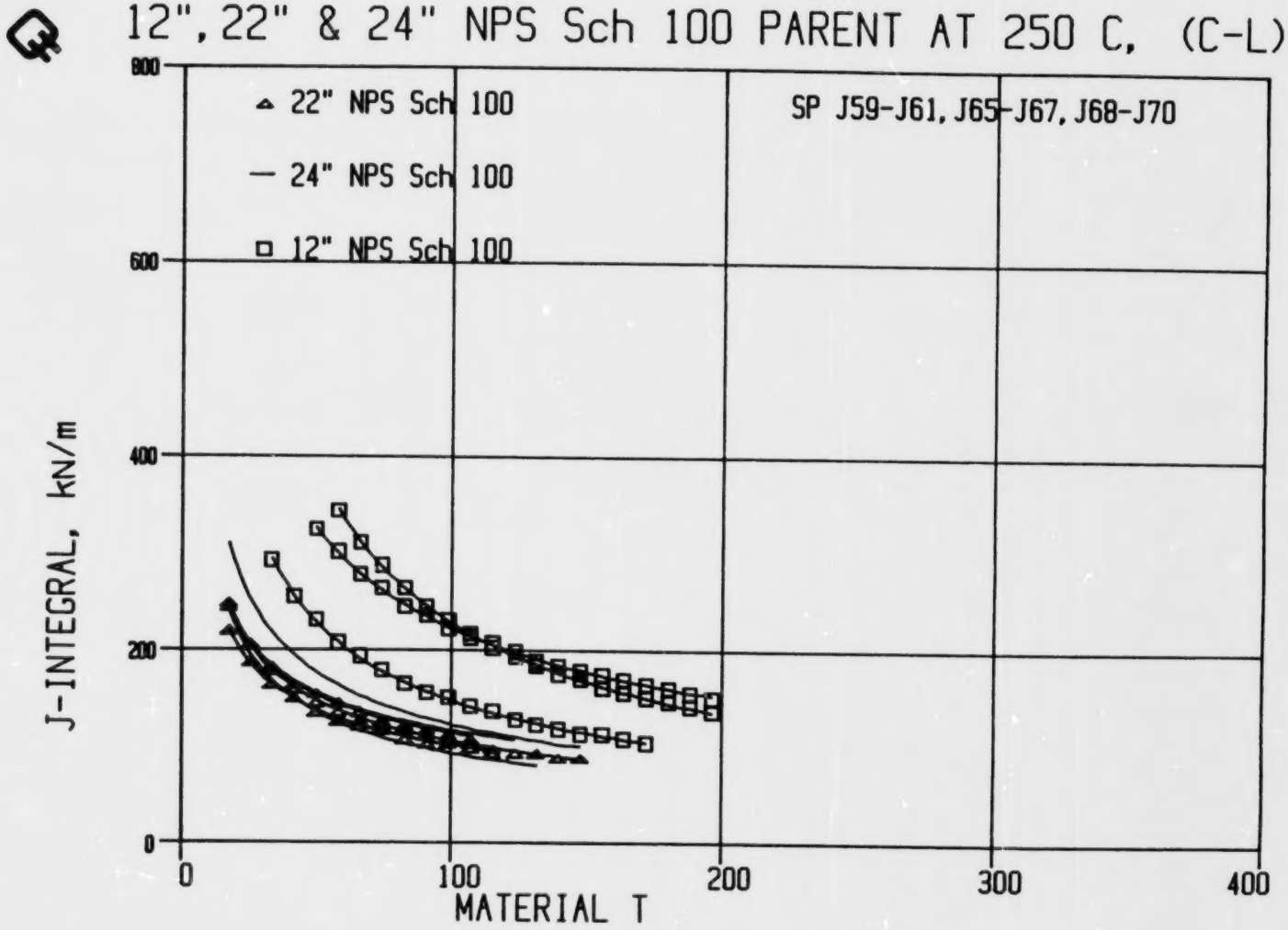

FIGURE 9

J-T CURVES FOR THREE PIPE SIZES

File JT 59-70
174362-RD

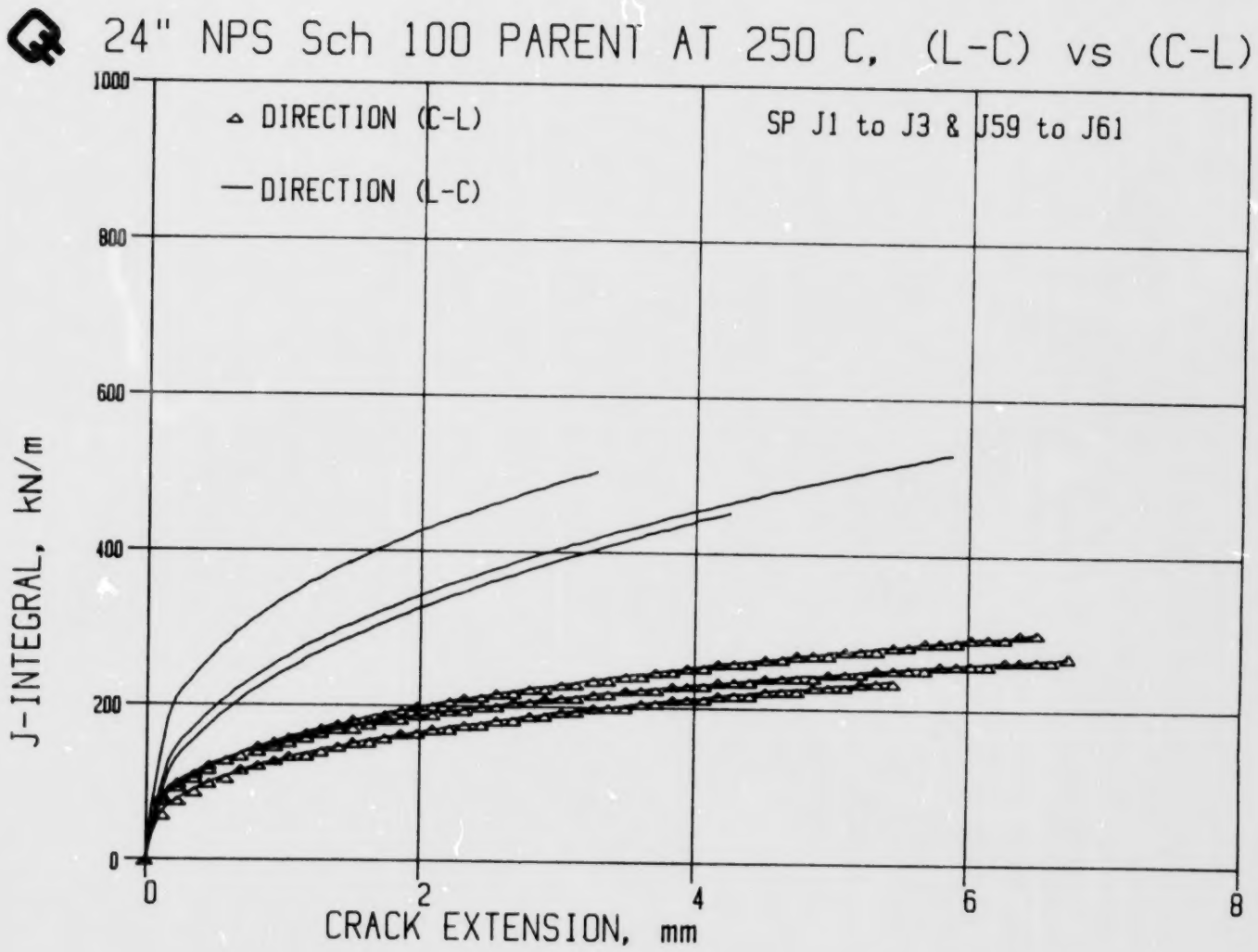

FIGURE 10

EFFECT OF ORIENTATION ON J-RESISTANCE CURVES

File J 01-03
174361-RD

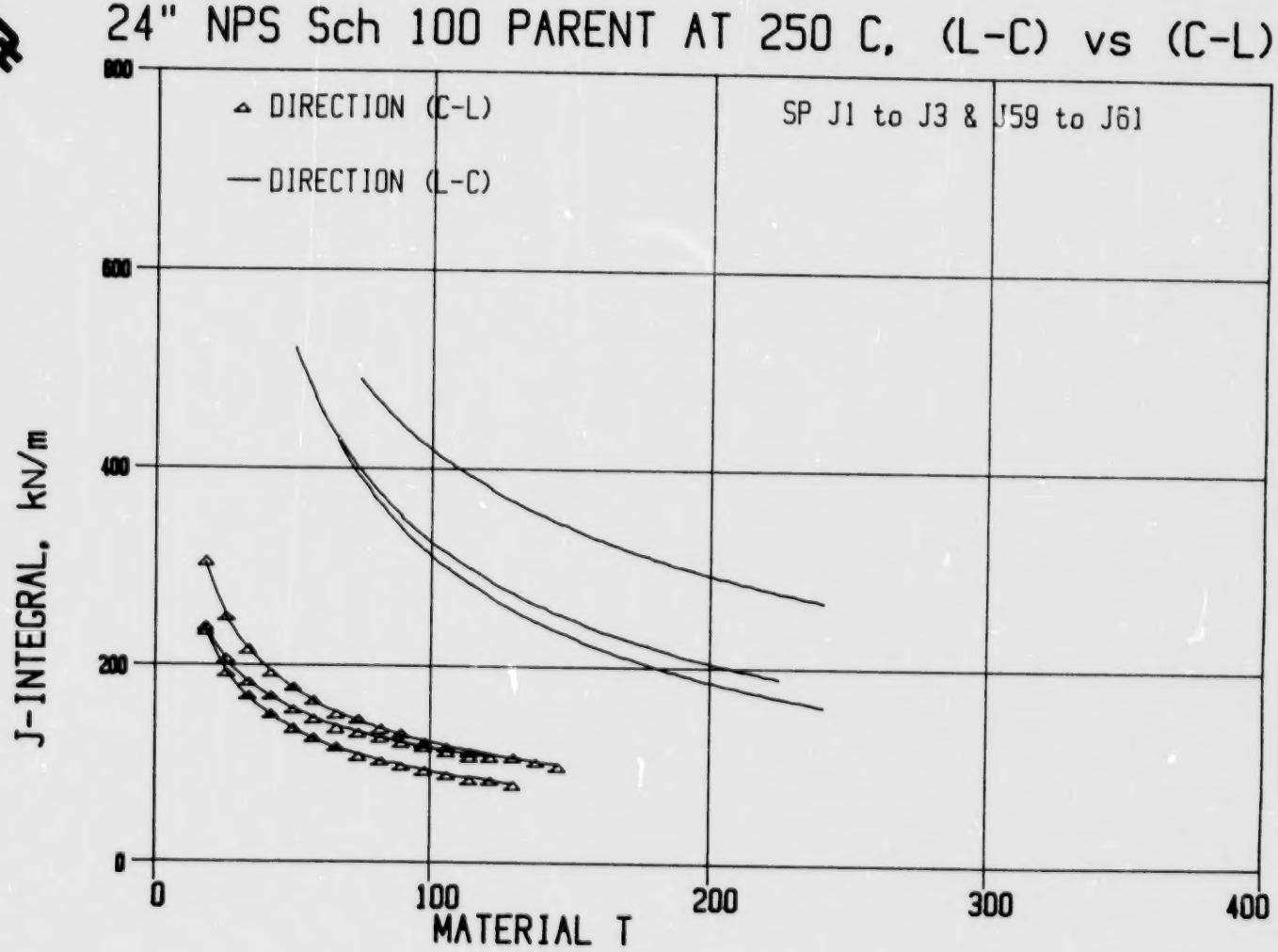

FIGURE 11
EFFECT OF ORIENTATION ON J-T CURVES

File JT 01-03
174360-RD

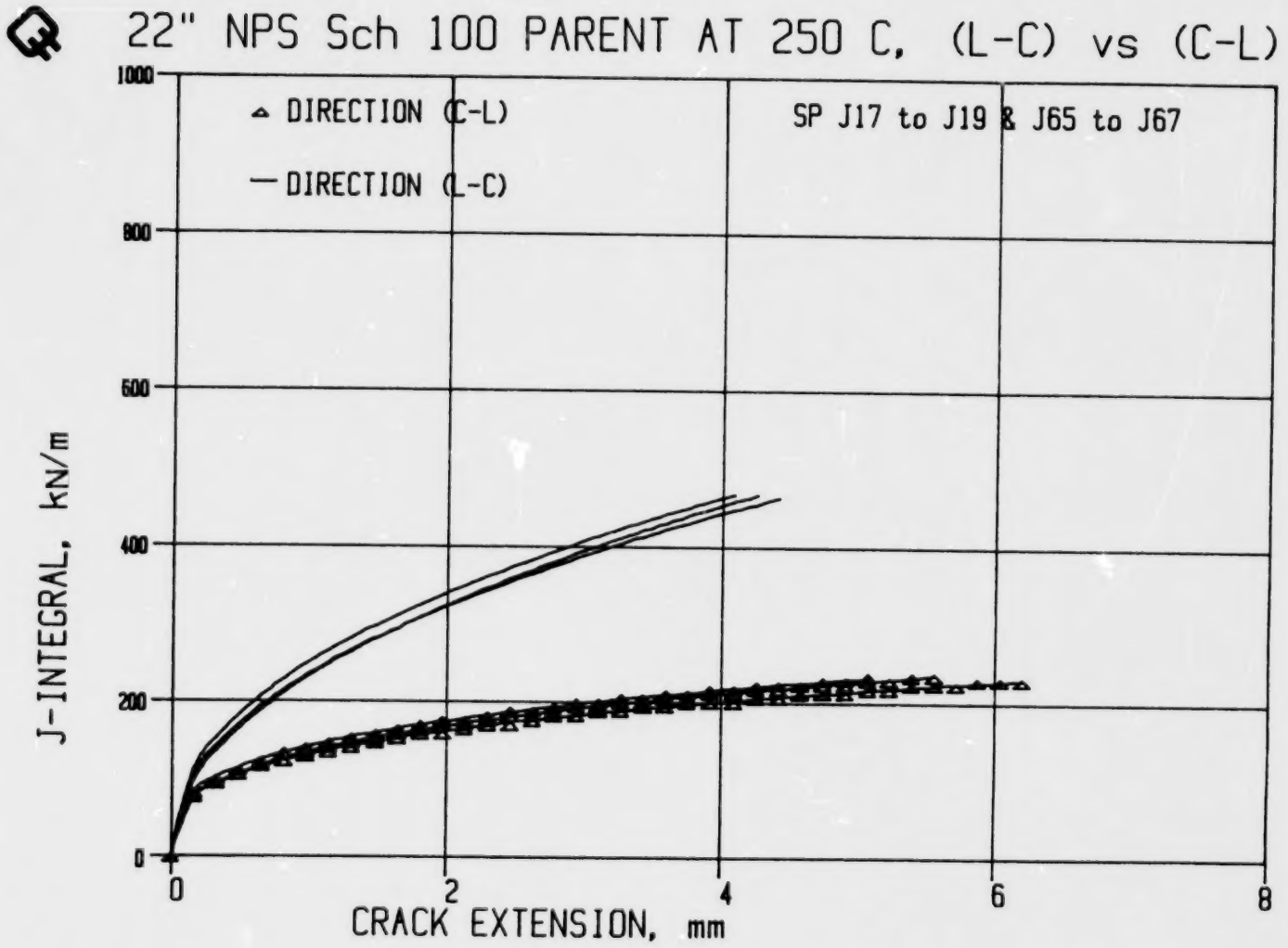

FIGURE 12
EFFECT OF ORIENTATION ON J-RESISTANCE CURVES

File J 65-67
174359-RD

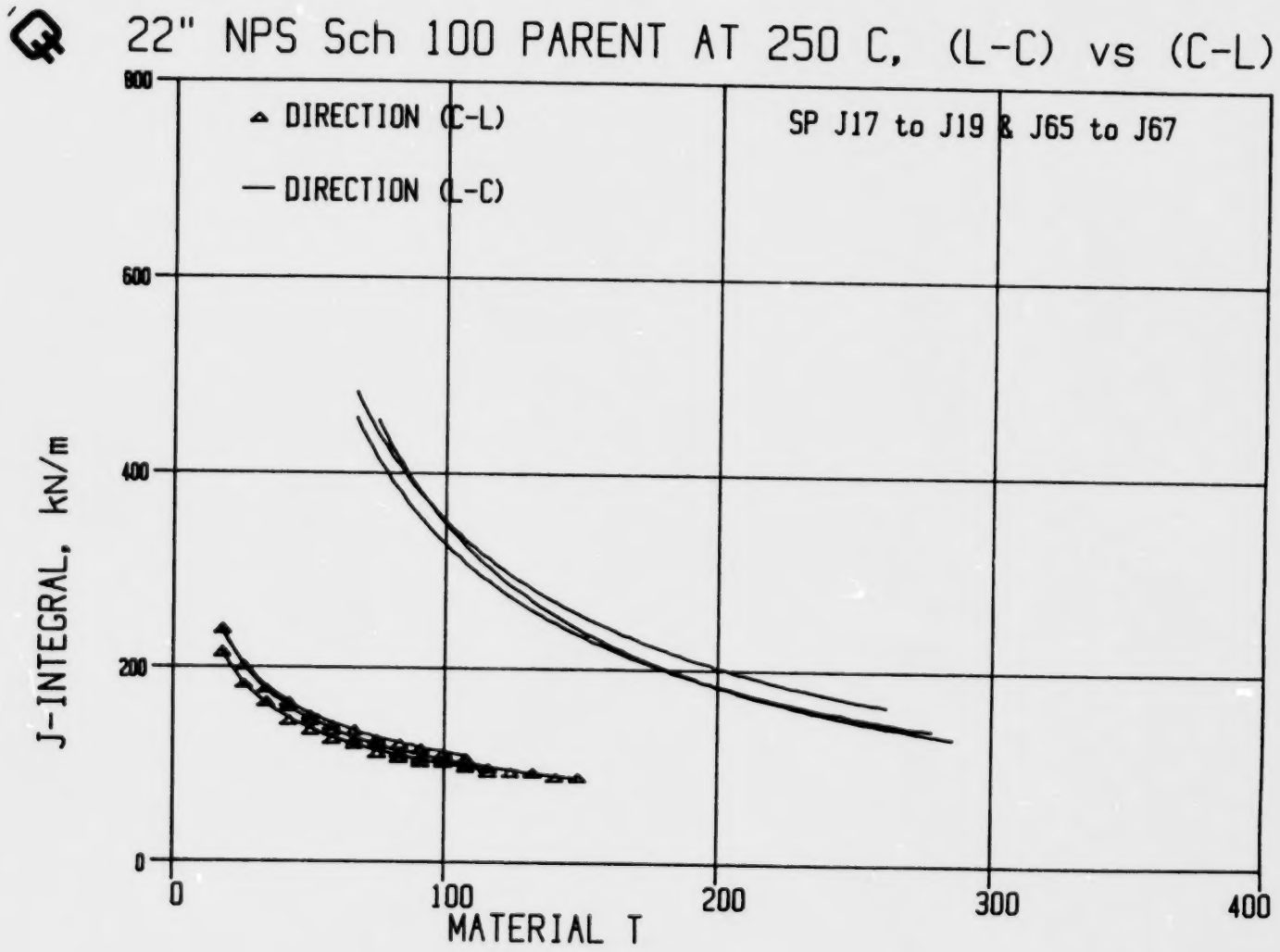

FIGURE 13
EFFECT OF ORIENTATION ON J-T CURVES

File JT 65-67
174358-RD

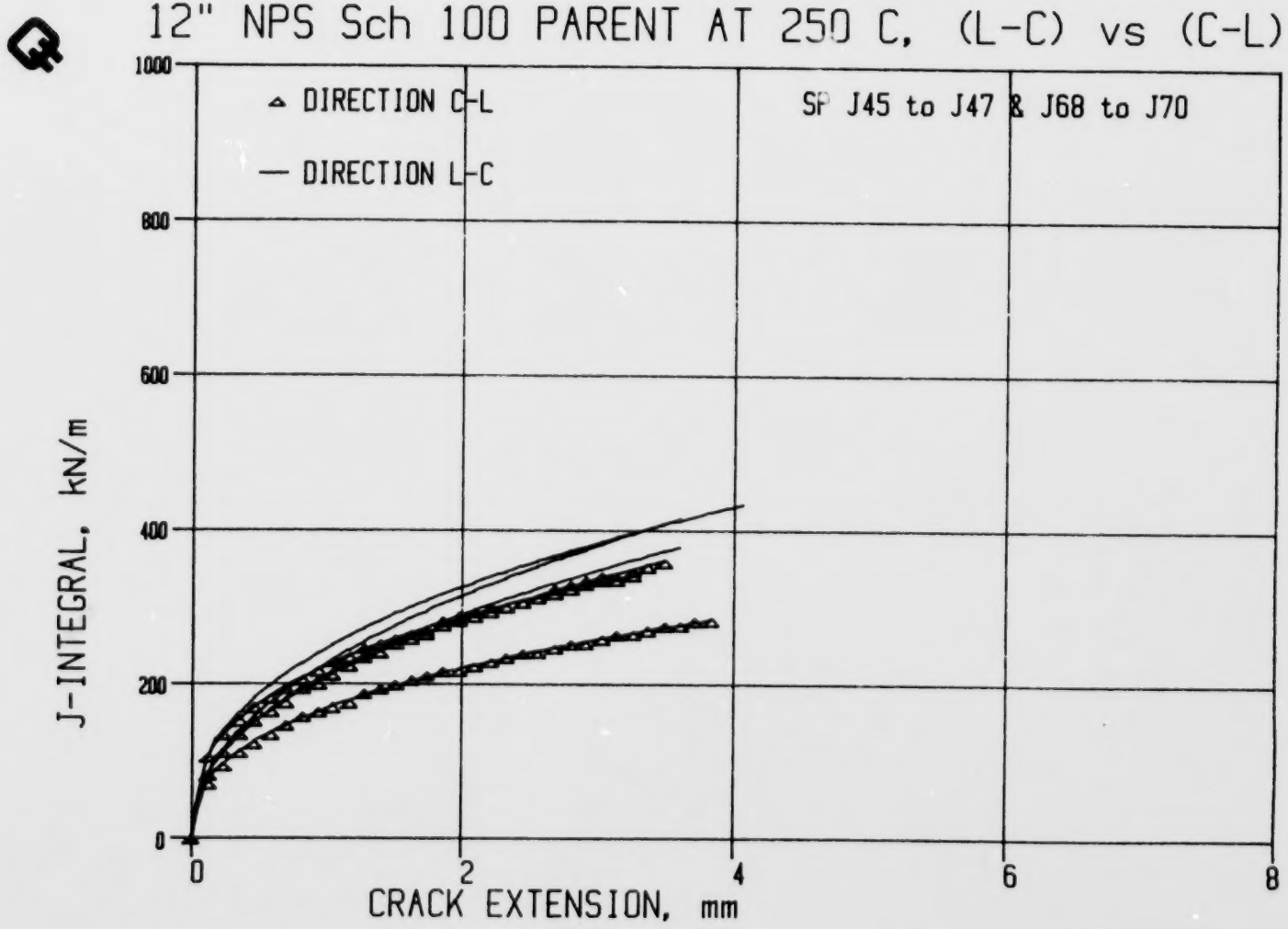

FIGURE 14

EFFECT OF ORIENTATION ON J-RESISTANCE CURVES

File J 45-47
17357-RD

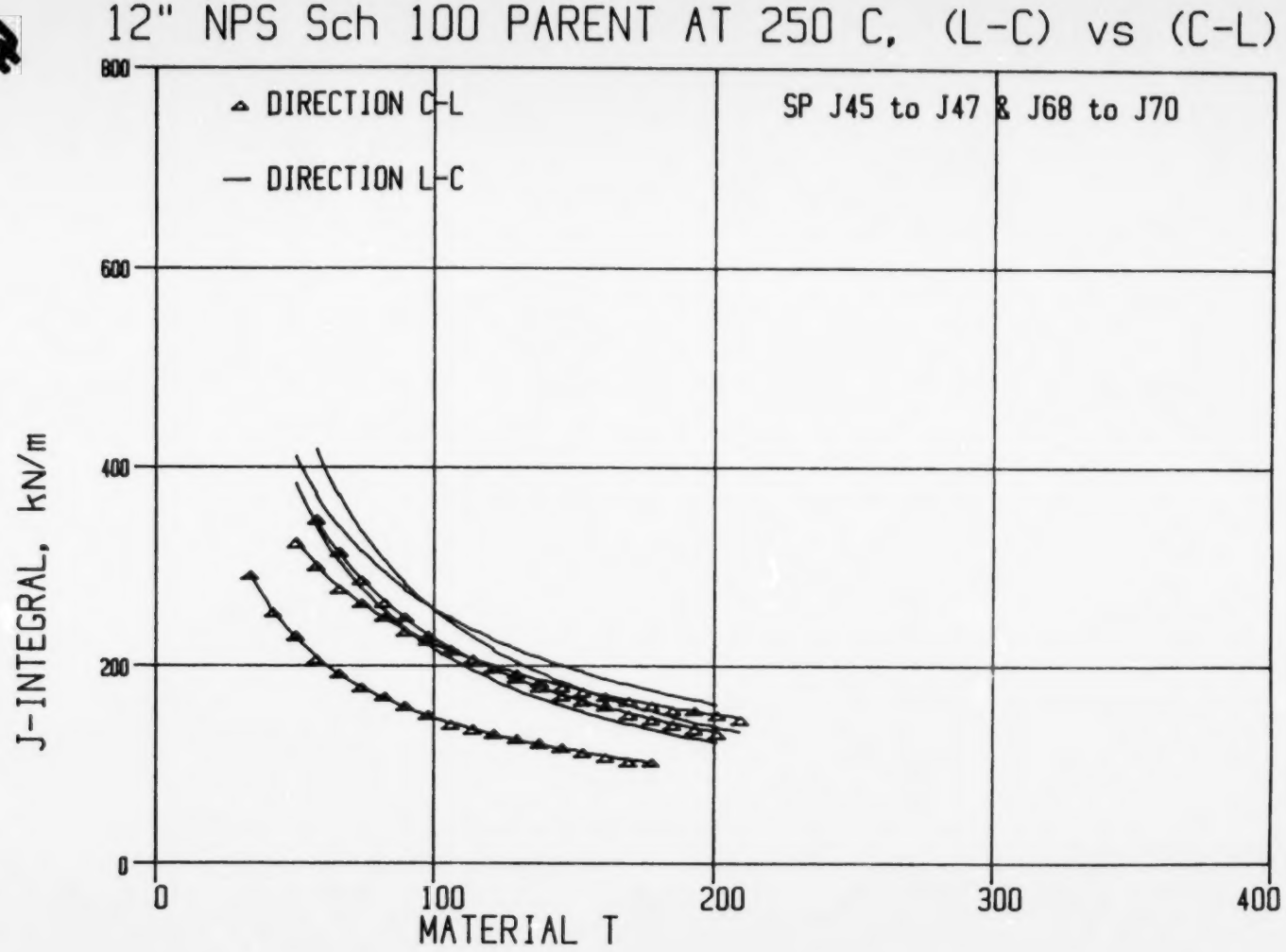

FIGURE 15
EFFECT OF ORIENTATION ON J-T CURVES

File JT 45-47
174356-RD

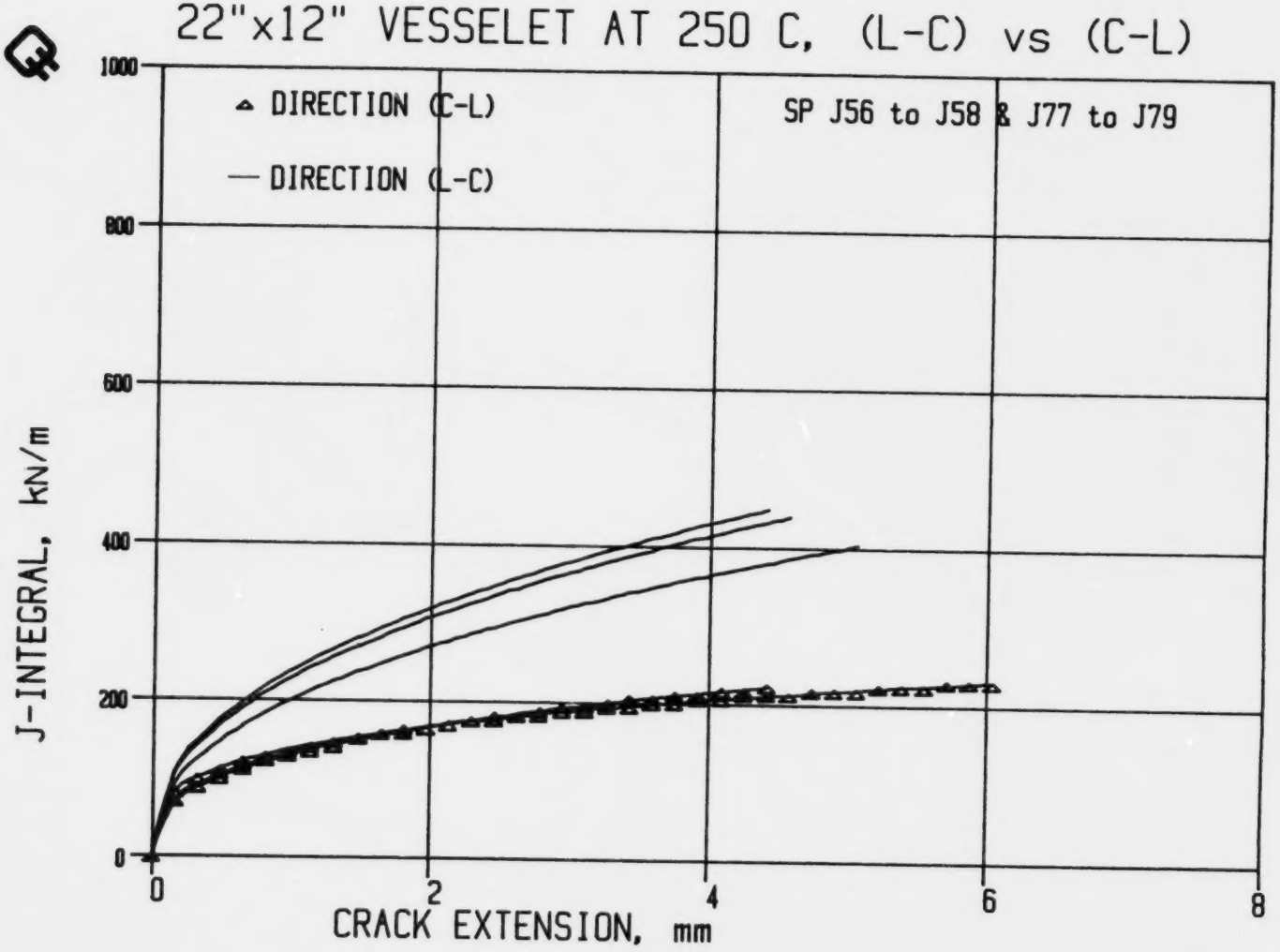

FIGURE 16

EFFECT OF ORIENTATION ON J-RESISTANCE CURVES

File J 56-58
174355-RD

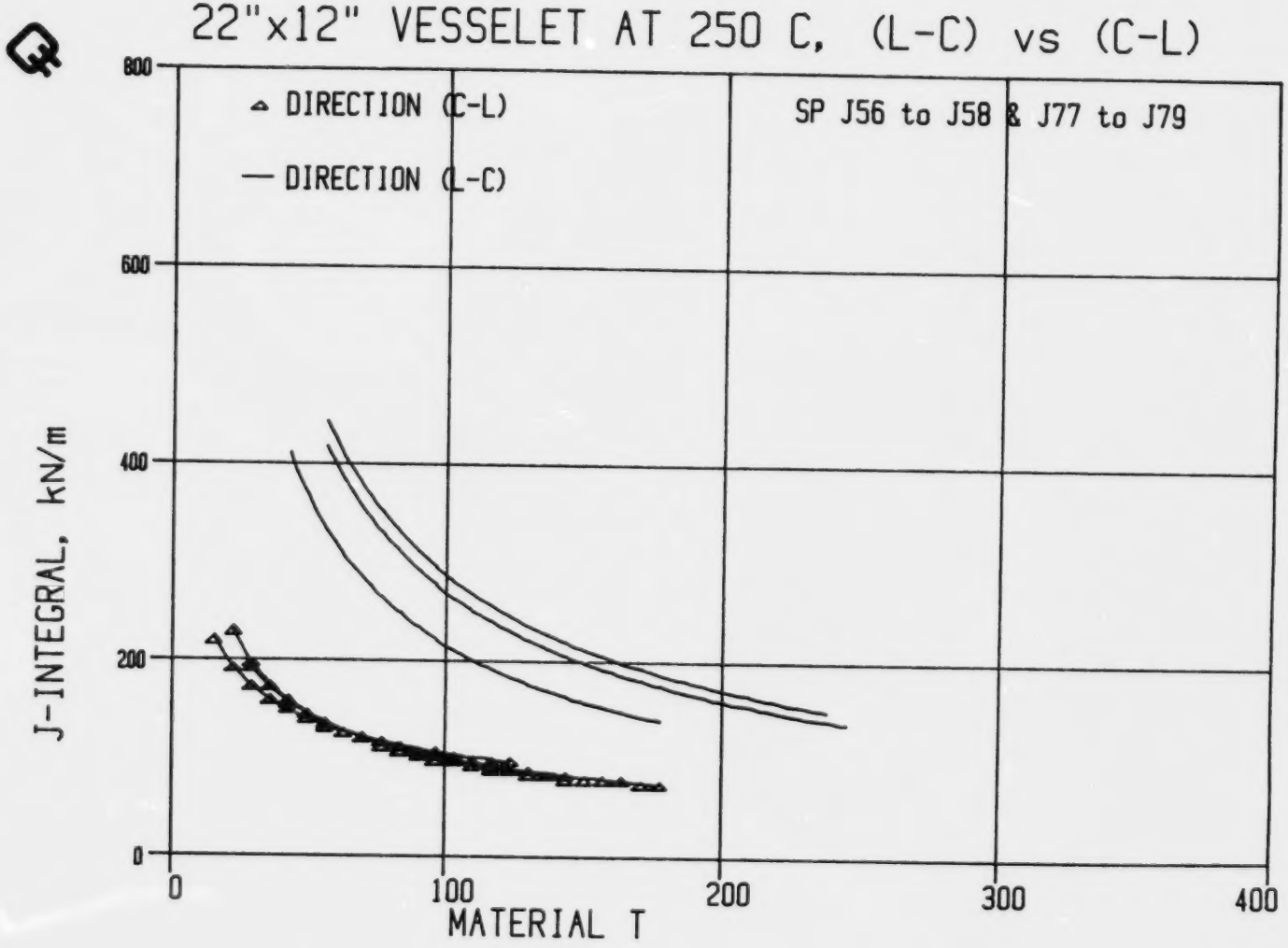

FIGURE 17

EFFECT OF ORIENTATION ON J-T CURVES

File JT 56-58
174354-RD

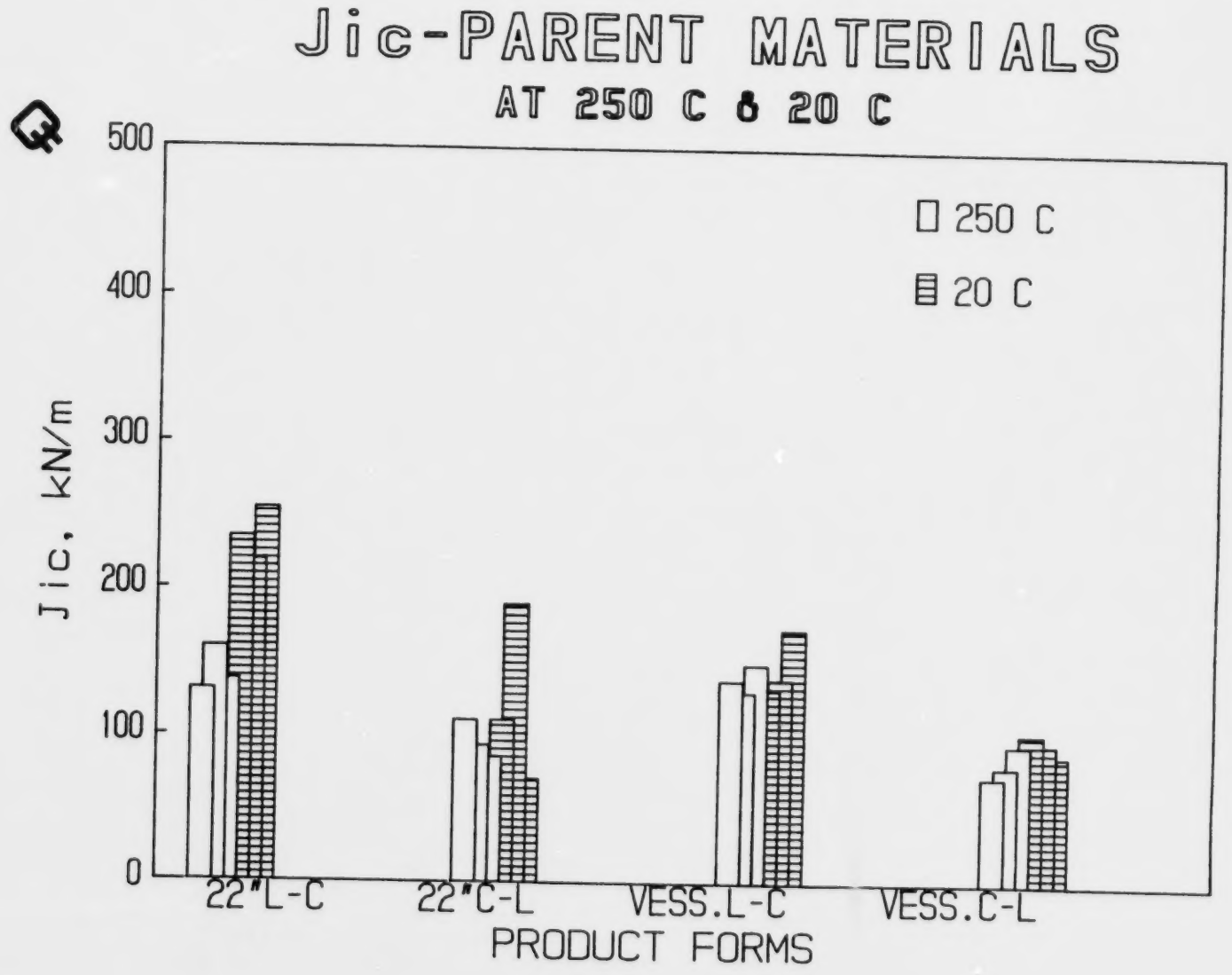

FIGURE 18

VARIATION OF J_{IC} WITH TEMPERATURE FOR TWO PRODUCT FORMS

File JC PARENT ENG
174310-RD

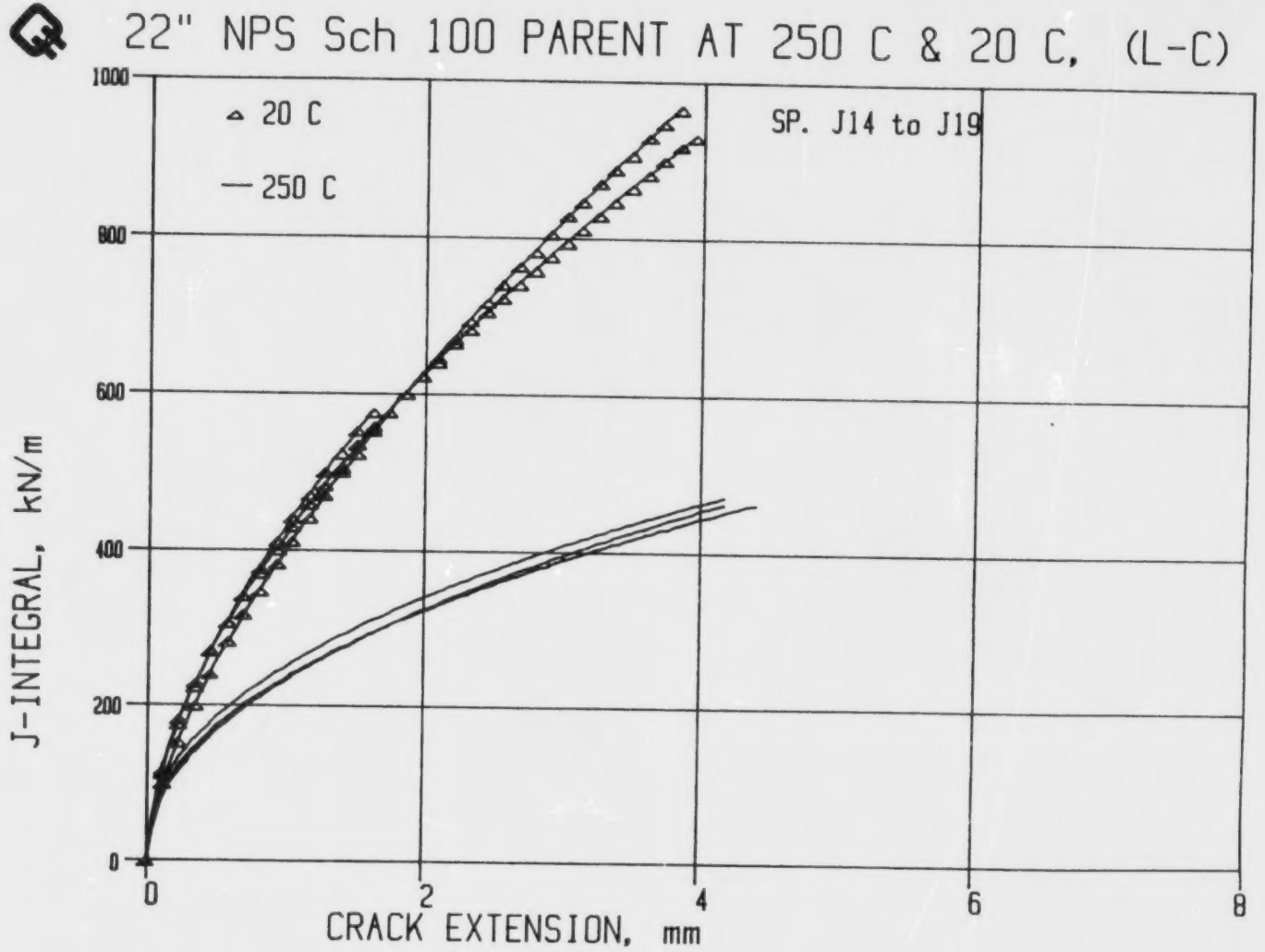

FIGURE 19

EFFECT OF TEST TEMPERATURE ON J-RESISTANCE CURVES

File J 14-19
174353-RD

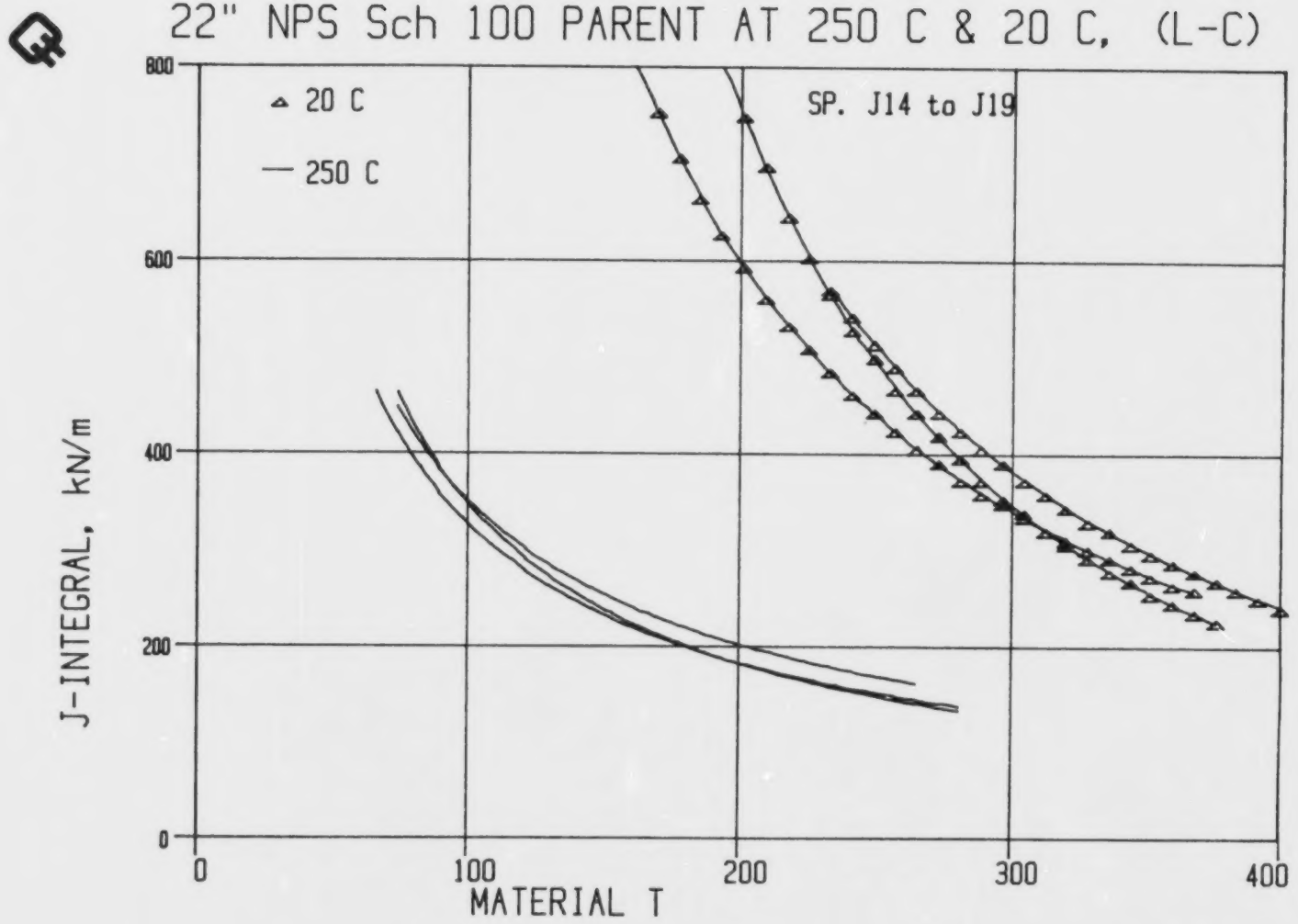

FIGURE 20

EFFECT OF TEST TEMPERATURE ON J-T CURVES

File JT 14-19
174352-RD

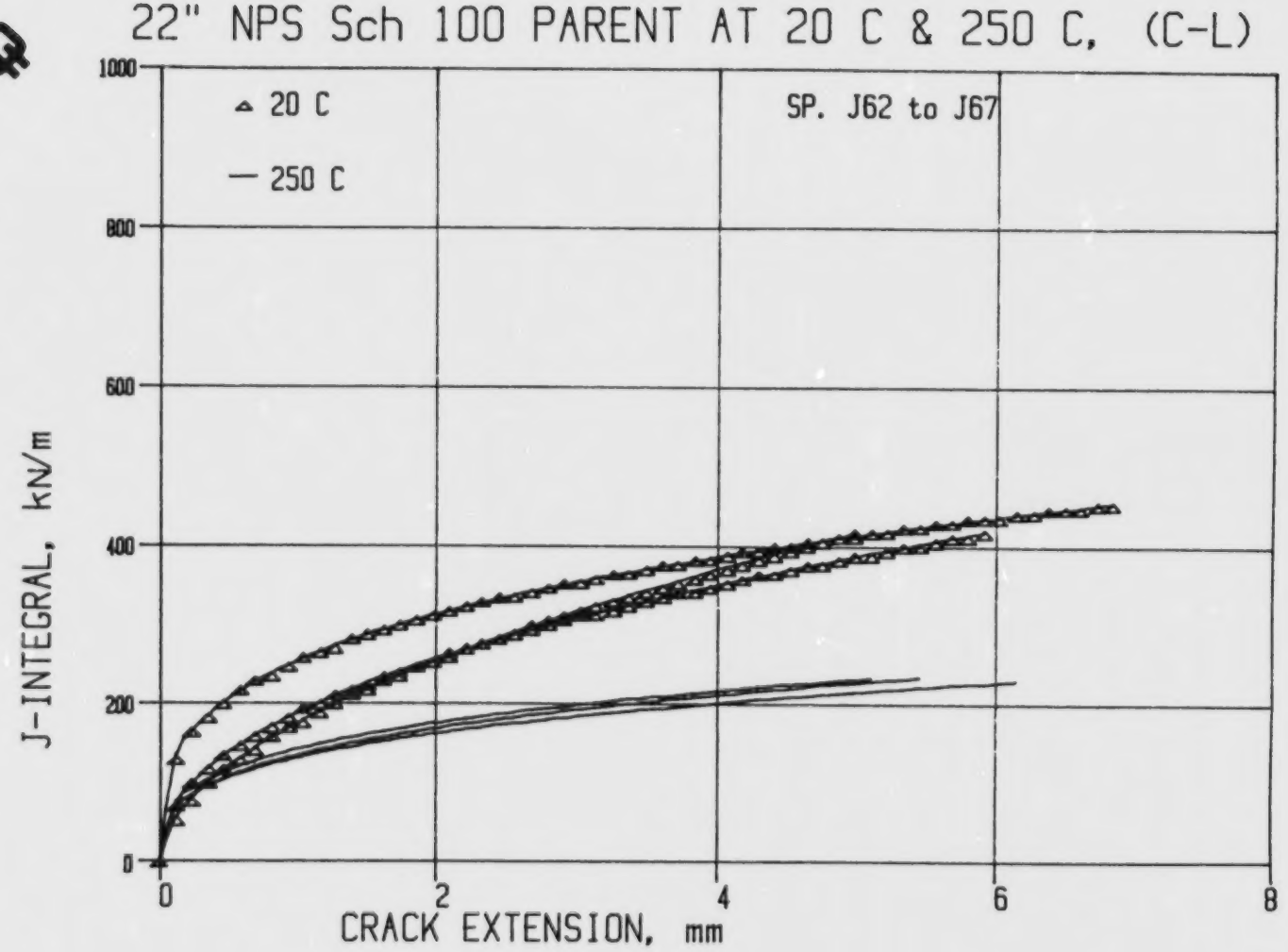

FIGURE 21
EFFECT OF TEST TEMPERATURE ON J-RESISTANCE CURVES

File J 62-67
174351-RD

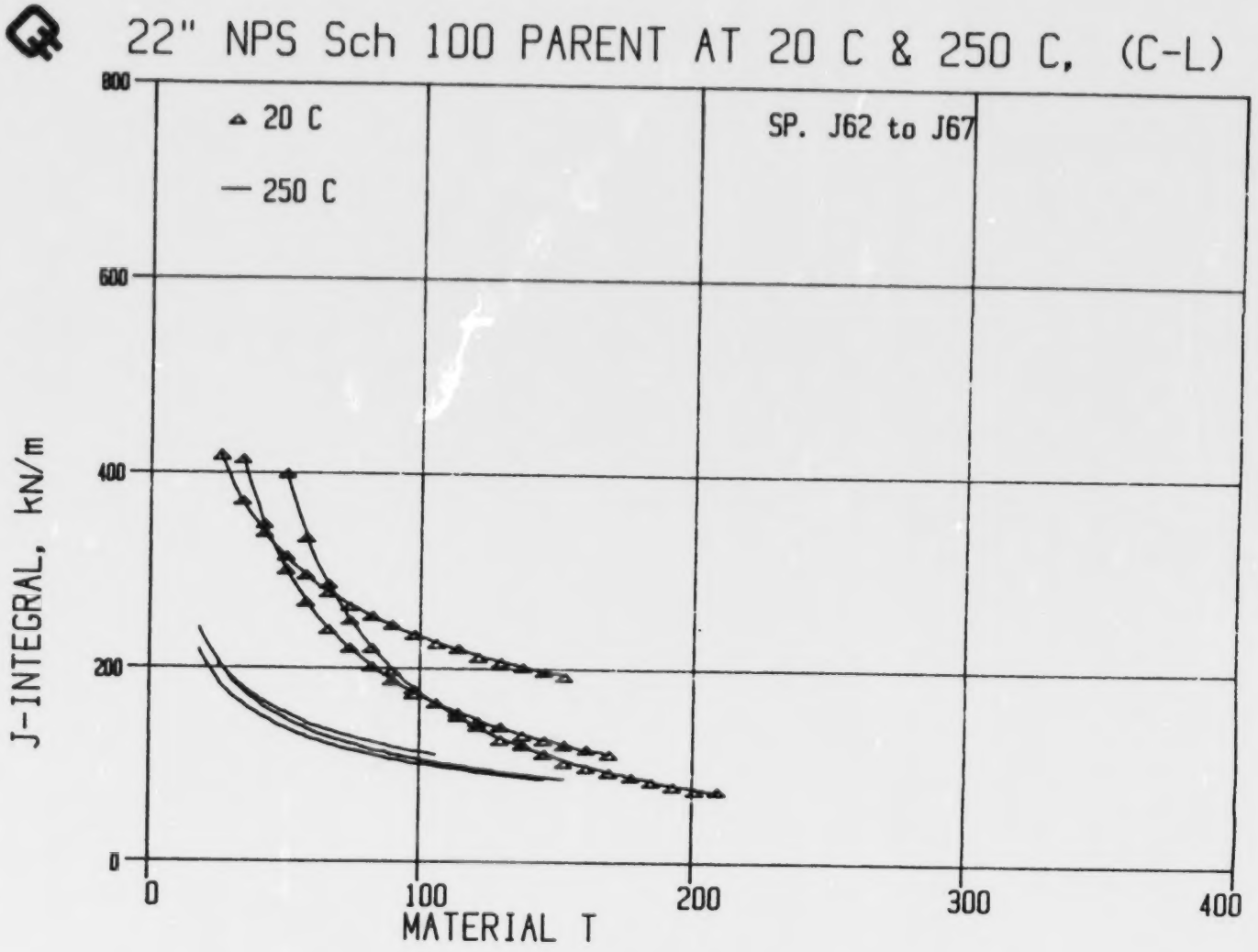

FIGURE 22

EFFECT OF TEST TEMPERATURE ON J-T CURVES

File JT 62-67
174350-RD

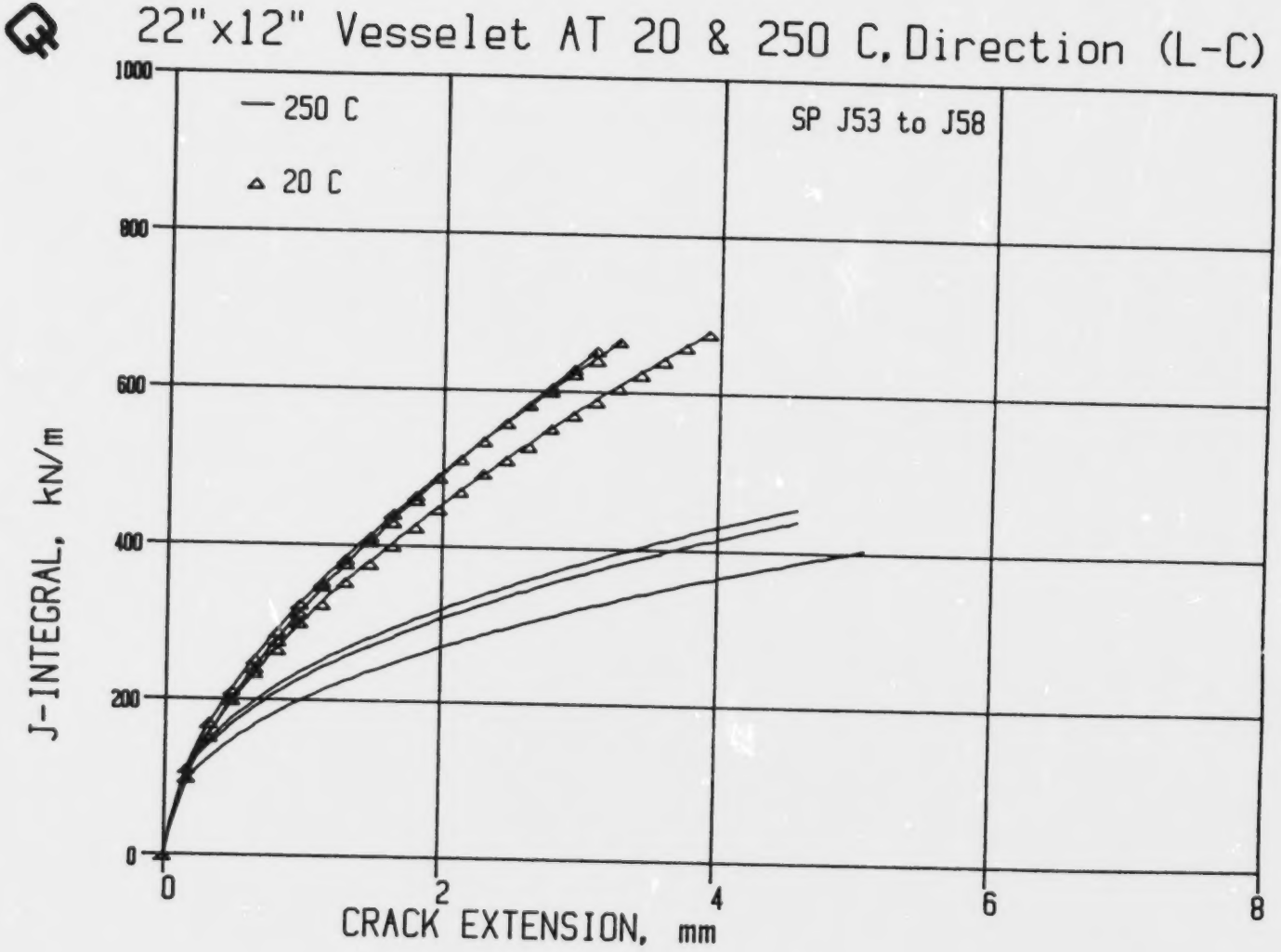

FIGURE 23
EFFECT OF TEST TEMPERATURE ON J-RESISTANCE CURVES

File J 53-58
174349-RD

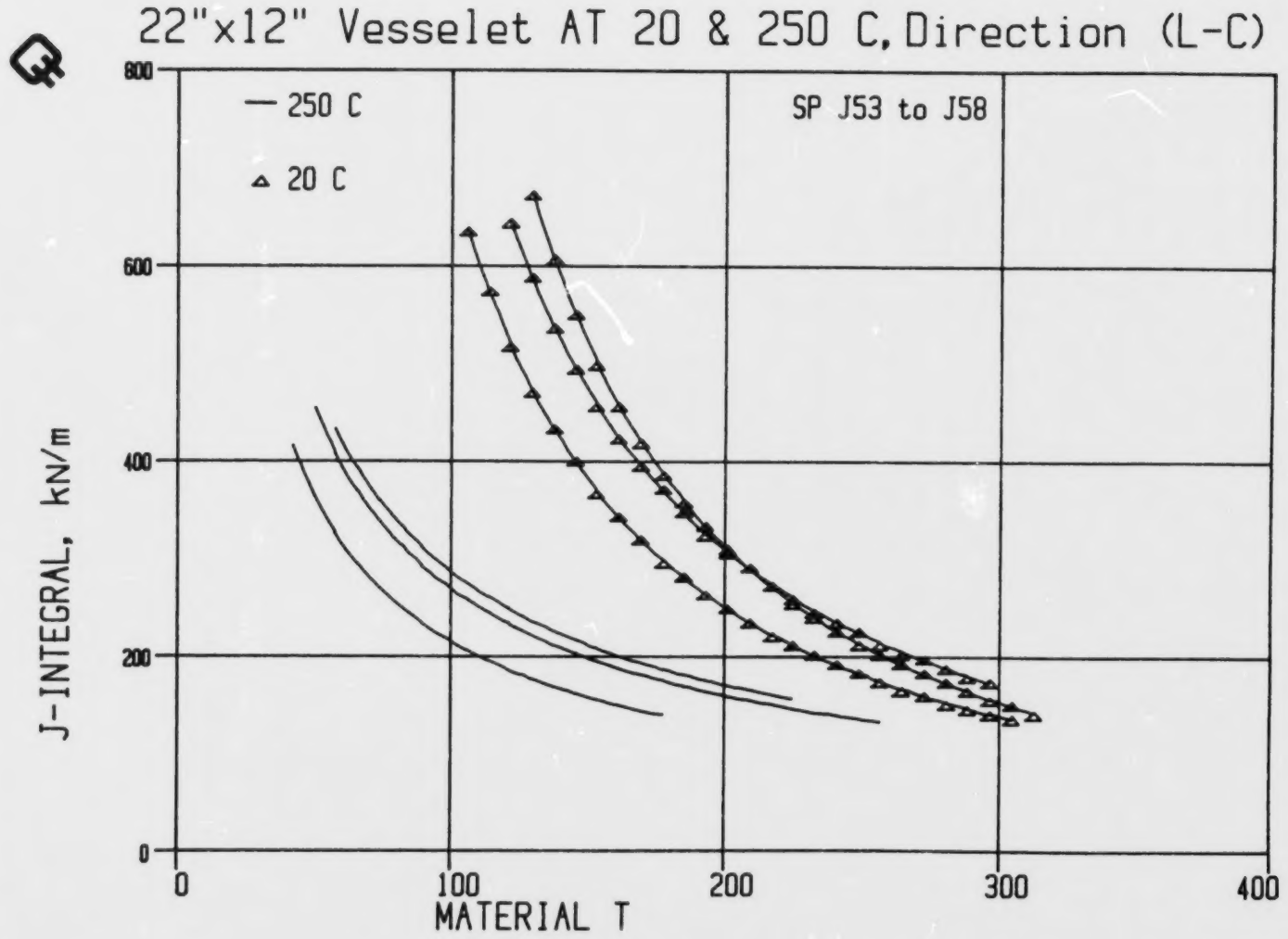

FIGURE 24

EFFECT OF TEST TEMPERATURE ON J-T CURVES

File JT 53-58
174348-RD

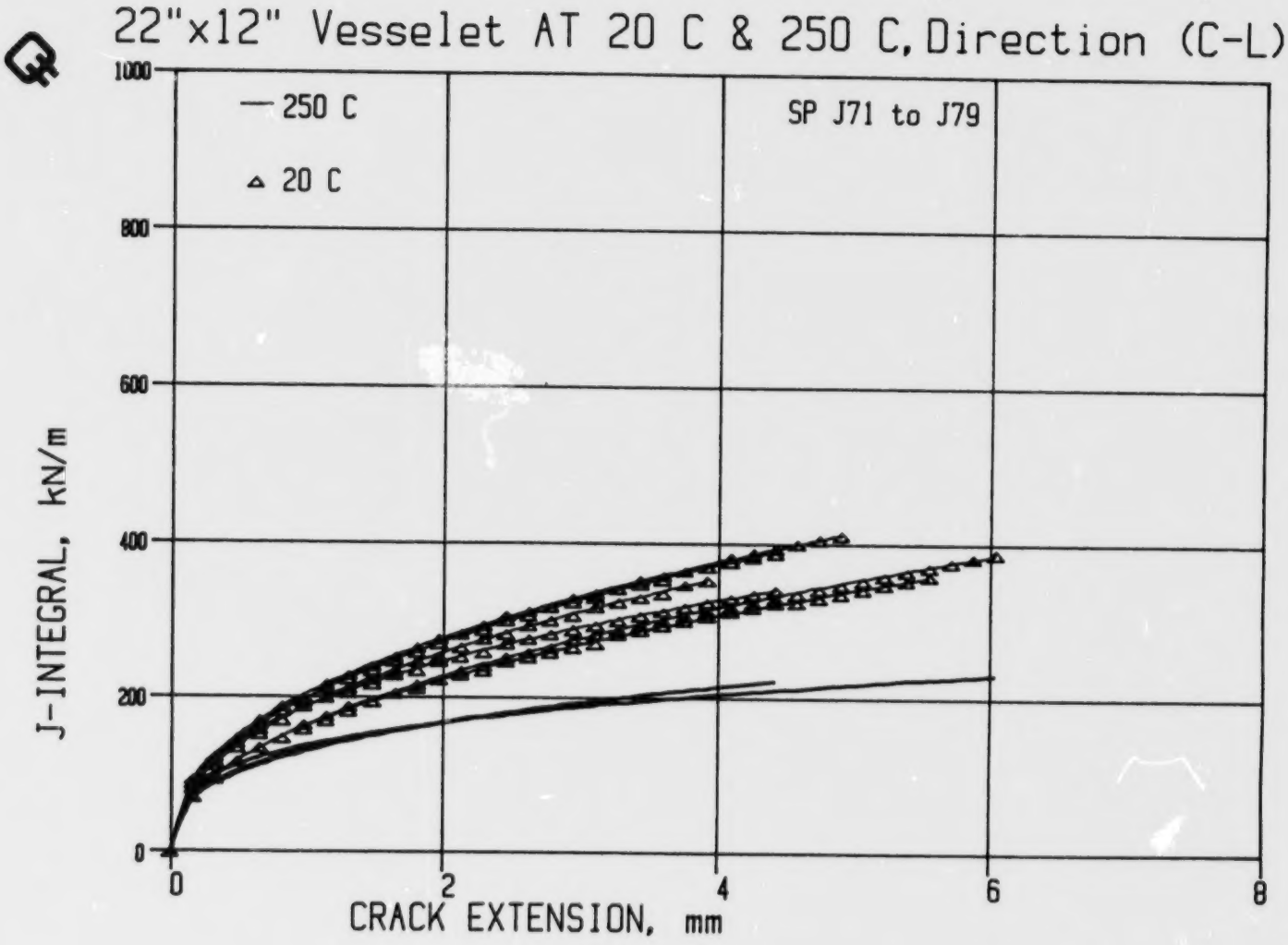

FIGURE 25
EFFECT OF TEST TEMPERATURE ON J-RESISTANCE CURVES

File J 71-79
174347-RD

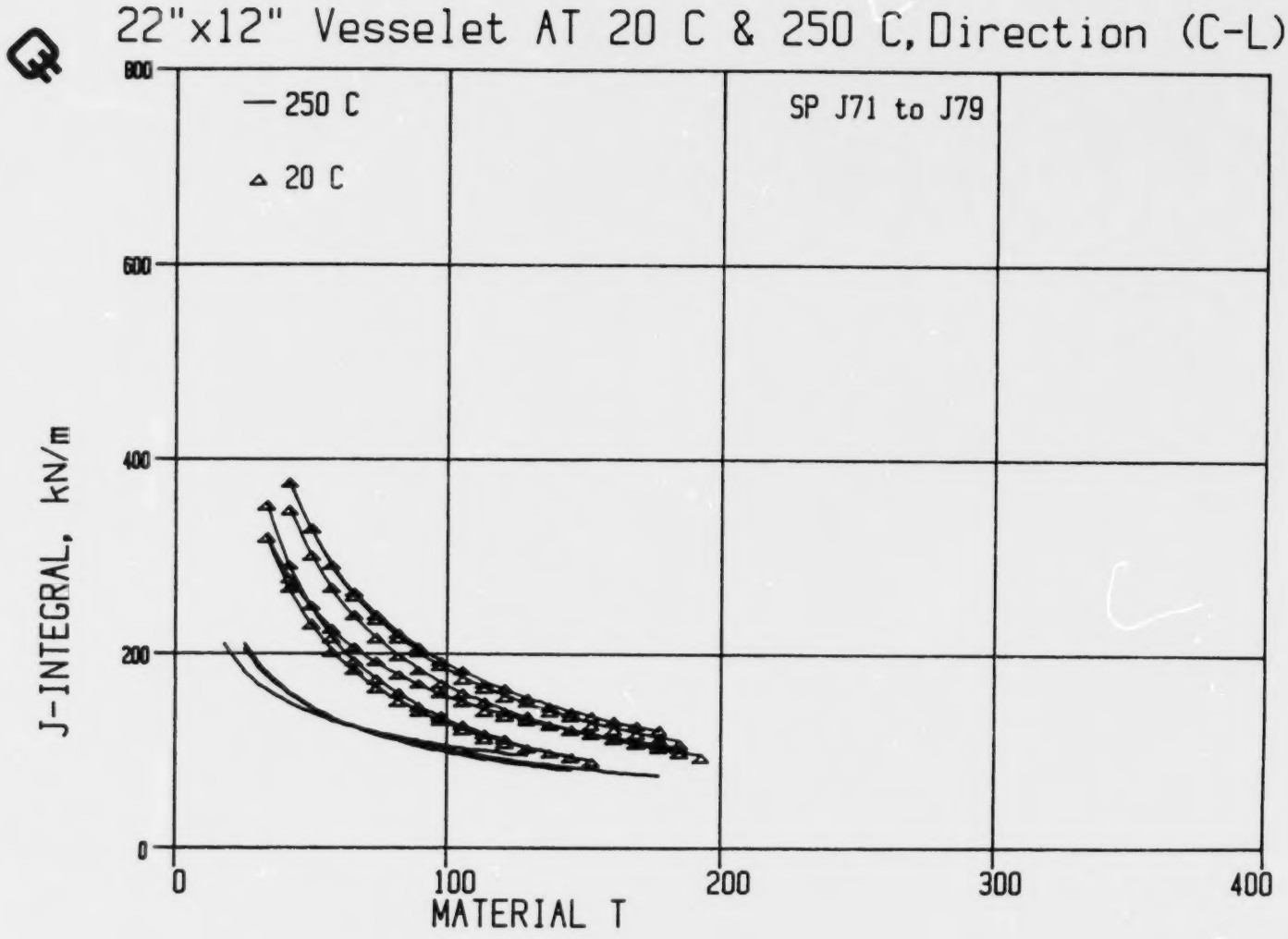

FIGURE 26
EFFECT OF TEST TEMPERATURE ON J-T CURVES

File JT 71-79
174346-RD

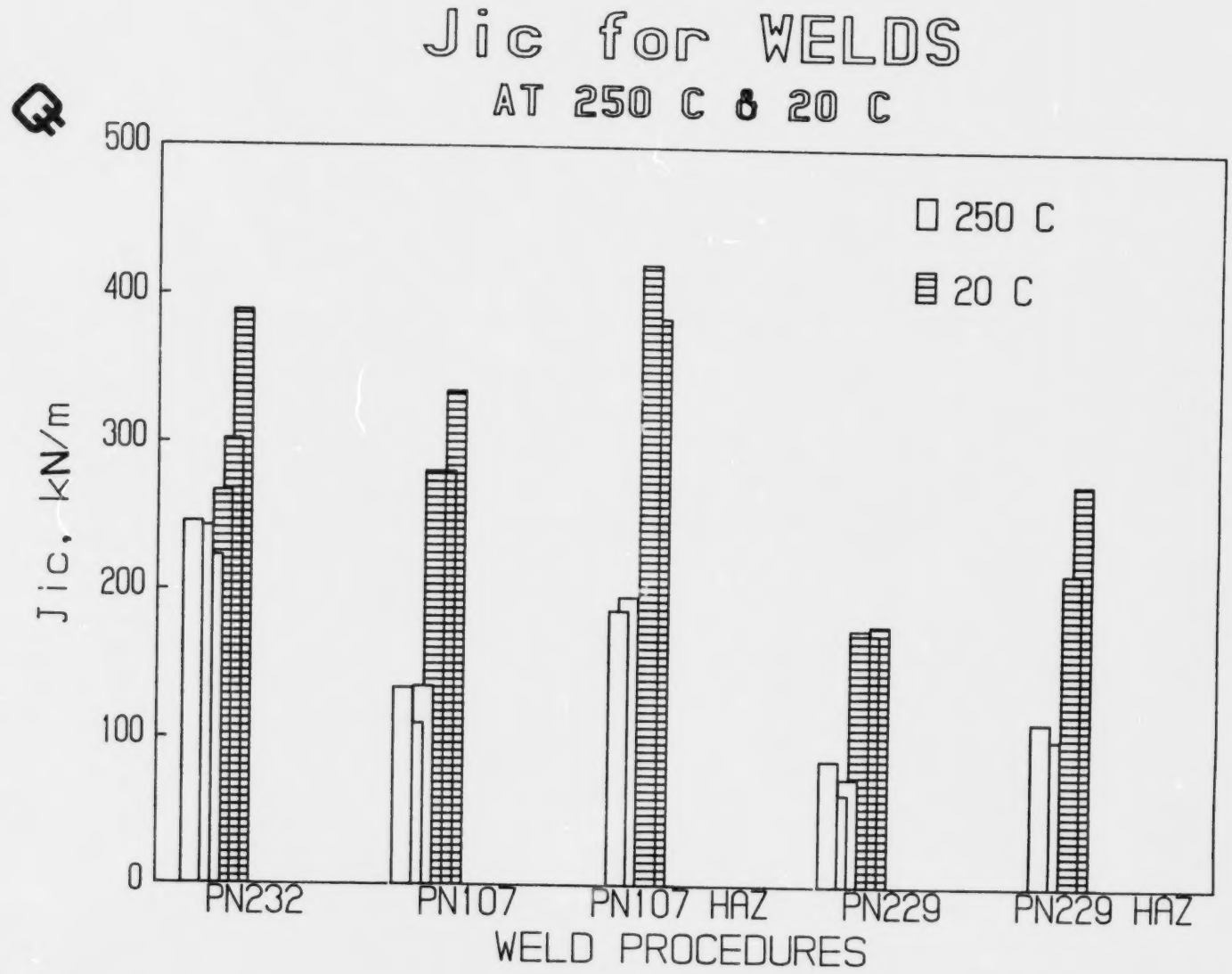

FIGURE 27

VARIATION OF J_{IC} WITH TEMPERATURE FOR THREE WELD PROCEDURES

File JC WELD
174309-RD

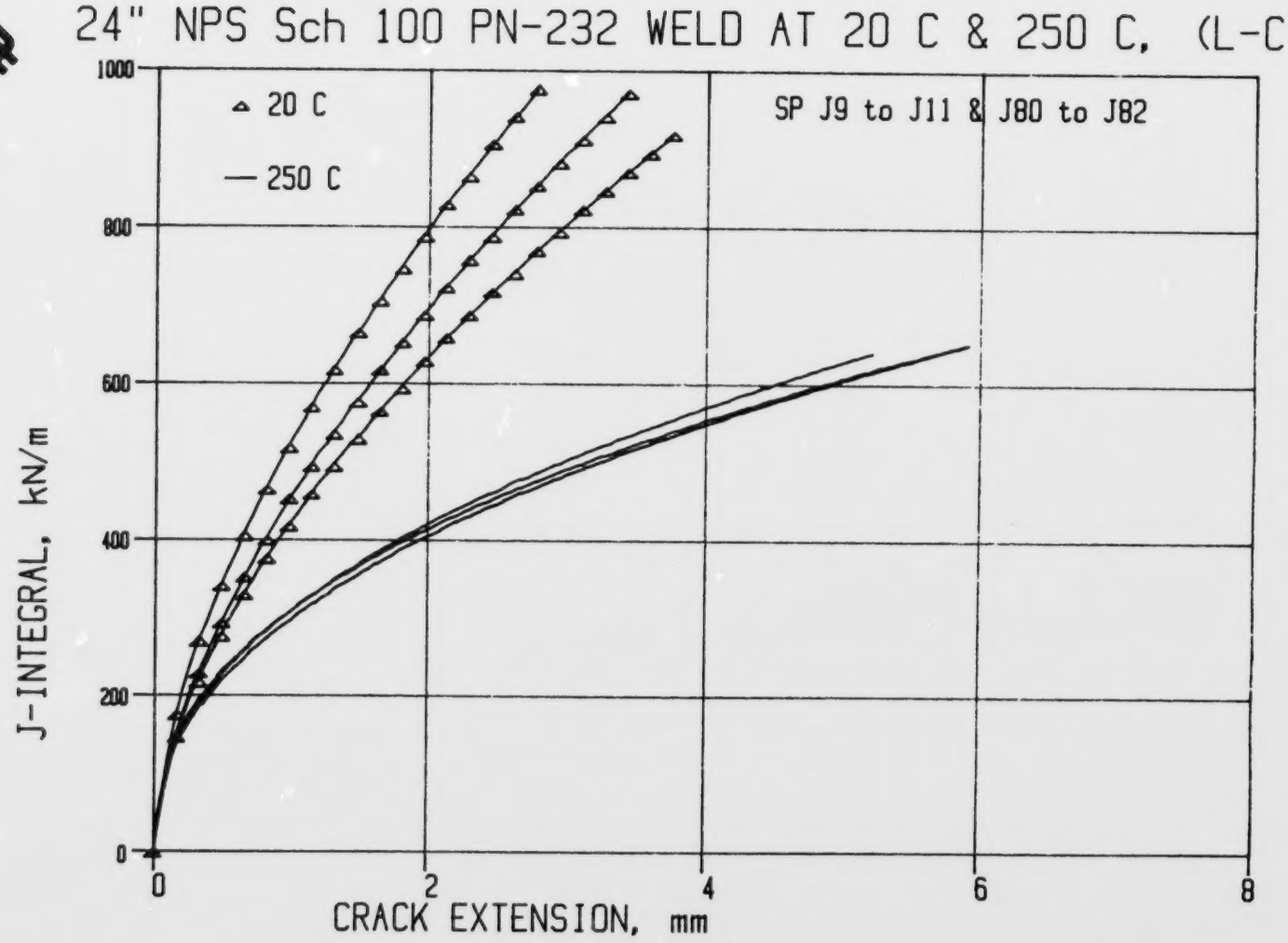

FIGURE 28
EFFECT OF TEST TEMPERATURE ON J-RESISTANCE CURVES

File J 80-82
174345-RD

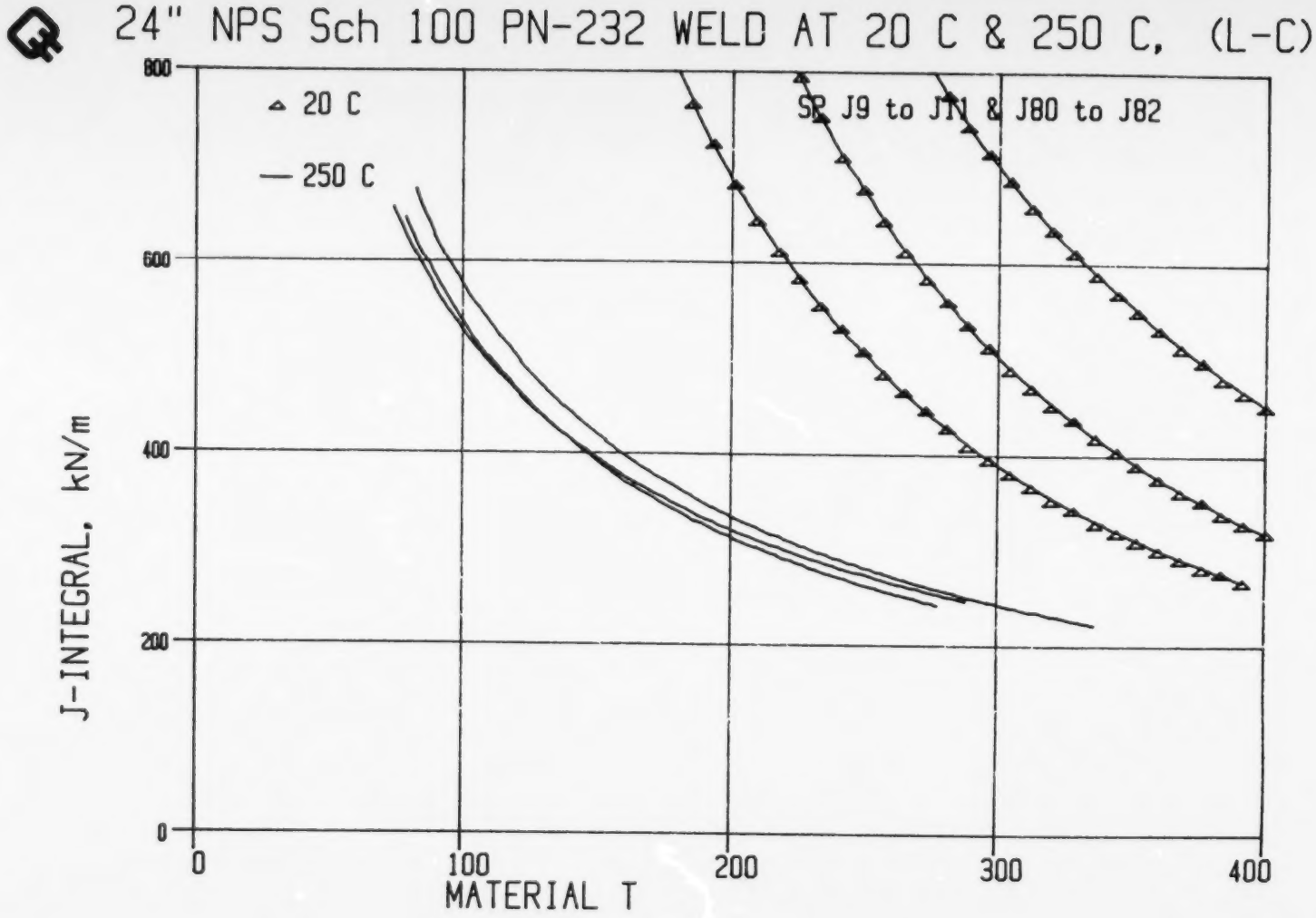

FIGURE 29

EFFECT OF TEST TEMPERATURE ON J-T CURVES

File JT 80-82
174344-RD

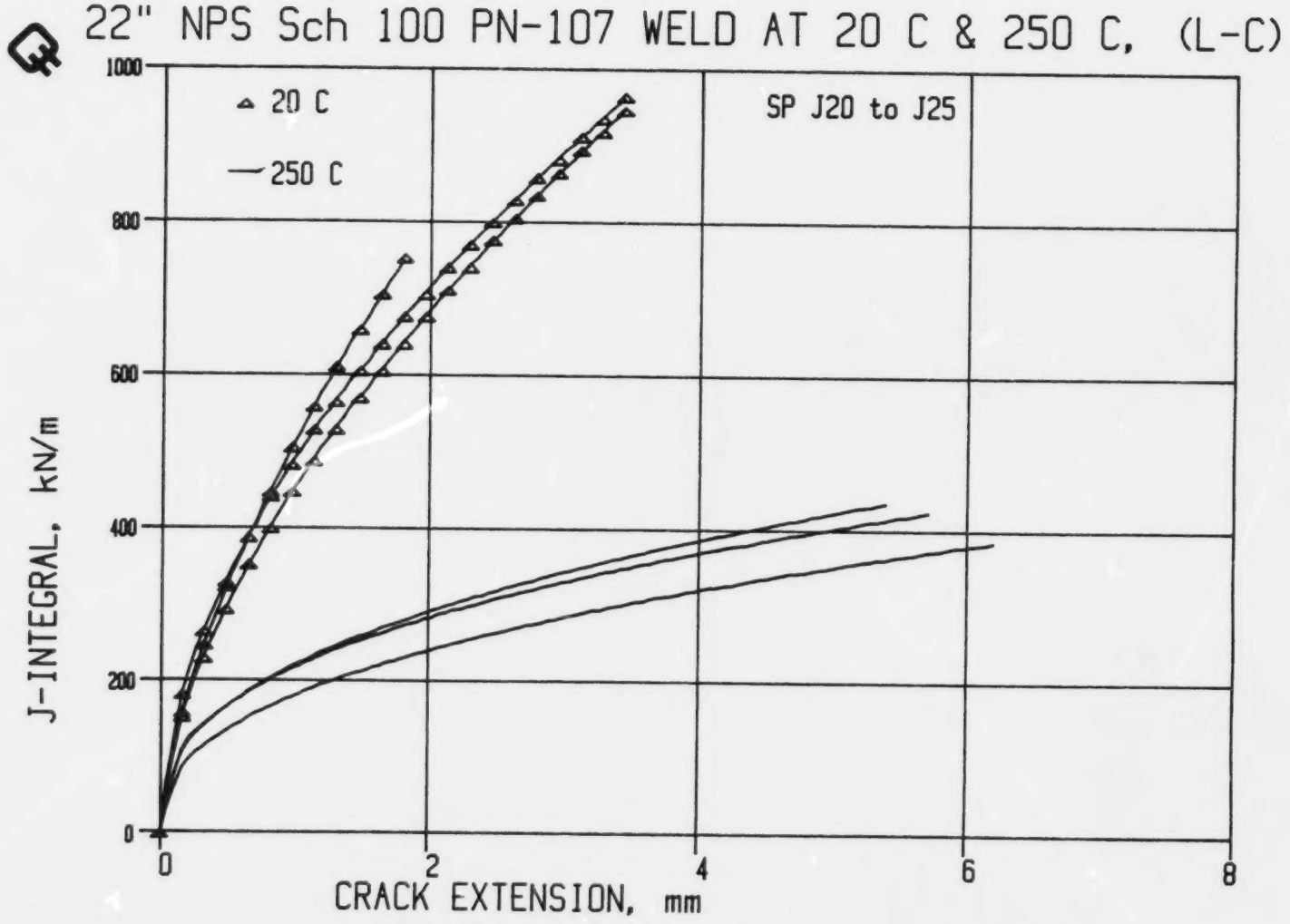

FIGURE 30

EFFECT OF TEST TEMPERATURE ON J-RESISTANCE CURVES

File J 20-25
174343-RD

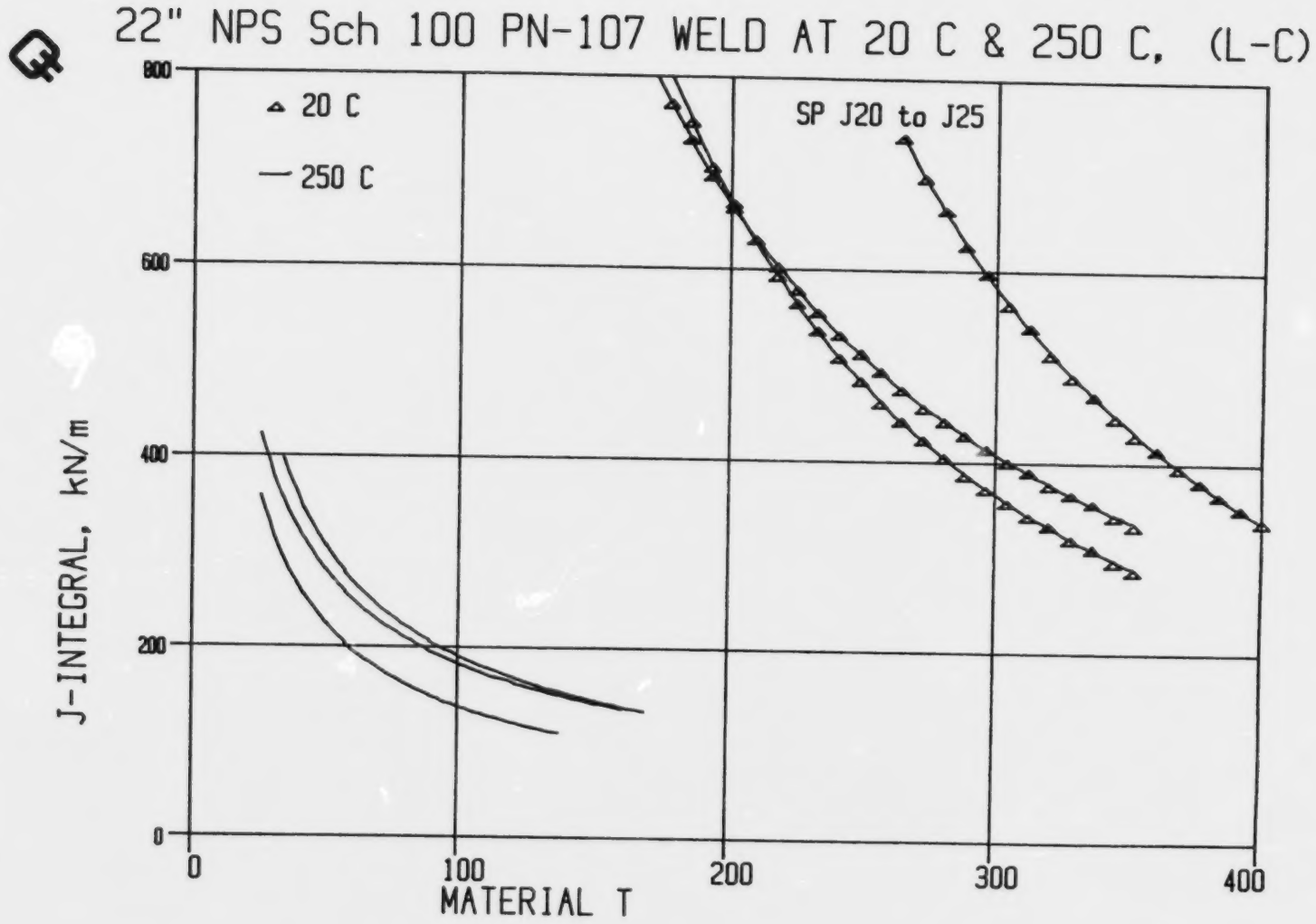

FIGURE 31
EFFECT OF TEST TEMPERATURE ON J-T CURVES

File JT 20-25
174342-RD

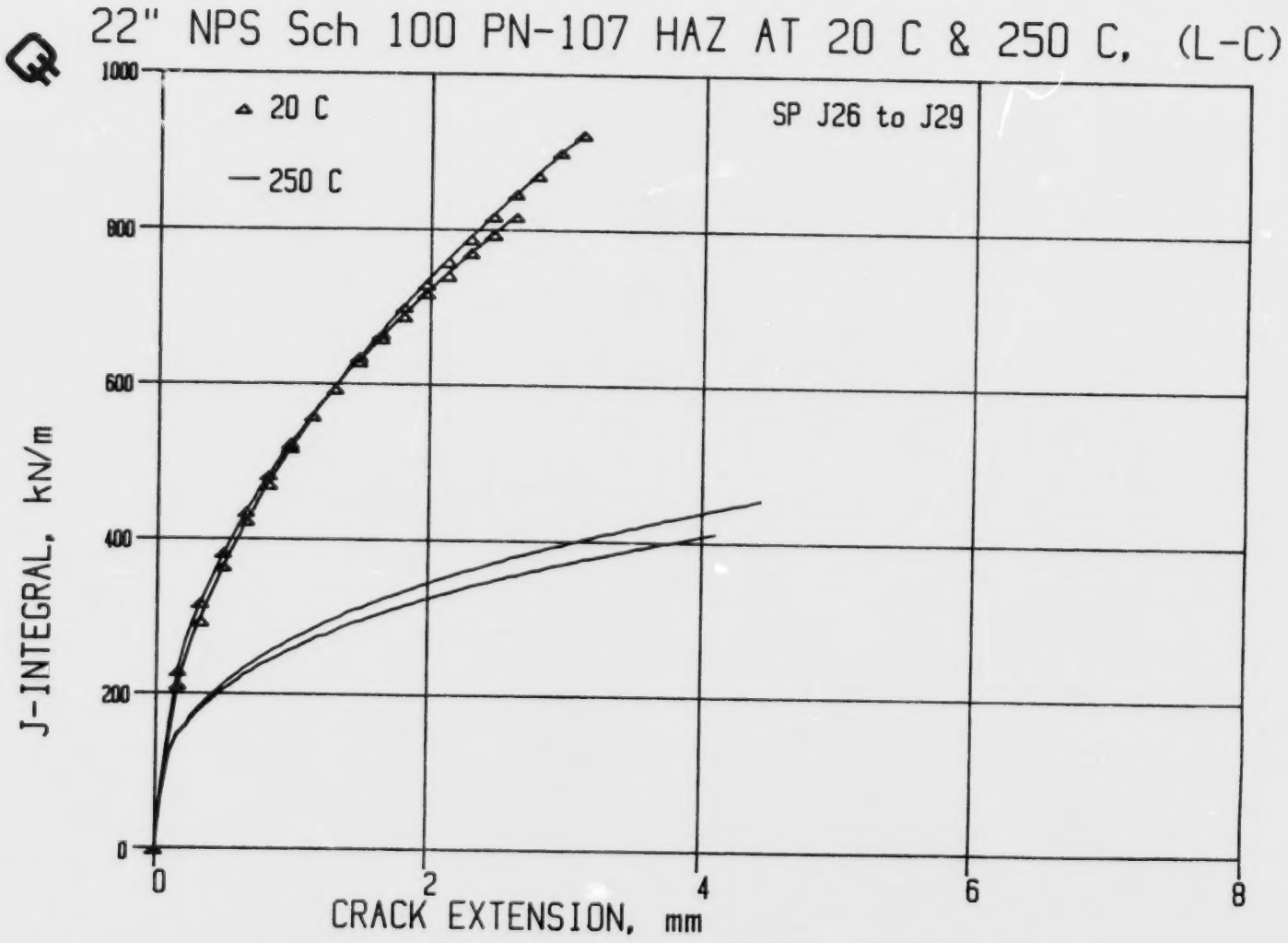

FIGURE 32

EFFECT OF TEST TEMPERATURE ON J-RESISTANCE CURVES

File J 26-29
174341-RD

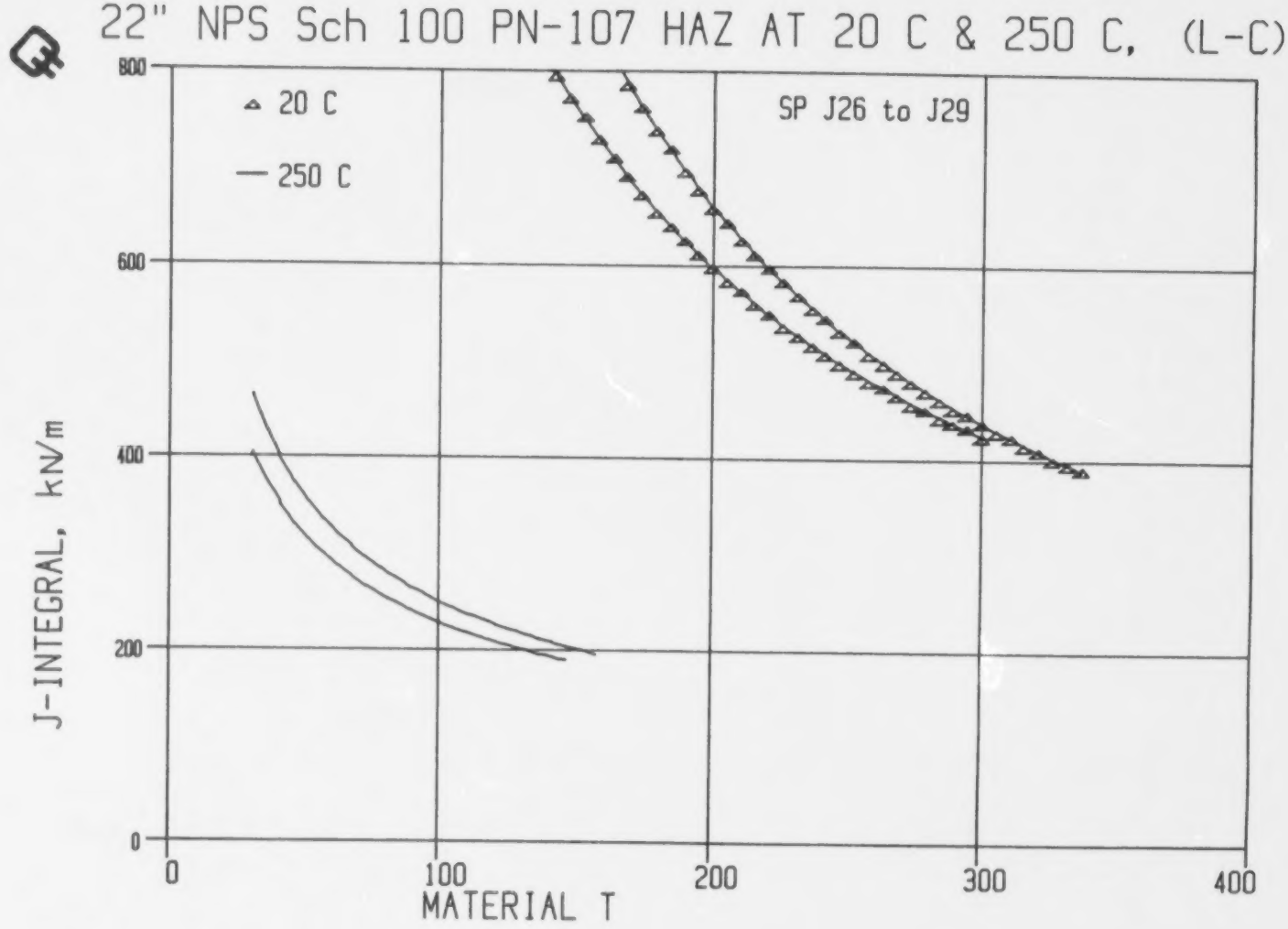

FIGURE 33

EFFECT OF TEST TEMPERATURE ON J-T CURVES

File JT 26-29
174340-RD

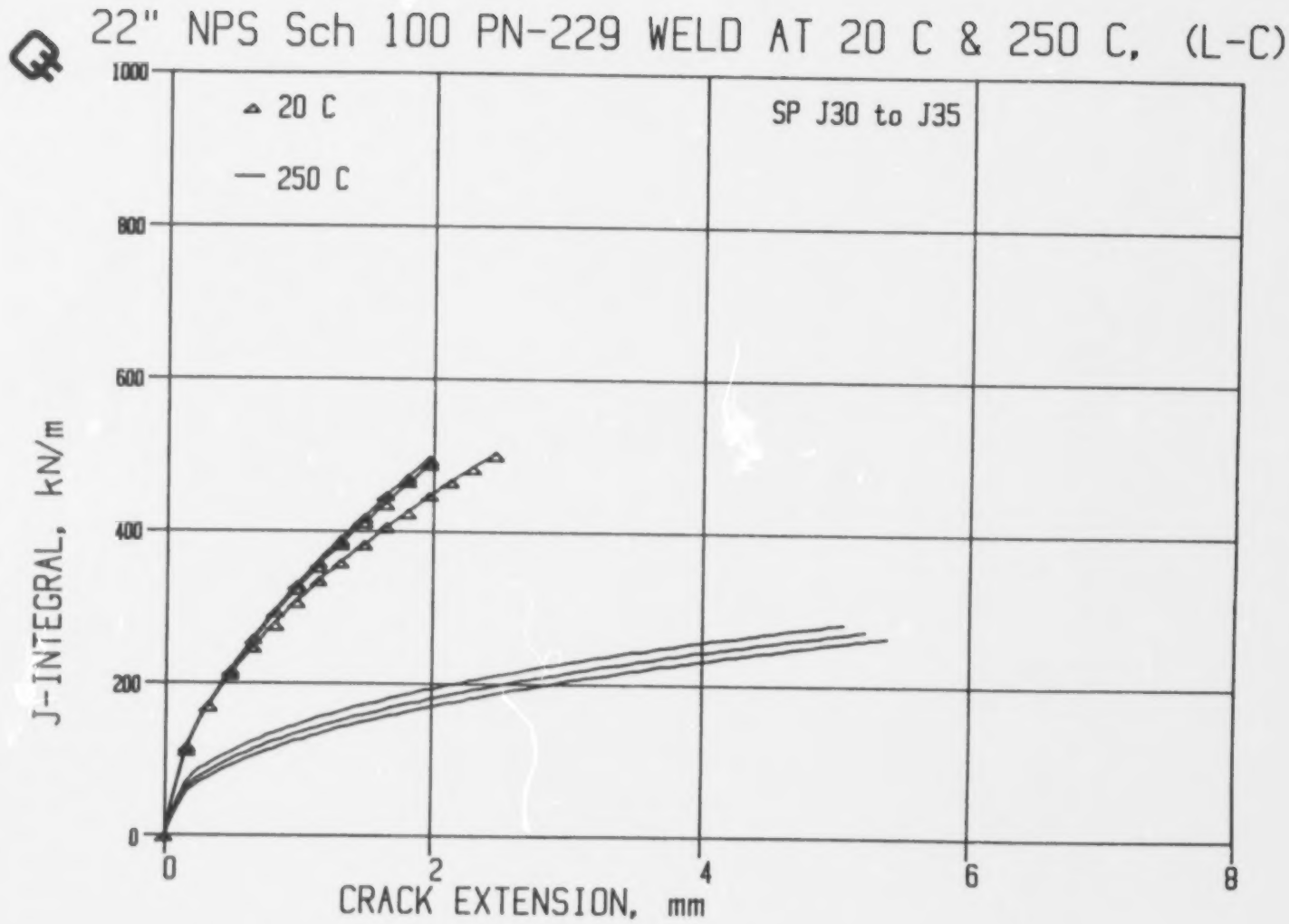

FIGURE 34

EFFECT OF TEST TEMPERATURE ON J-RESISTANCE CURVES

File J 30-35
174339-RD

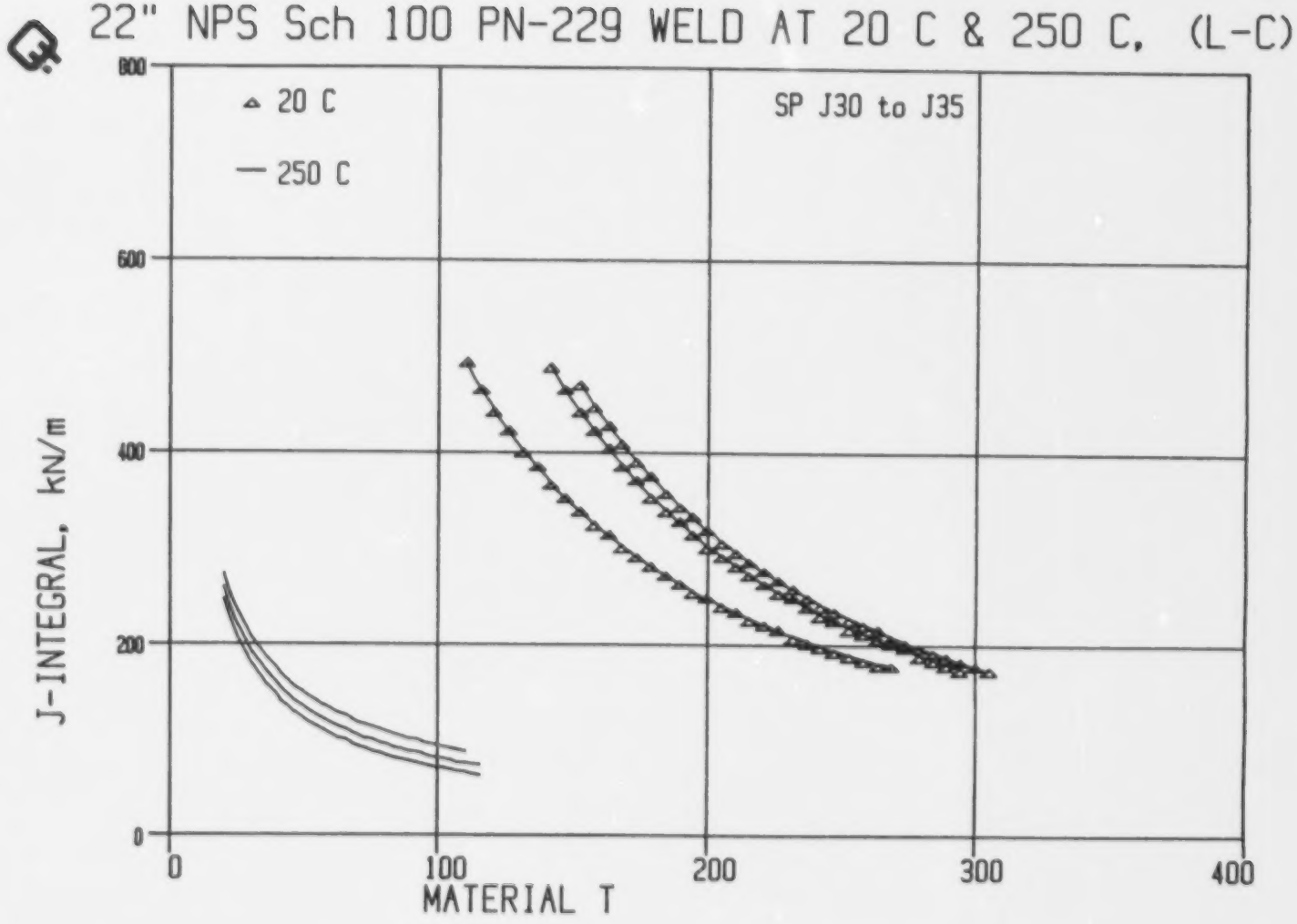

FIGURE 35
EFFECT OF TEST TEMPERATURE ON J-T CURVES

File JT 30-35
174338-RD

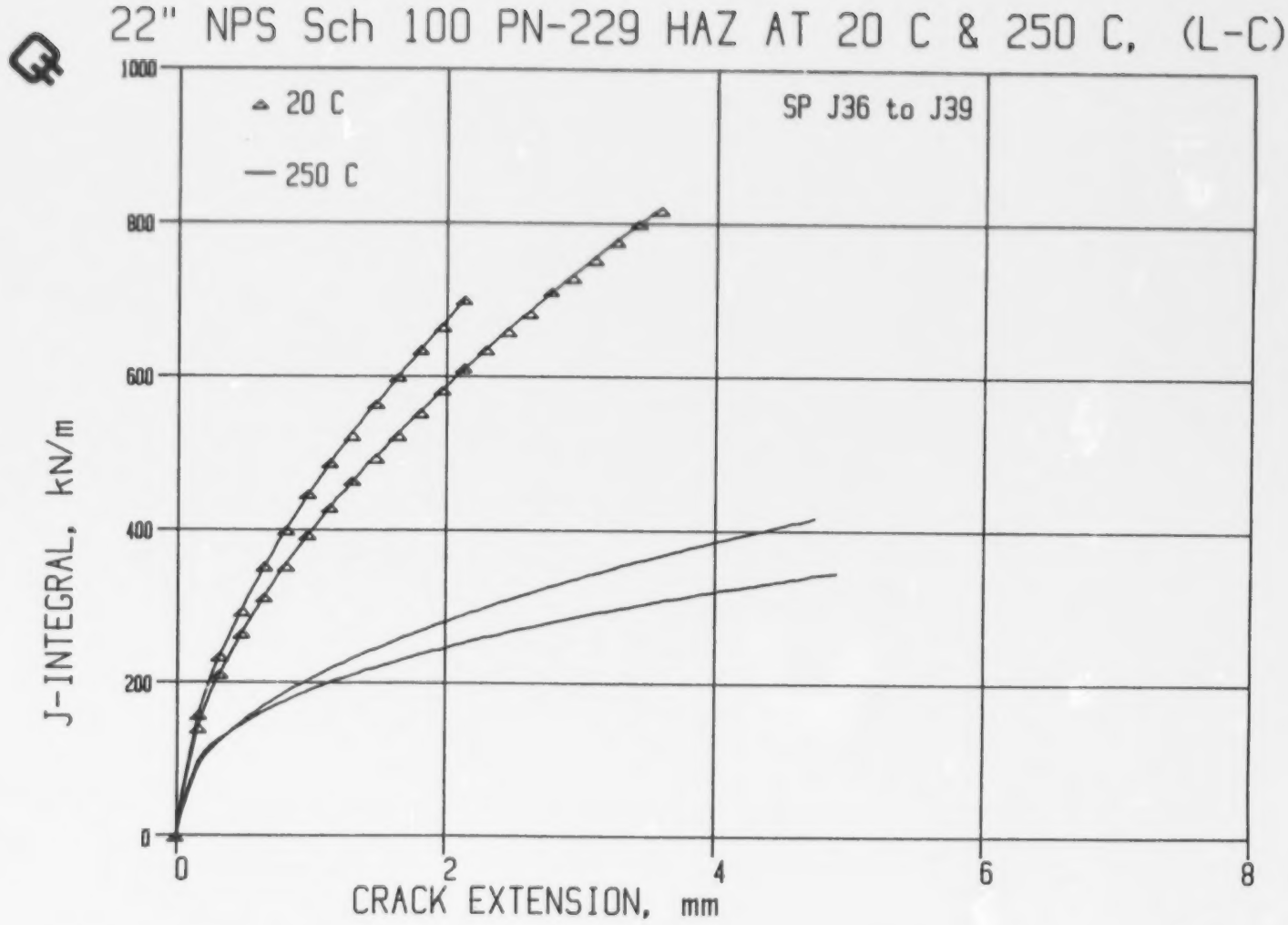

FIGURE 36

EFFECT OF TEST TEMPERATURE ON J-RESISTANCE CURVES

File J 36-39
174337-RD

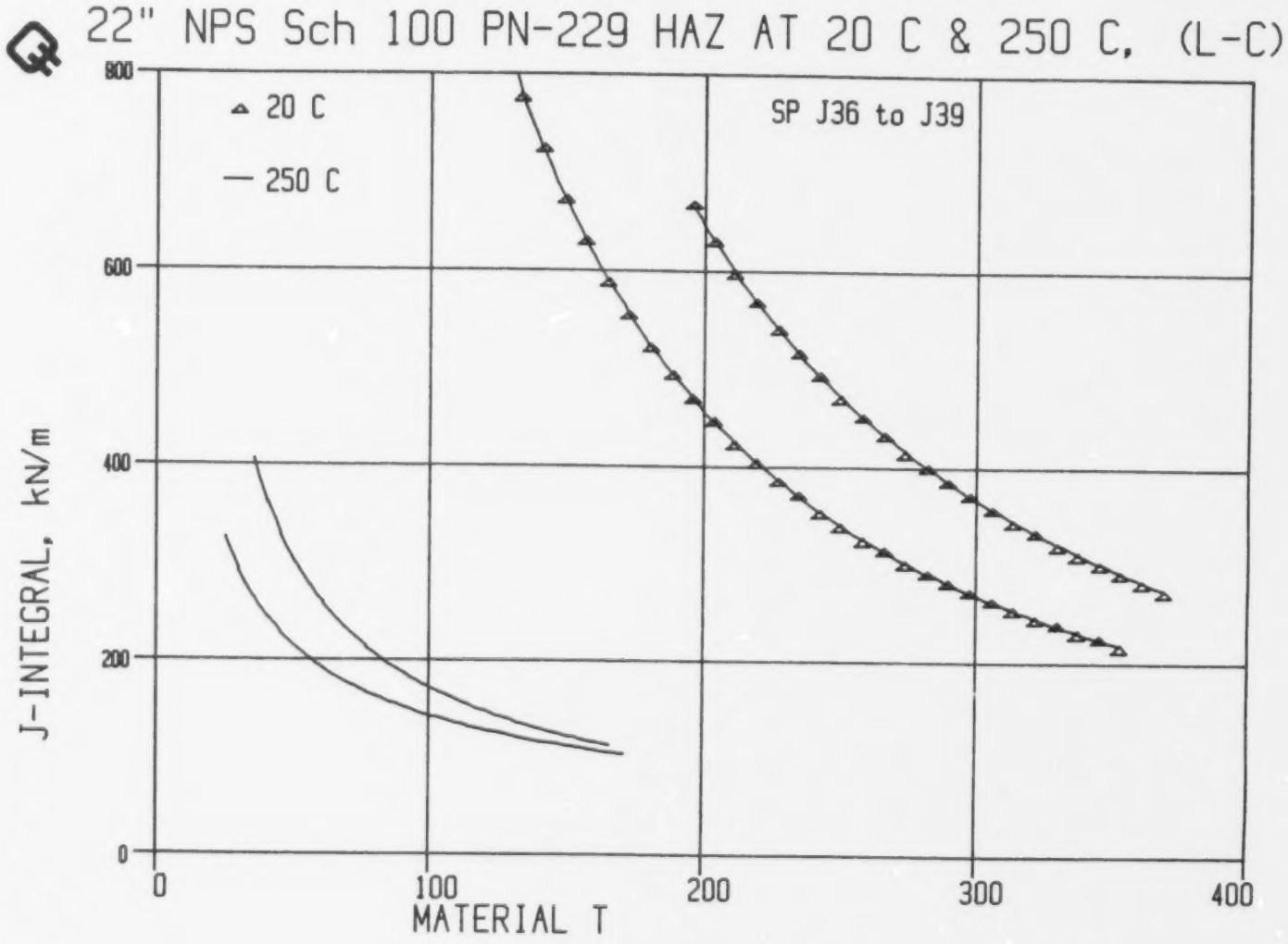

FIGURE 37

EFFECT OF TEST TEMPERATURE ON J-T CURVES

File JT 36-39
174336-RD

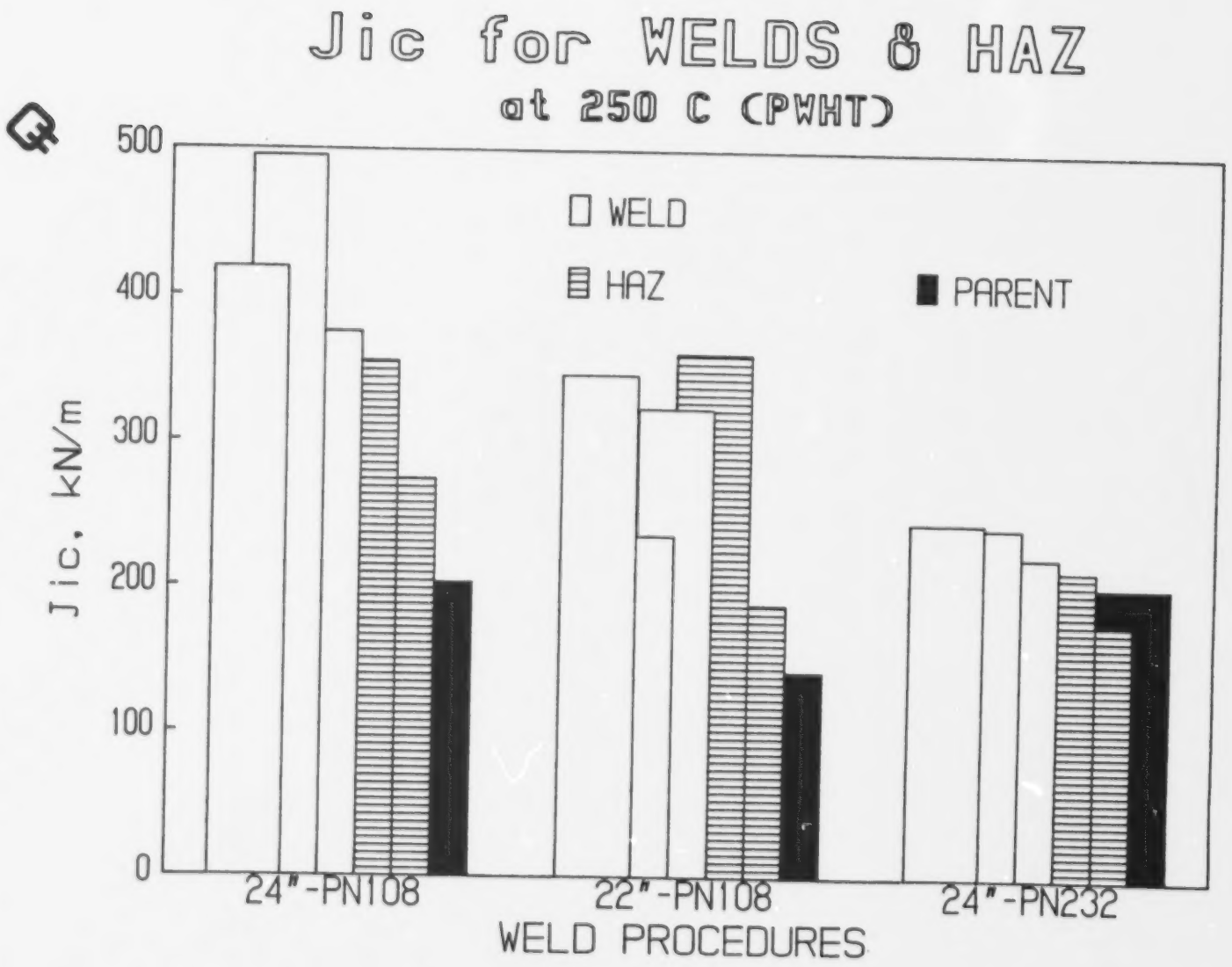

FIGURE 38

WELD AND HAZ J_{IC} VALUES

File JC HAZ1
174308-RD

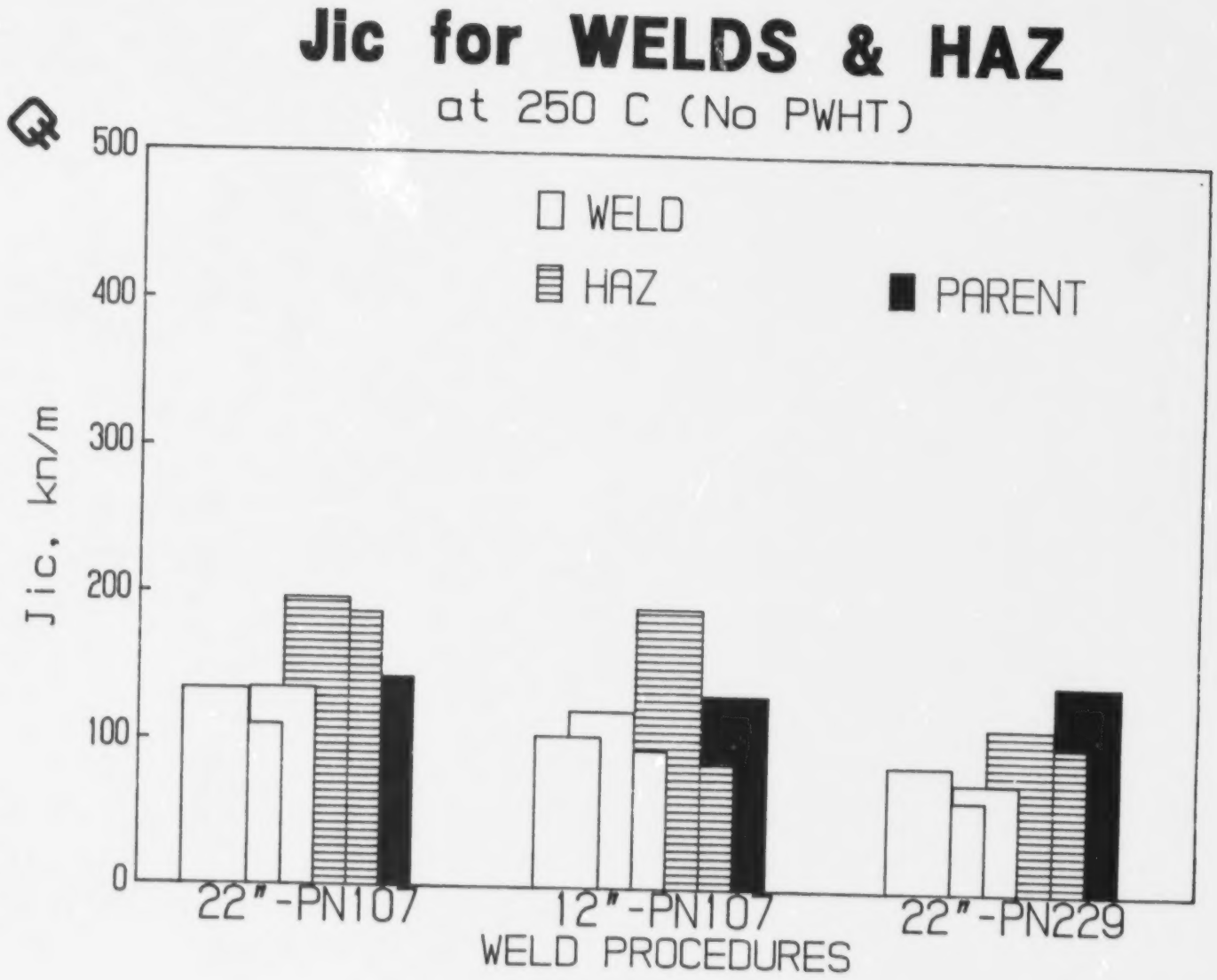

FIGURE 39

WELD AND HAZ J_{IC} VALUES

File JC HAZ2
174307-RD

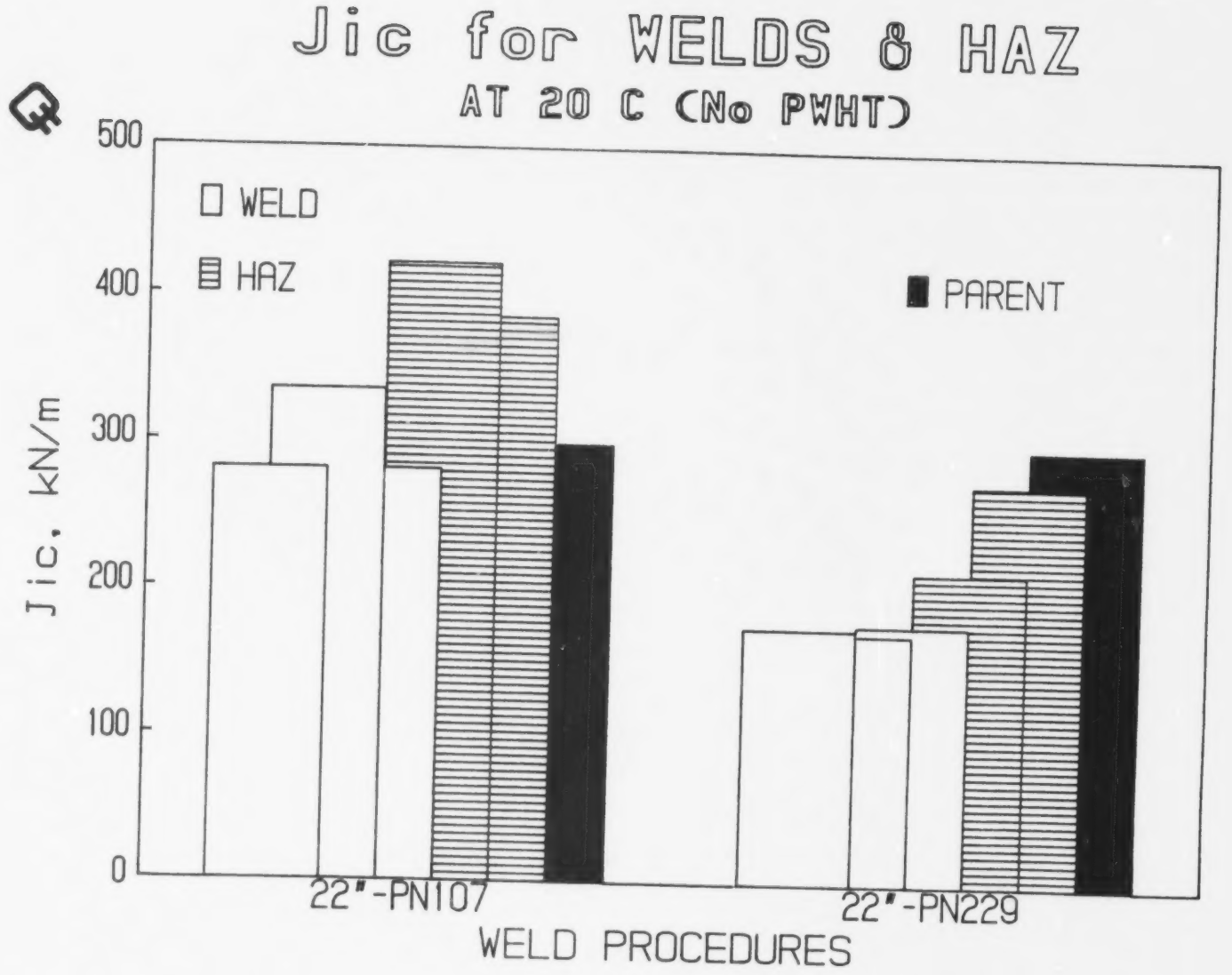

FIGURE 40

WELD AND HAZ J_{IC} VALUES

File JC HAZ3
174306-RD

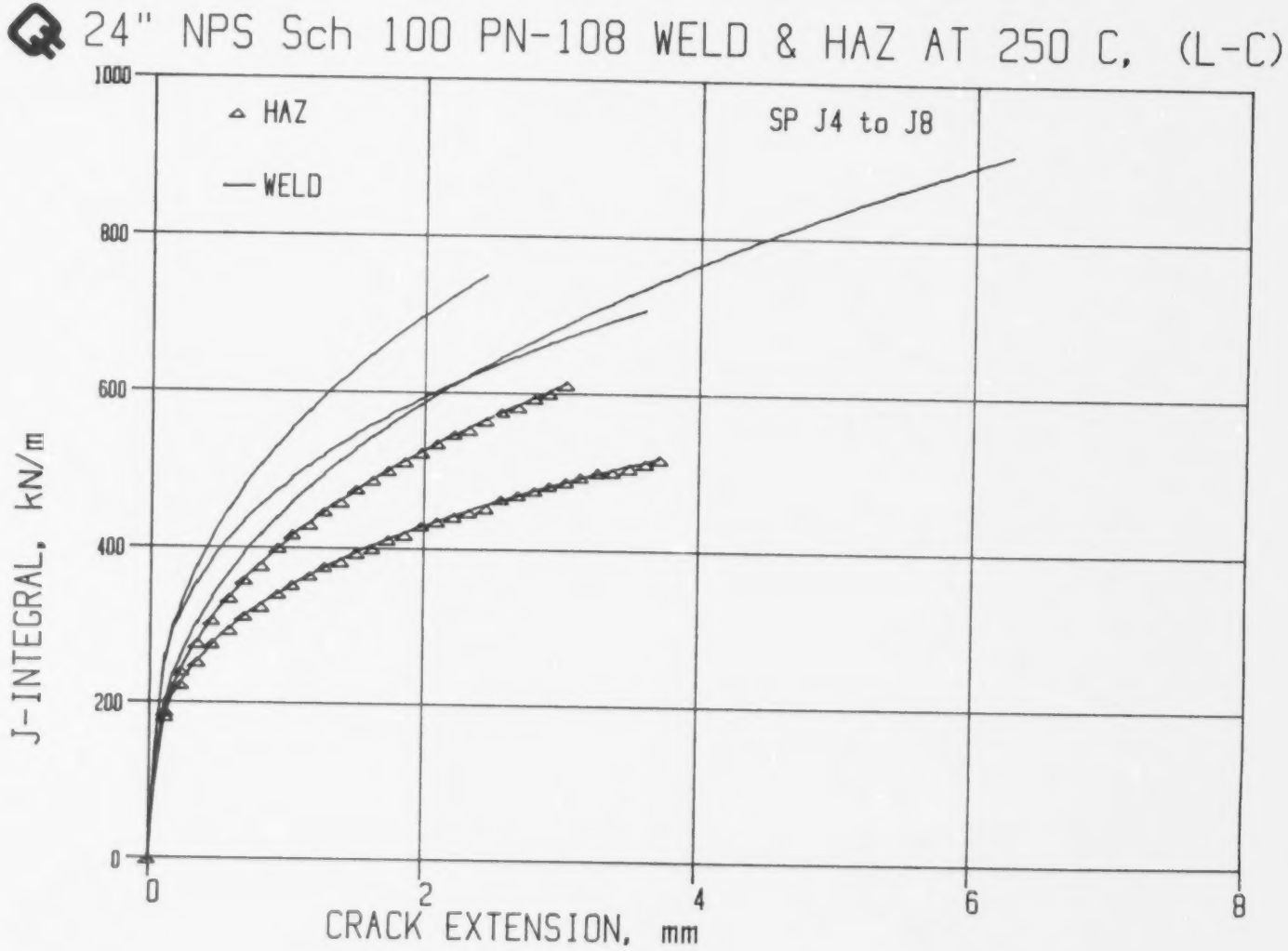

FIGURE 41

COMPARISON OF J-RESISTANCE CURVES FOR WELD AND HAZ

File J 04-08
174335-RD

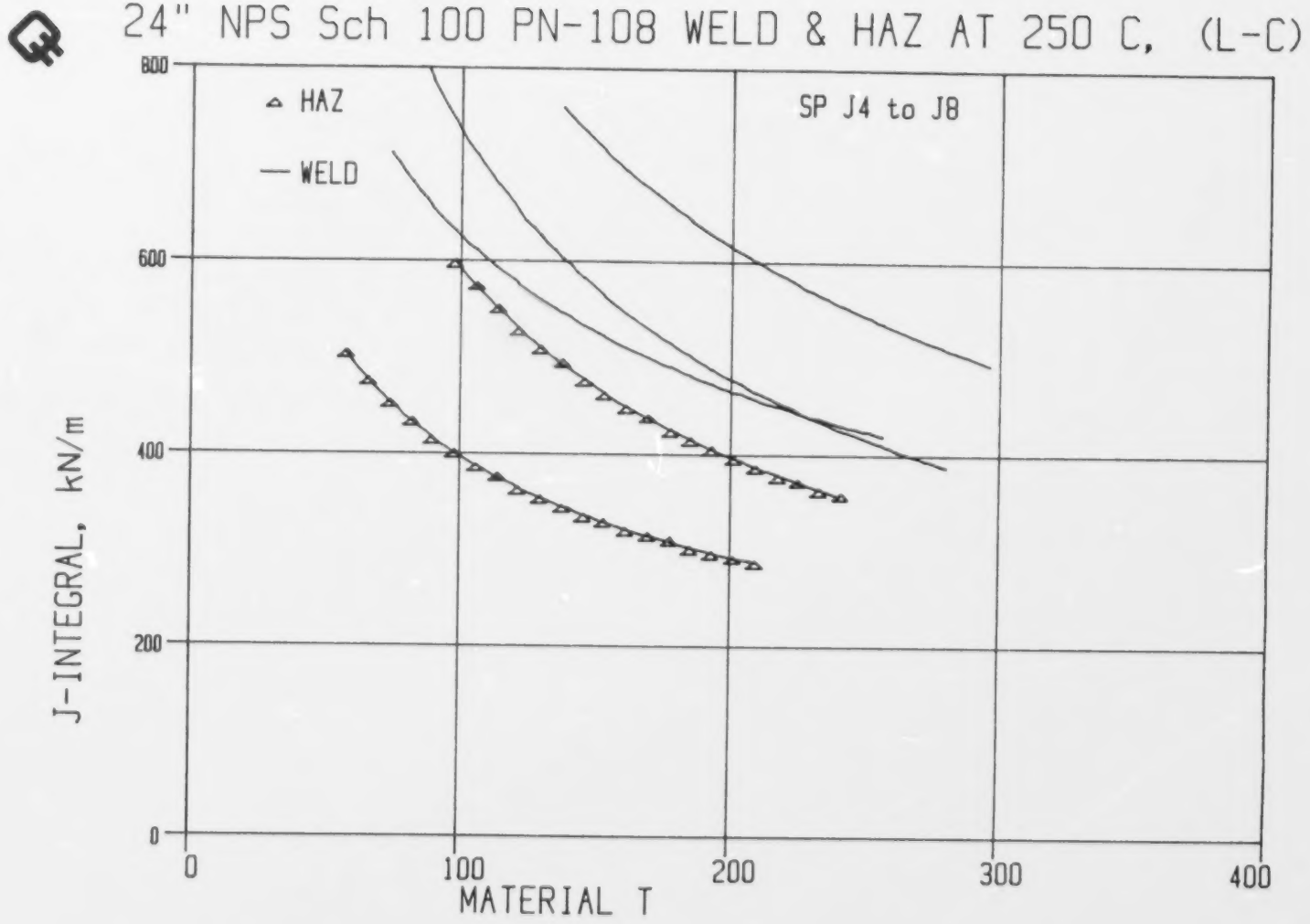

FIGURE 42
COMPARISON OF J-T CURVES FOR WELD AND HAZ

File JT 04-08
174334-RD

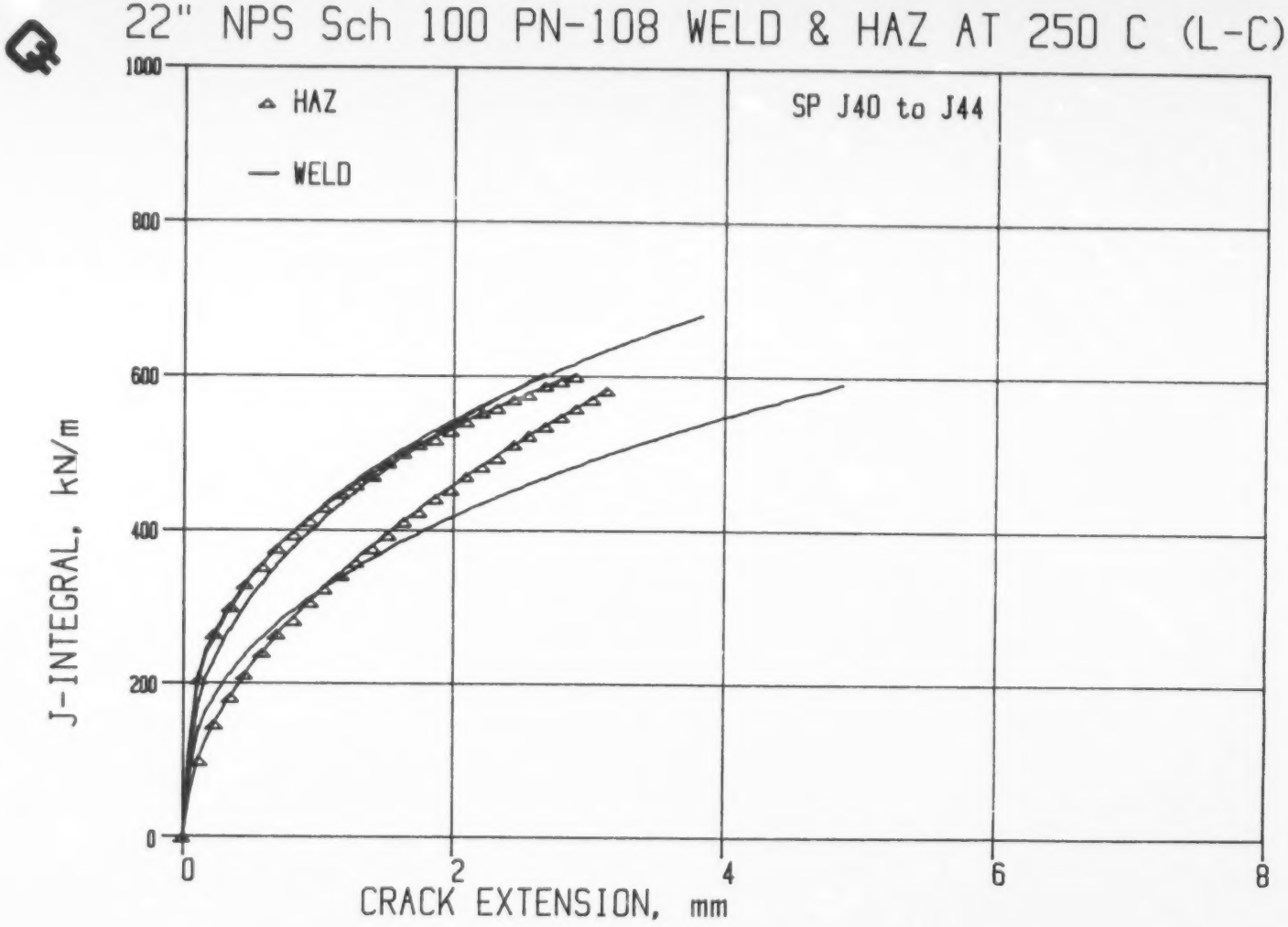

FIGURE 43

COMPARISON OF J-RESISTANCE CURVES FOR WELD AND HAZ

File J 40-44
174333-RD

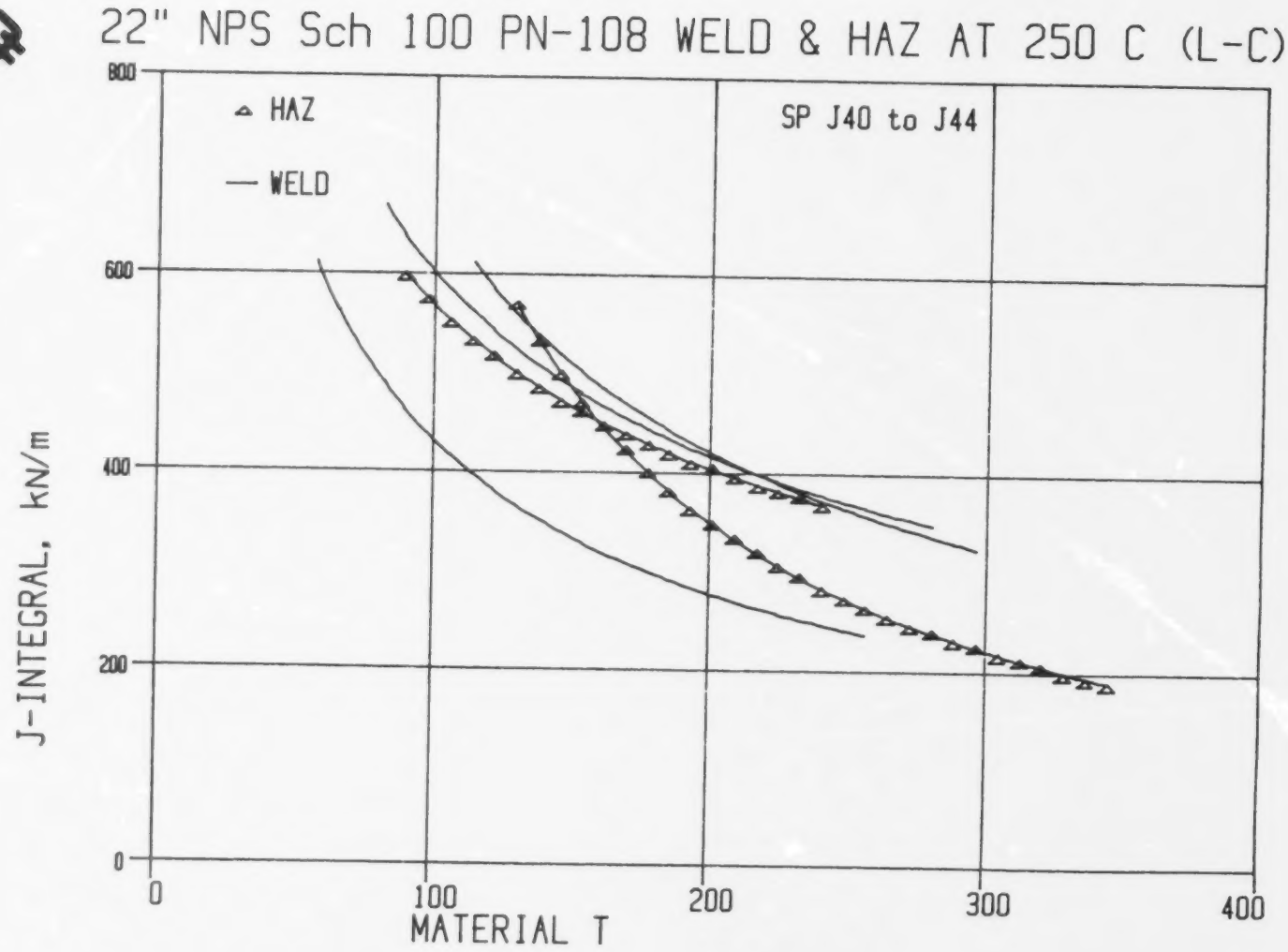

FIGURE 44
COMPARISON OF J-T CURVES FOR WELD AND HAZ

File JT 40-44
174332-RD

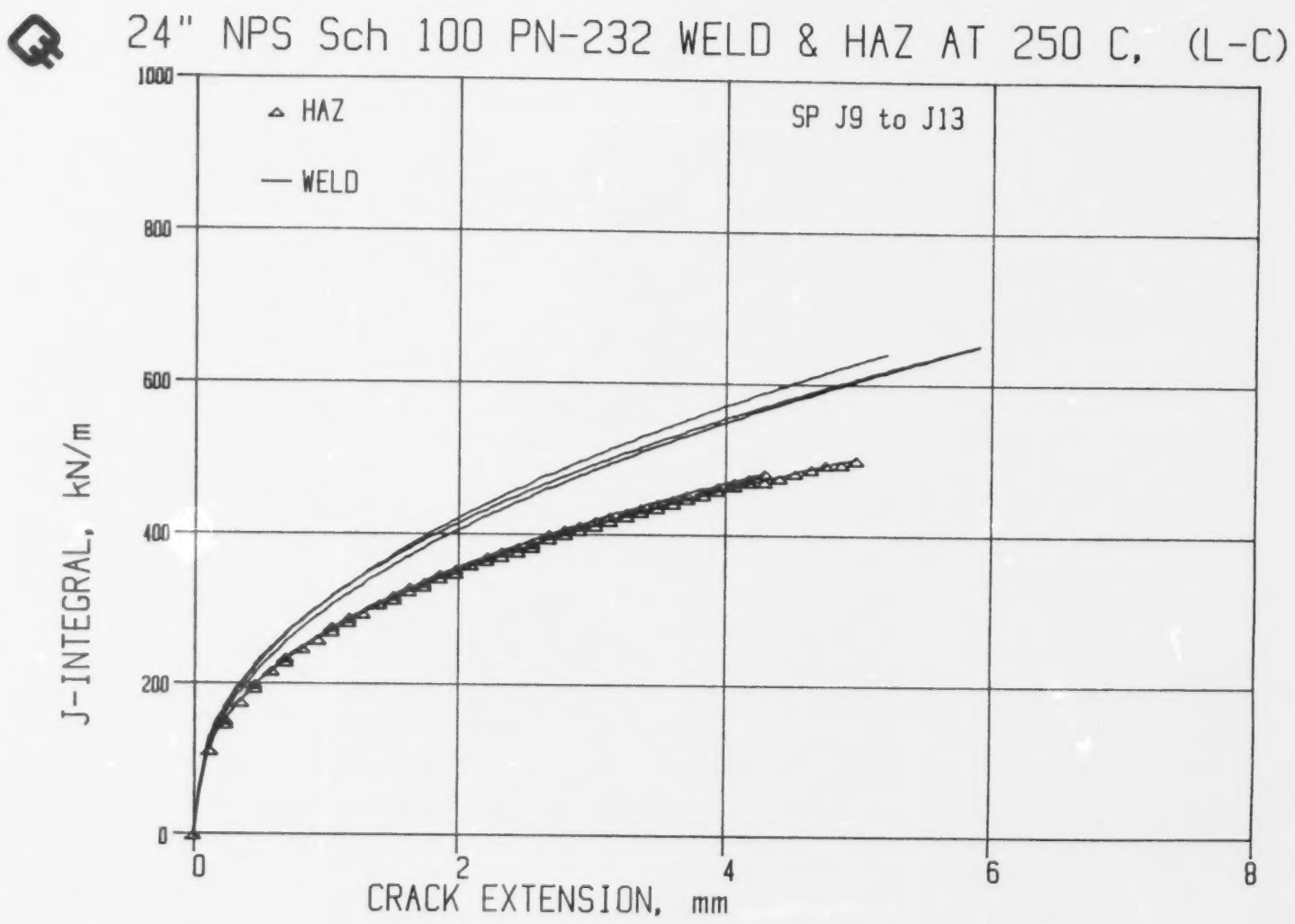

FIGURE 45

COMPARISON OF J-RESISTANCE CURVES FOR WELD AND HAZ

File J 09-13
174331-RD

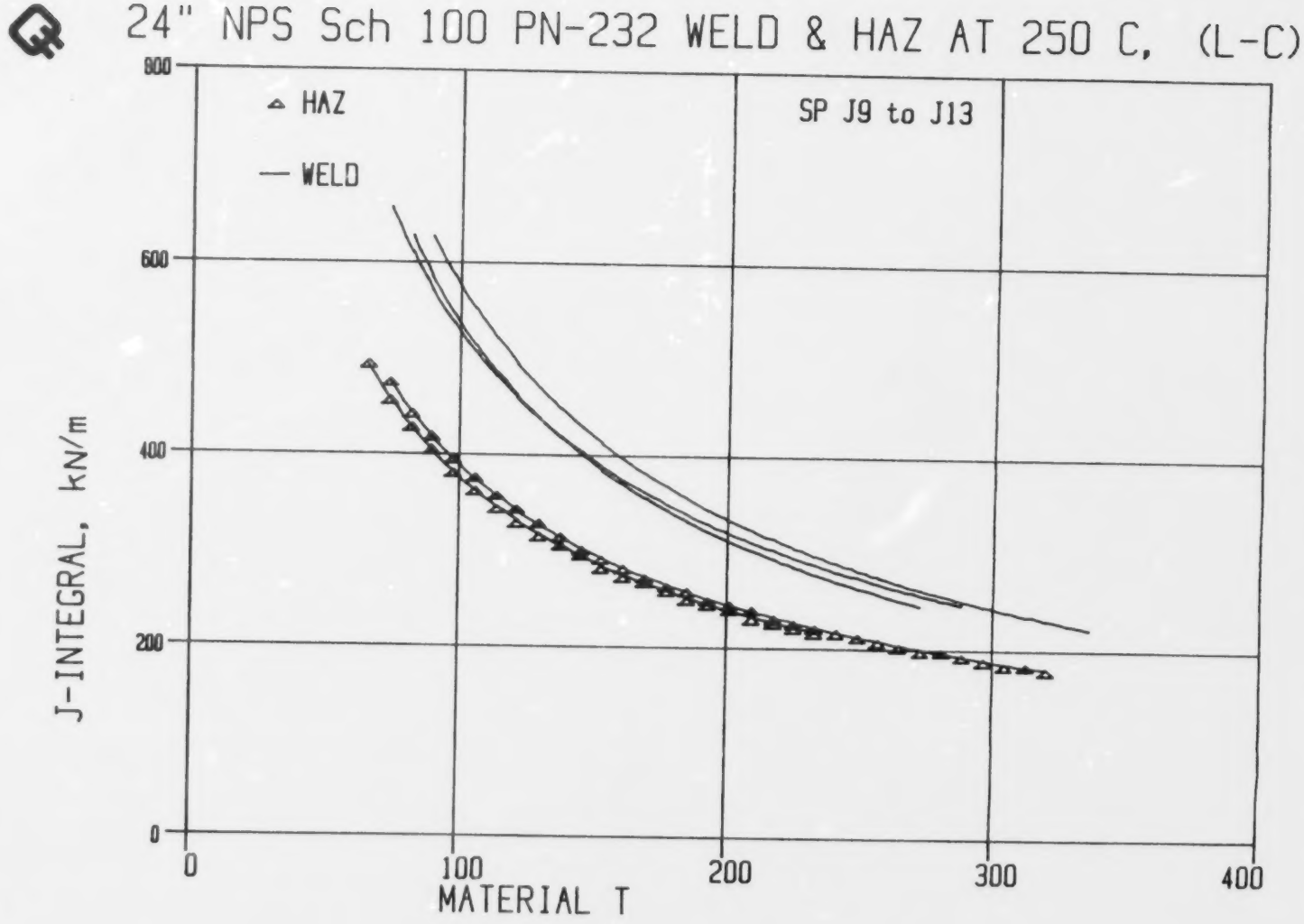

FIGURE 46
COMPARISON OF J-T CURVES FOR WELD AND HAZ

File JT 09-13
174330-RD

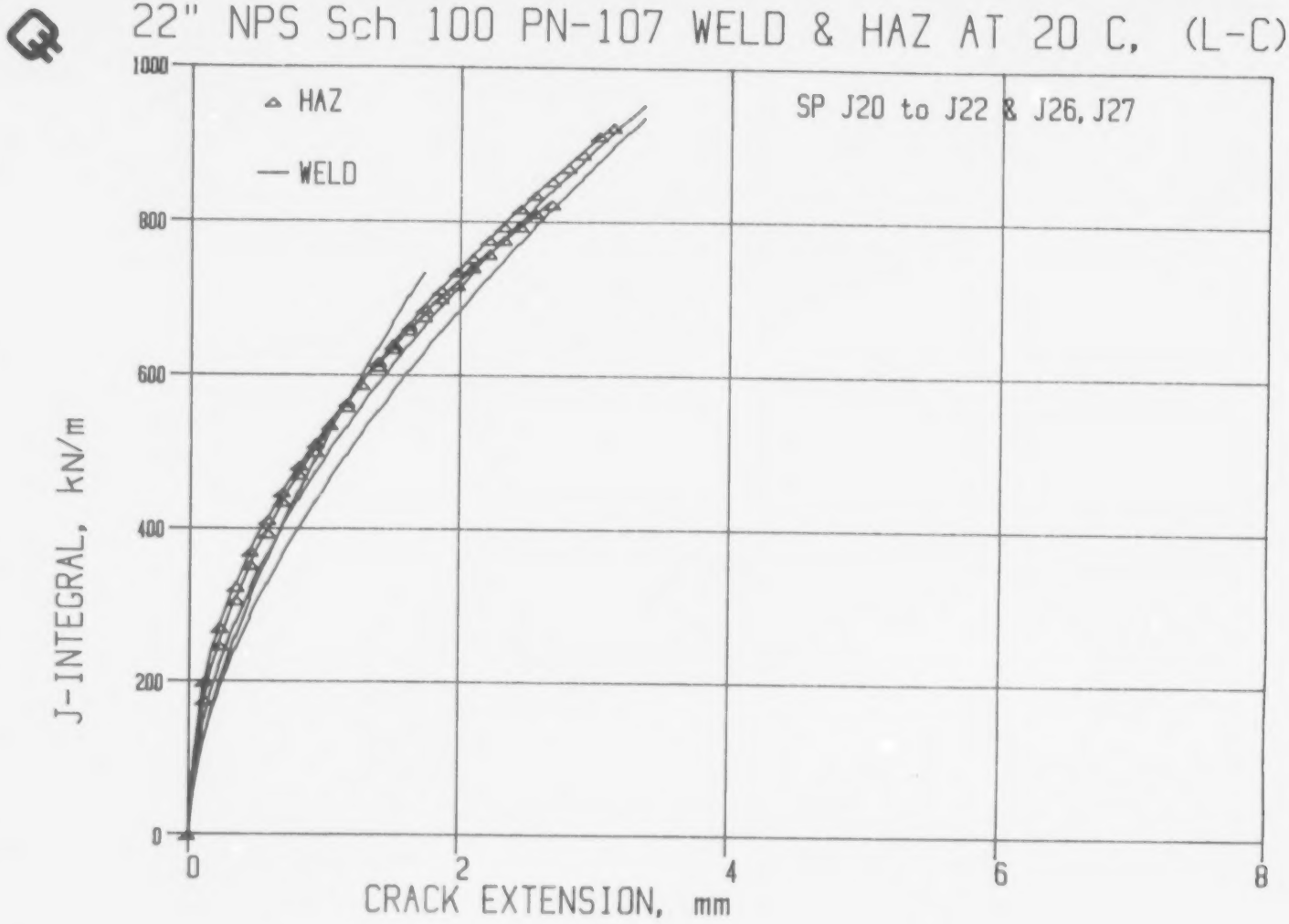

FIGURE 47

COMPARISON OF J-RESISTANCE CURVES FOR WELD AND HAZ

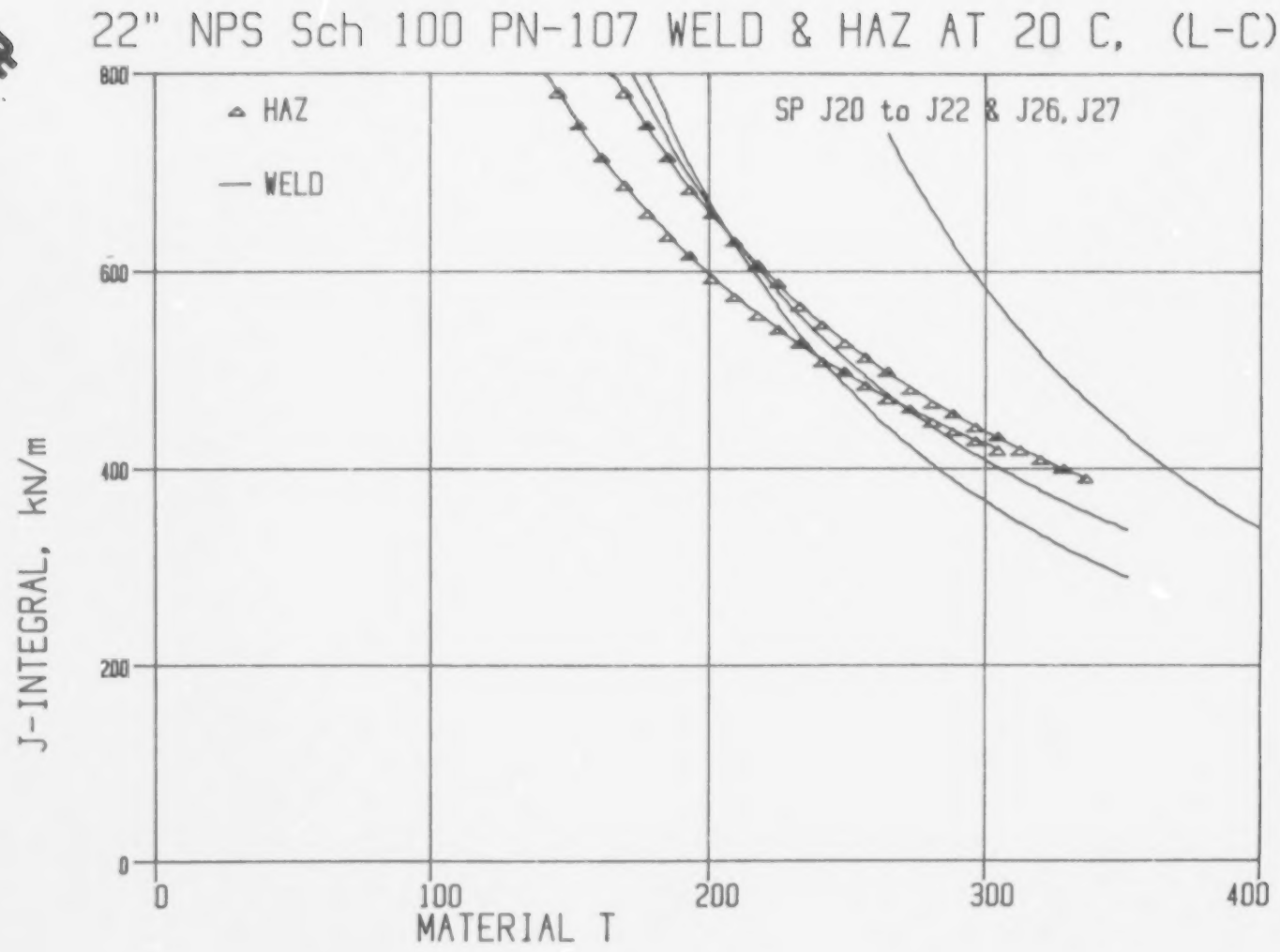

FIGURE 48

COMPARISON OF J-T CURVES FOR WELD AND HAZ

File JT 20-22
174328-RD

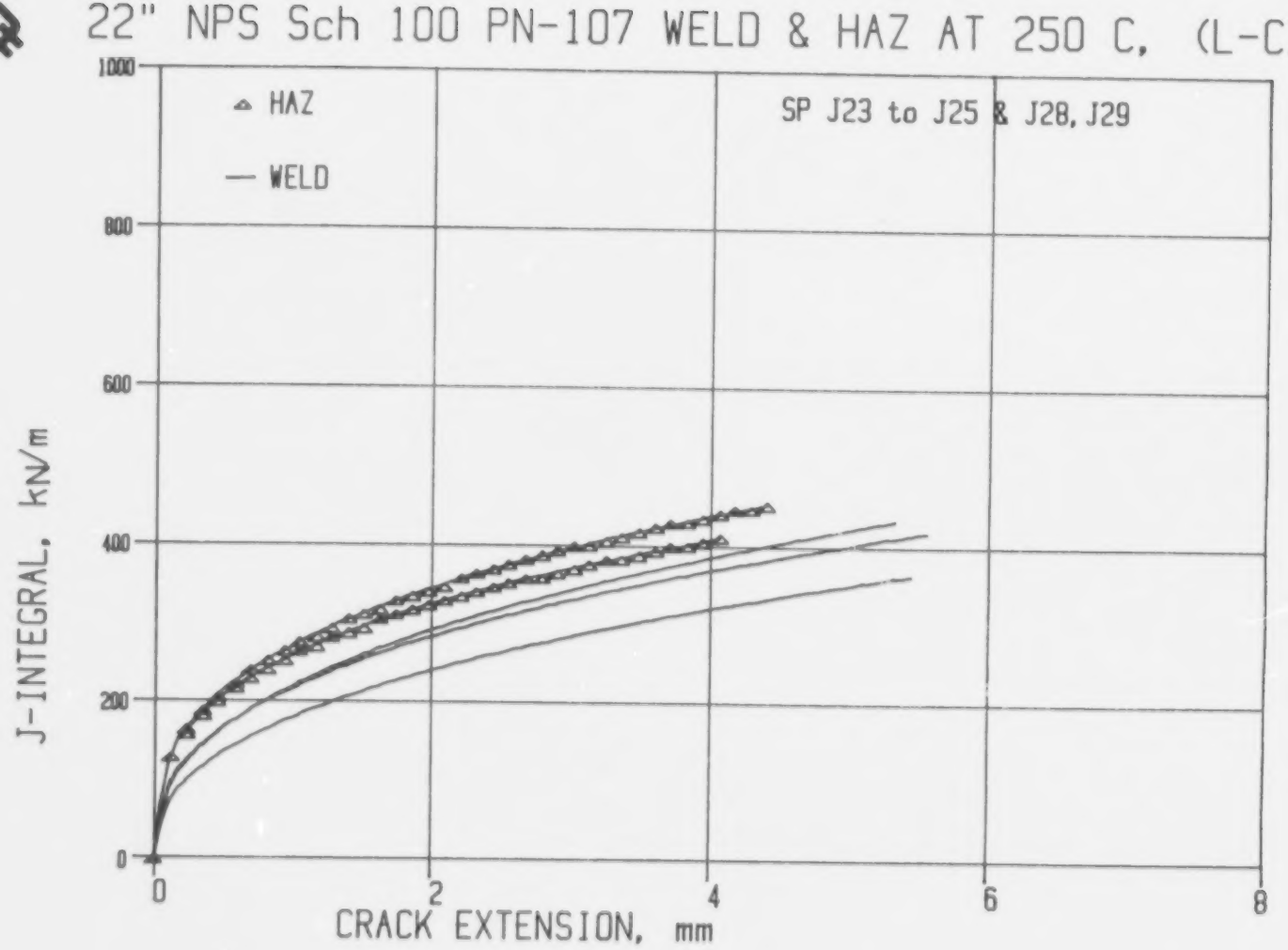

FIGURE 49
COMPARISON OF J-RESISTANCE CURVES FOR WELD AND HAZ

File J 23-25
174327-RD

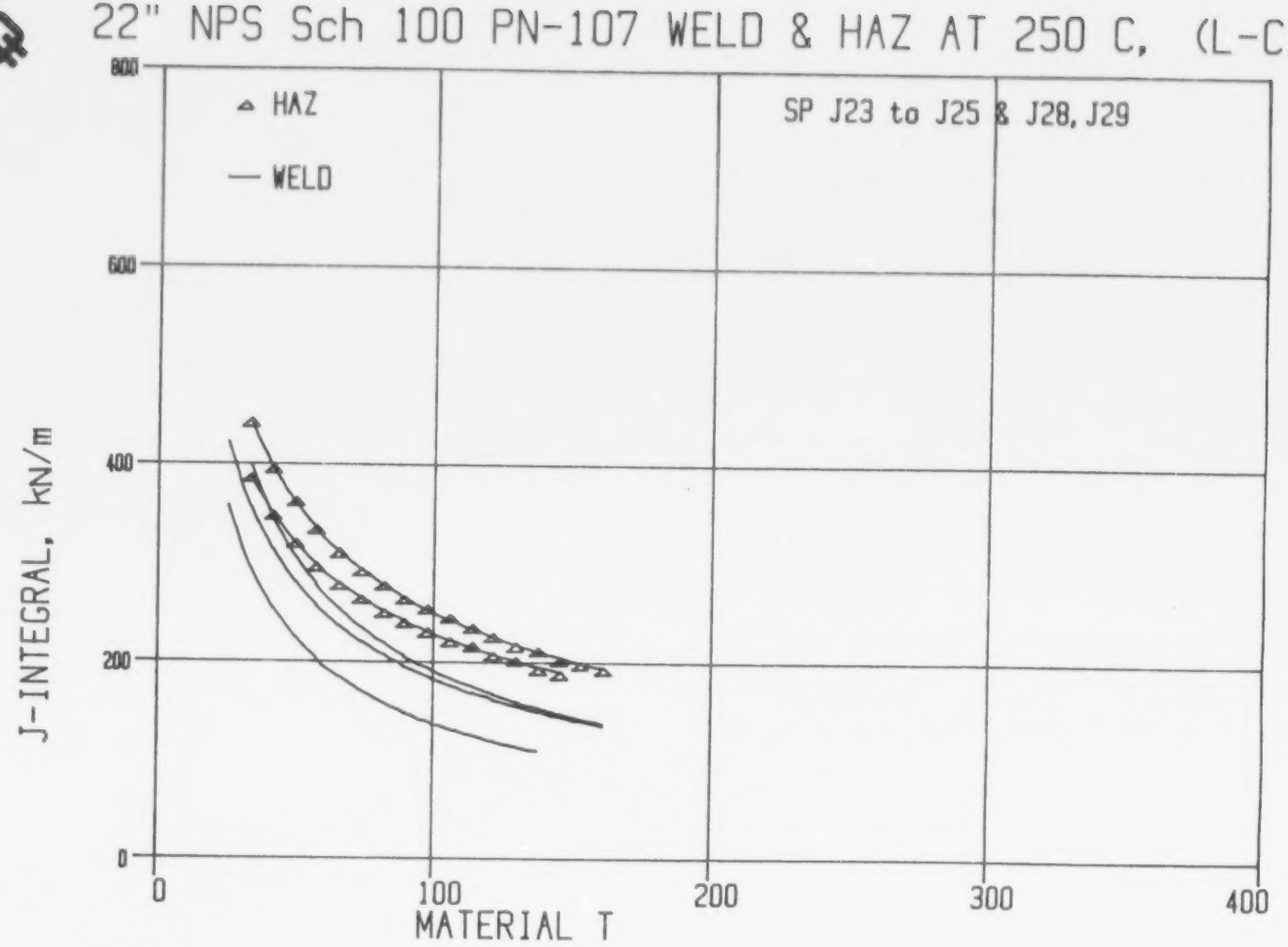

FIGURE 50

COMPARISON OF J-T CURVES FOR WELD AND HAZ

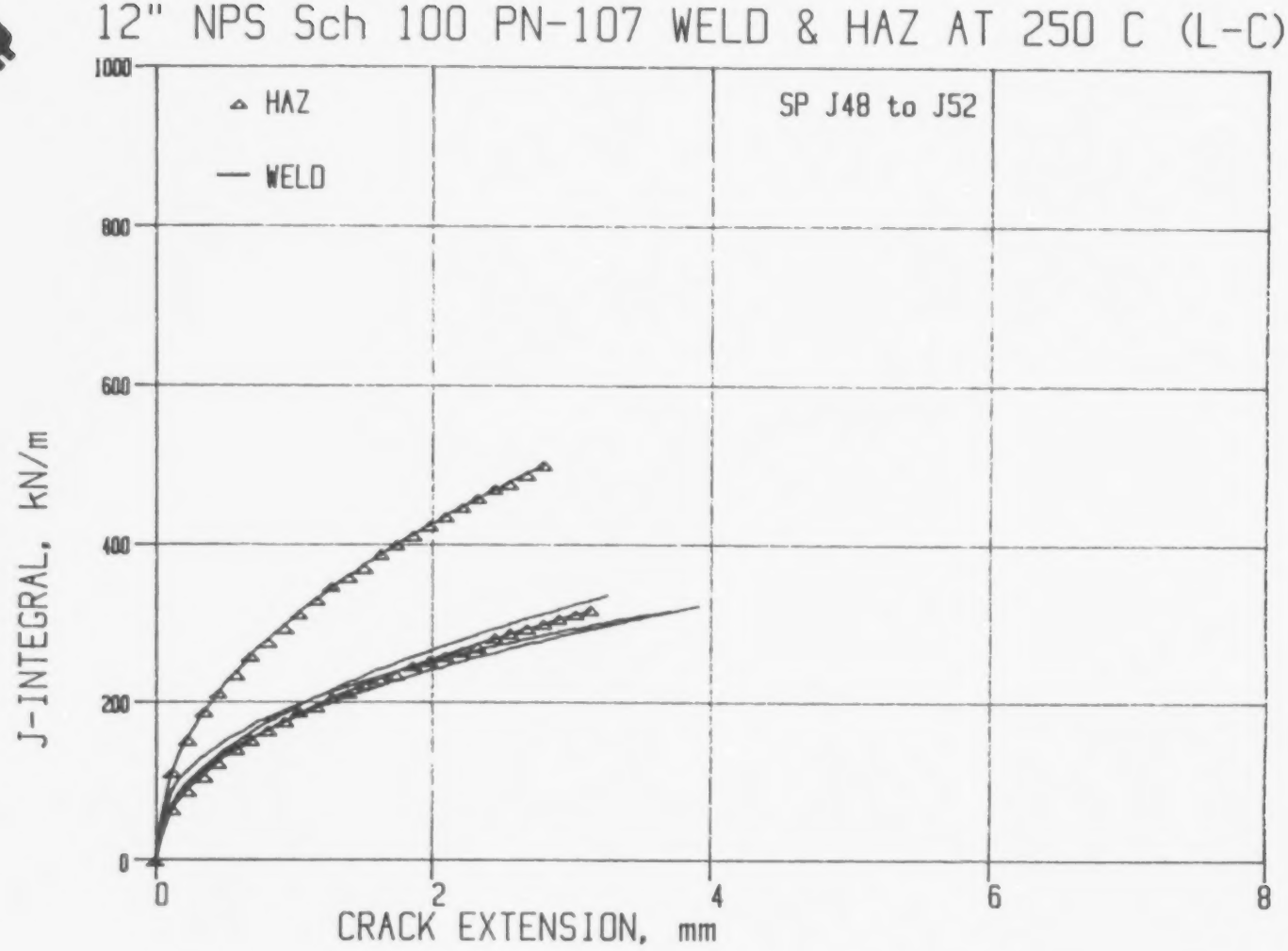

FIGURE 51

COMPARISON OF J-RESISTANCE CURVES FOR WELD AND HAZ

File J 48-52
174325-RD

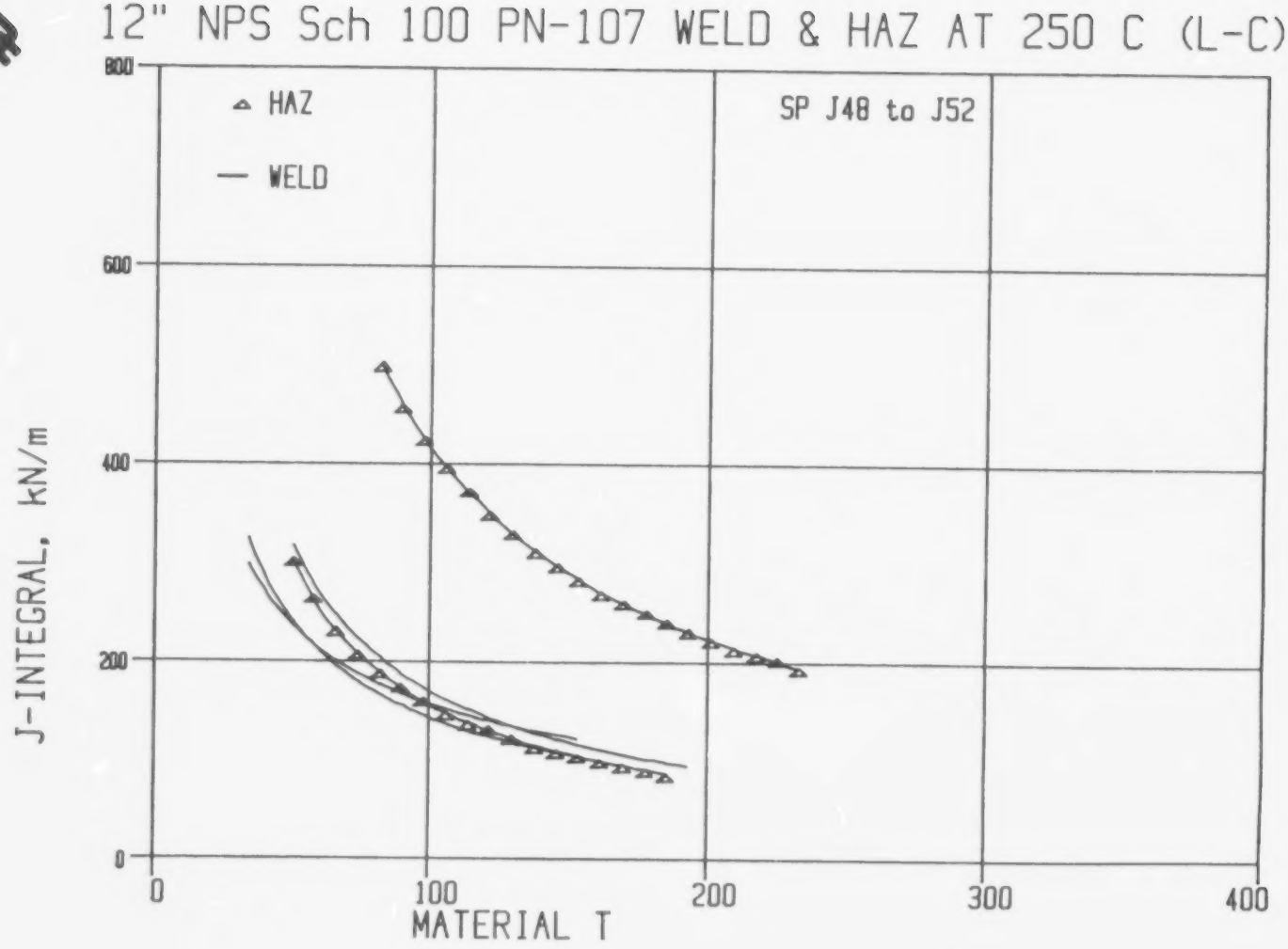

FIGURE 52

COMPARISON OF J-T CURVES FOR WELD AND HAZ

File JT 48-52
174324-RD

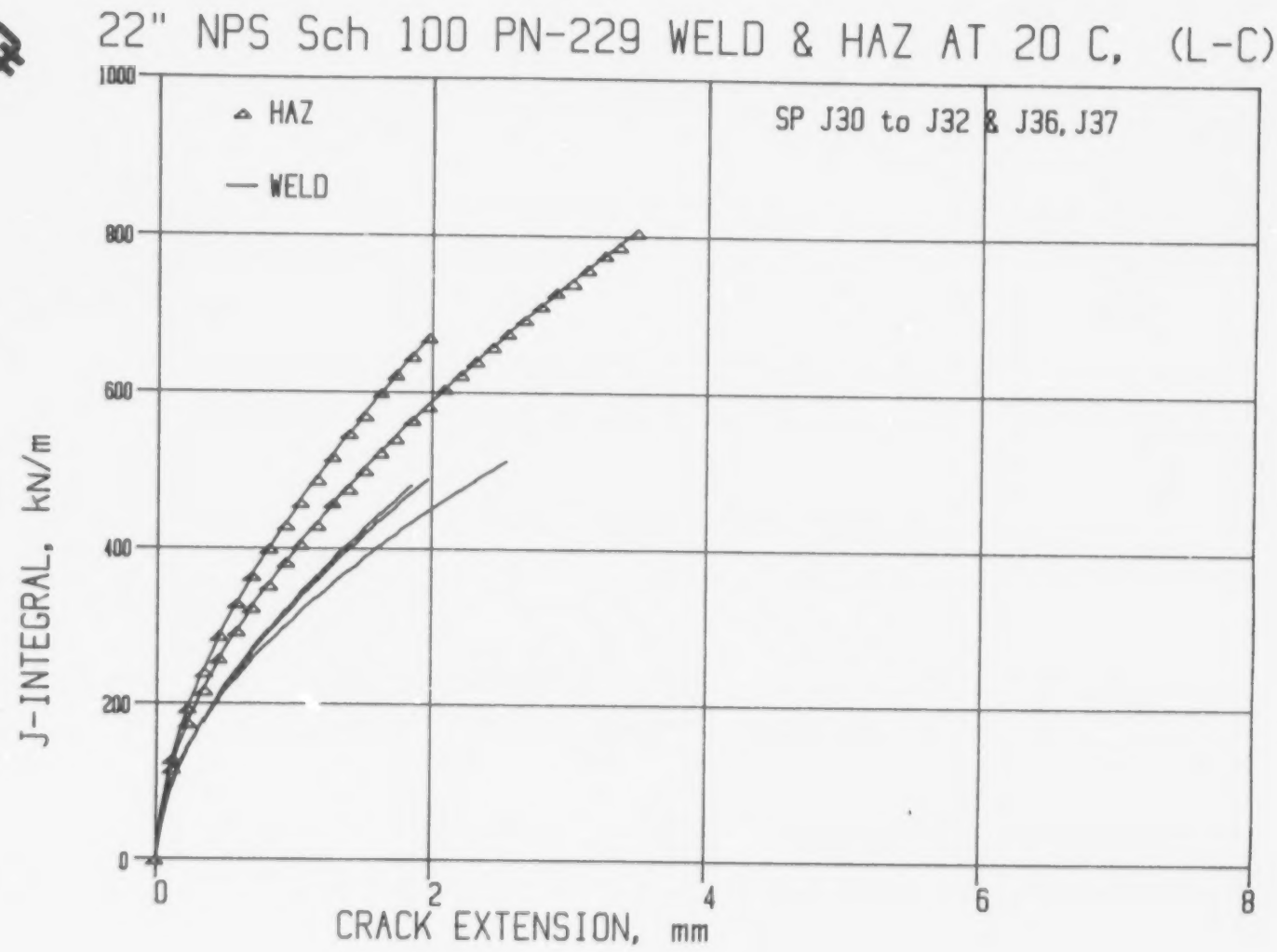

FIGURE 53

COMPARISON OF J-RESISTANCE CURVES FOR WELD AND HAZ

File J 30-32
17323-RD

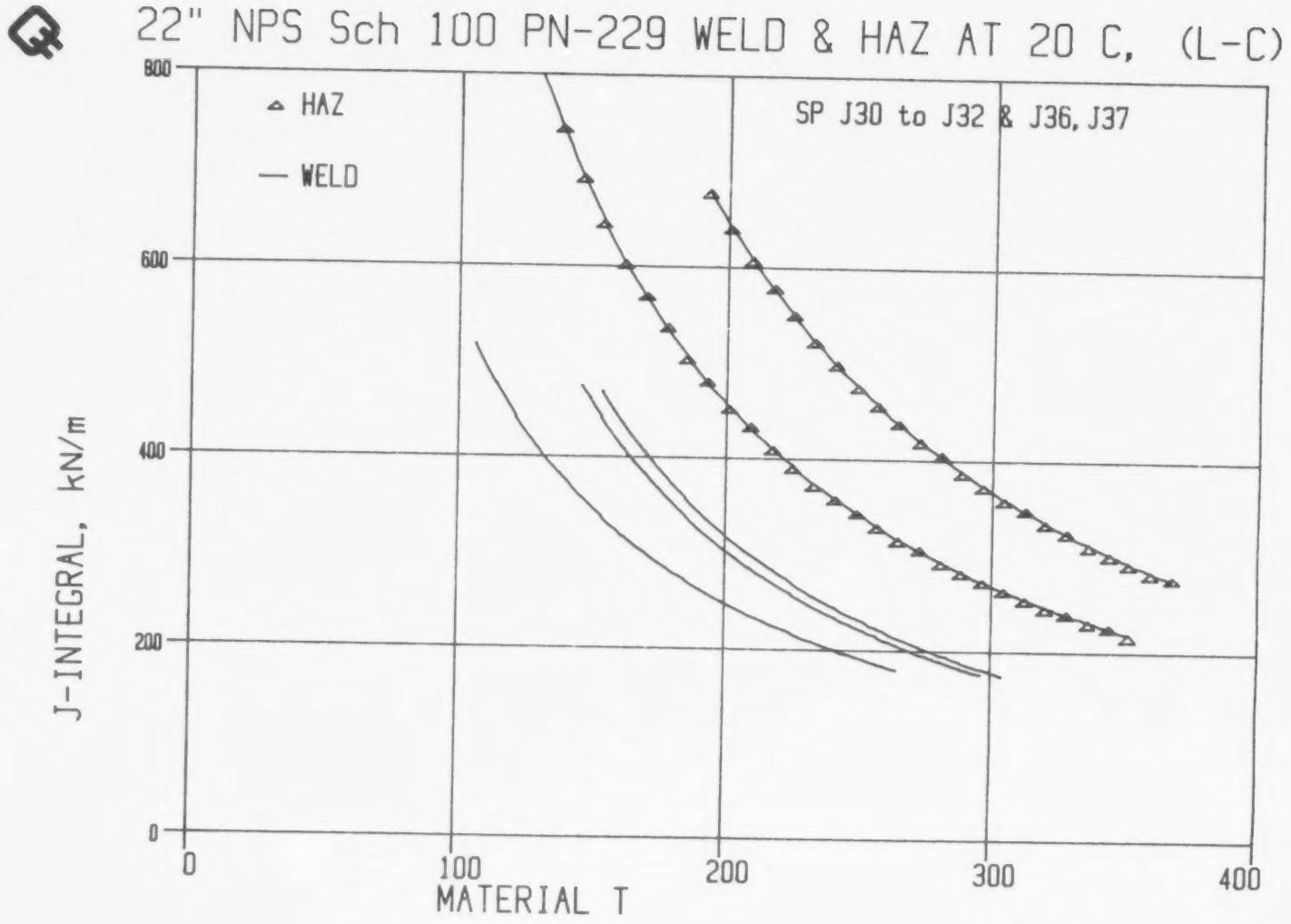

FIGURE 54

COMPARISON OF J-T CURVES FOR WELD AND HAZ

File JT 30-32
174322-RD

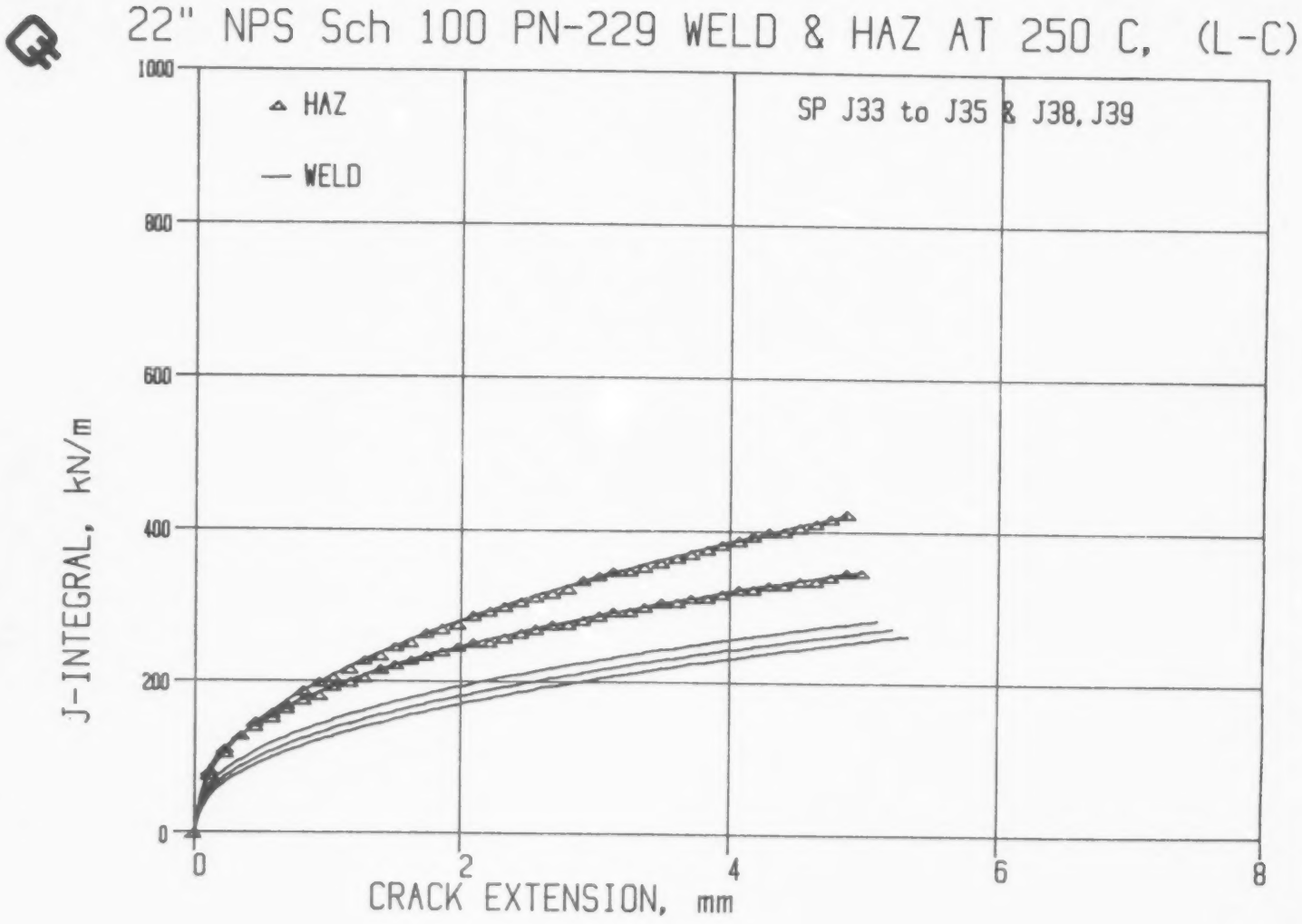

FIGURE 55

COMPARISON OF J-RESISTANCE CURVES FOR WELD AND HAZ

File J 33-35
174321-RD

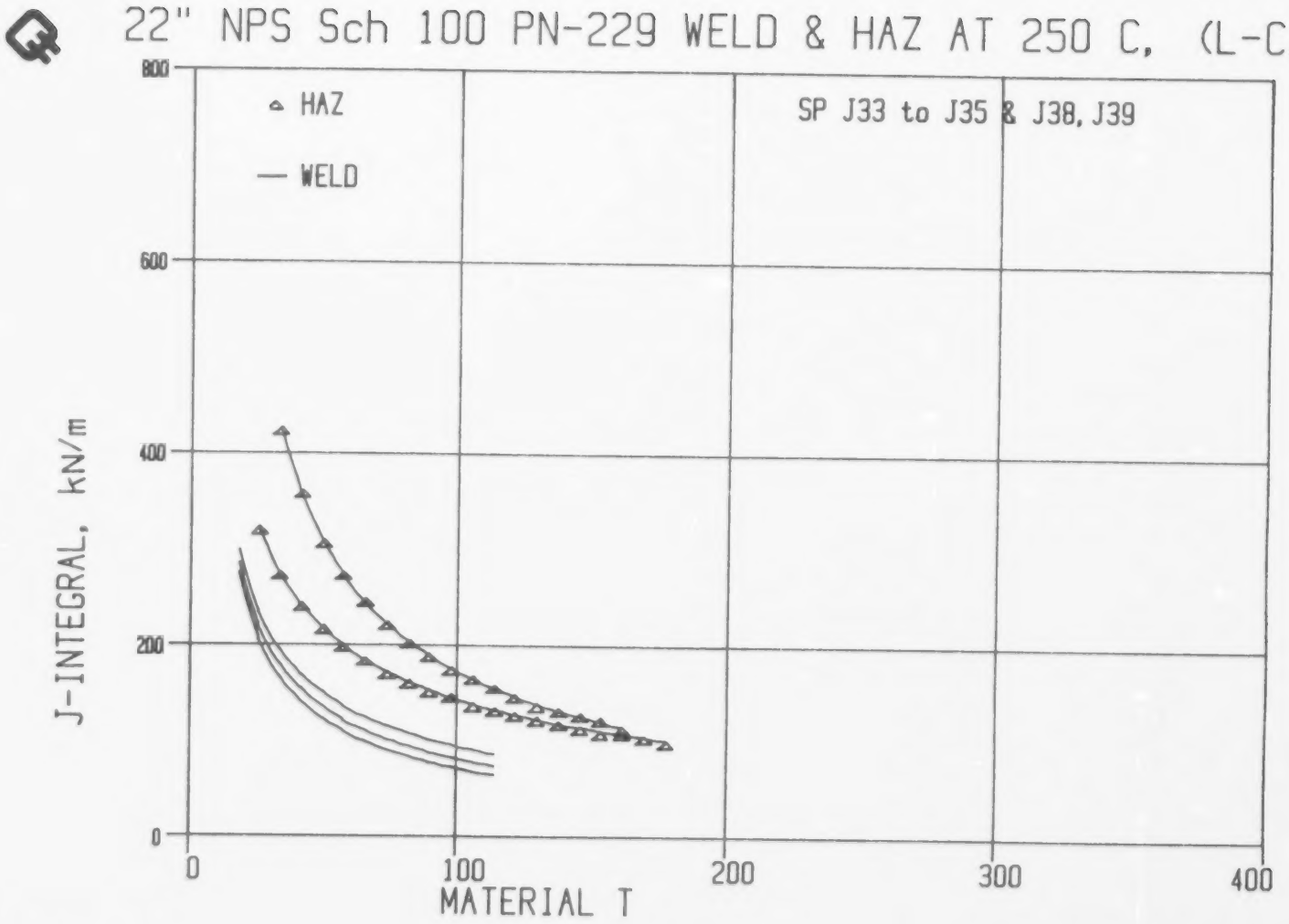

FIGURE 56

COMPARISON OF J-T CURVES FOR WELD AND HAZ

File JT 33-35
174320-RD

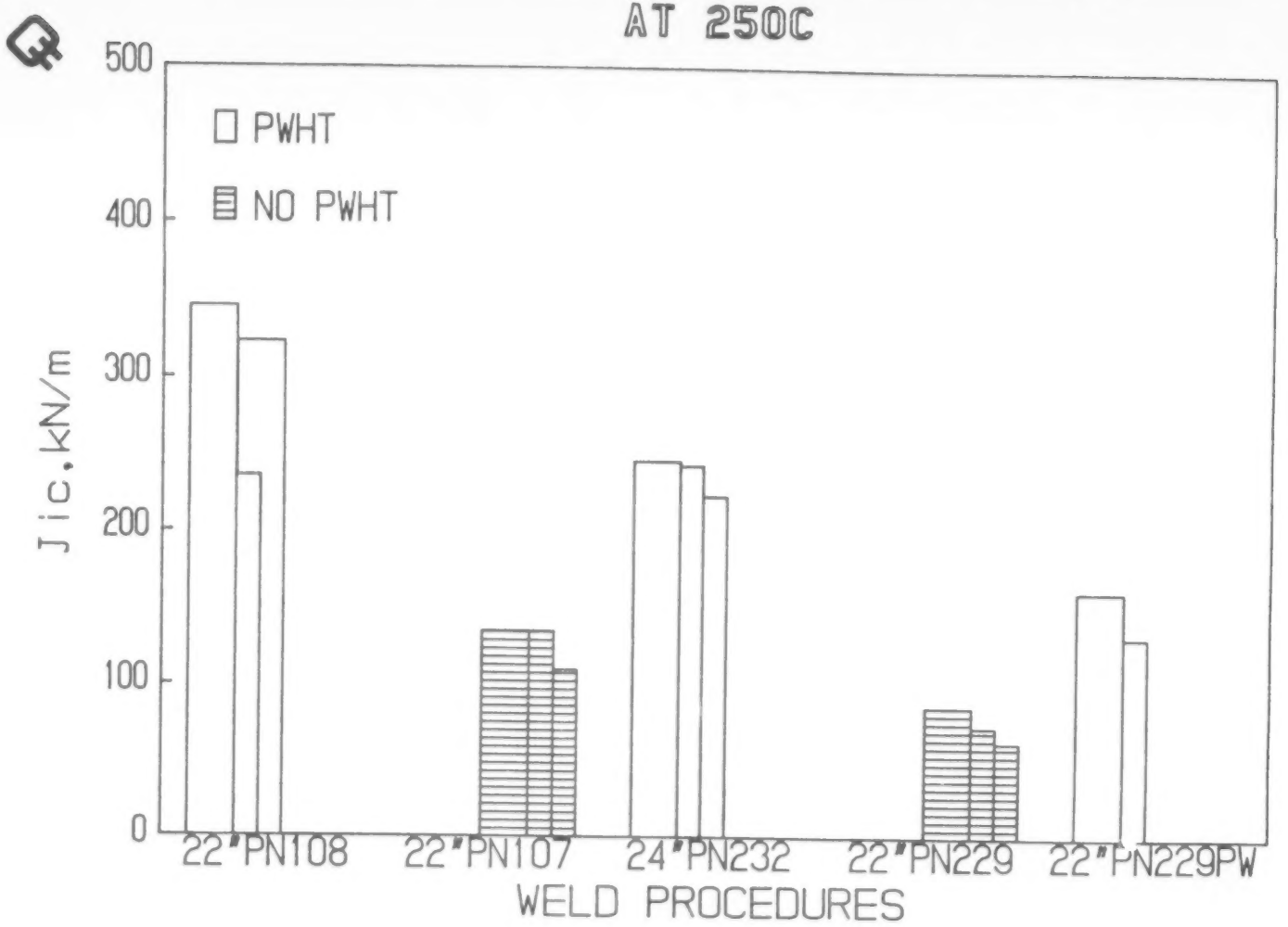

FIGURE 57

J_{IC} VALUES OF POST WELD HEAT TREATED VS NON HEAT TREATED WELDS

File JC PWHT
174305-RD

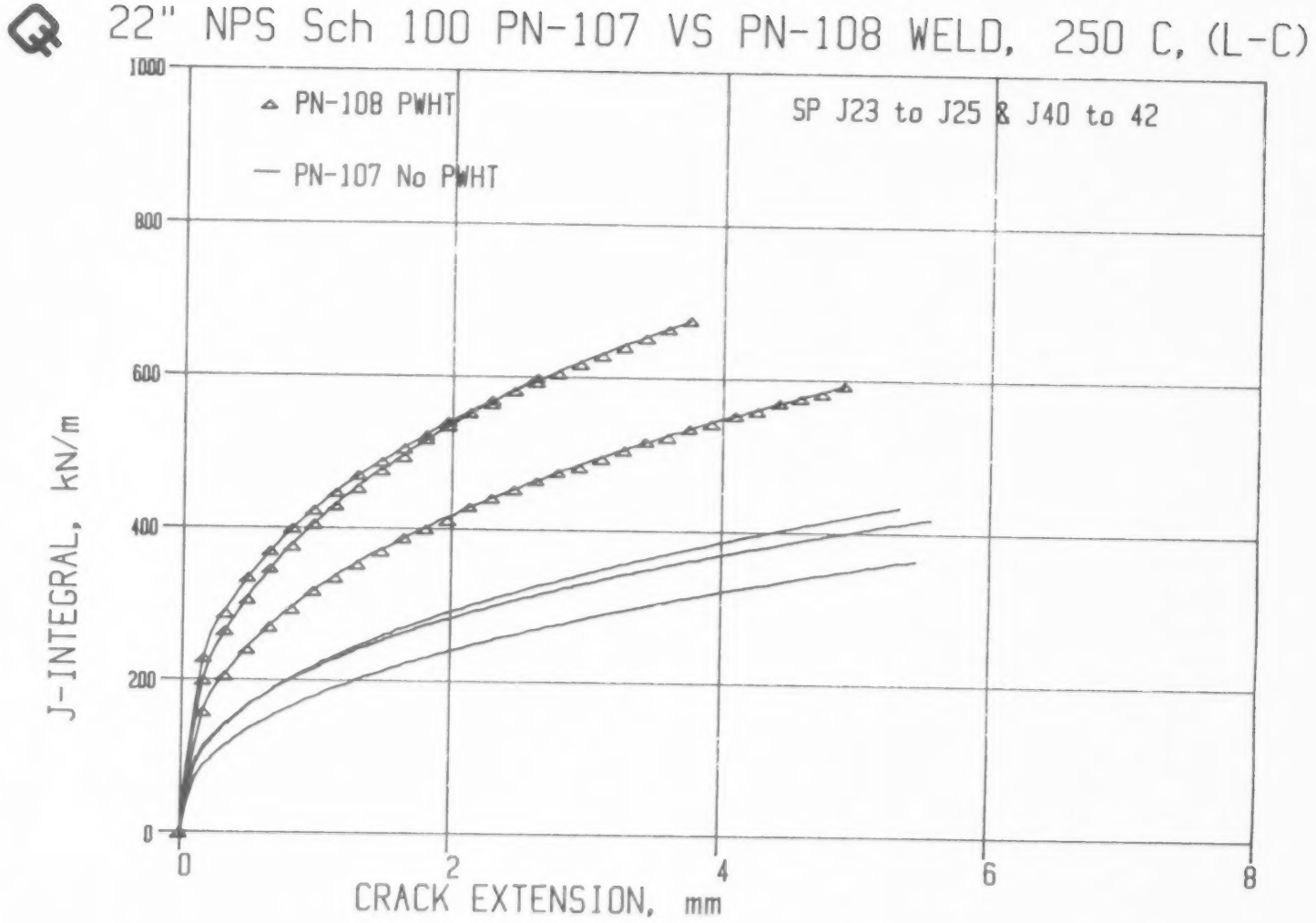

FIGURE 58
COMPARISON OF J-RESISTANCE CURVES FOR PWHT VS NON PWHT WELDS

File J 40-42
174319-RD

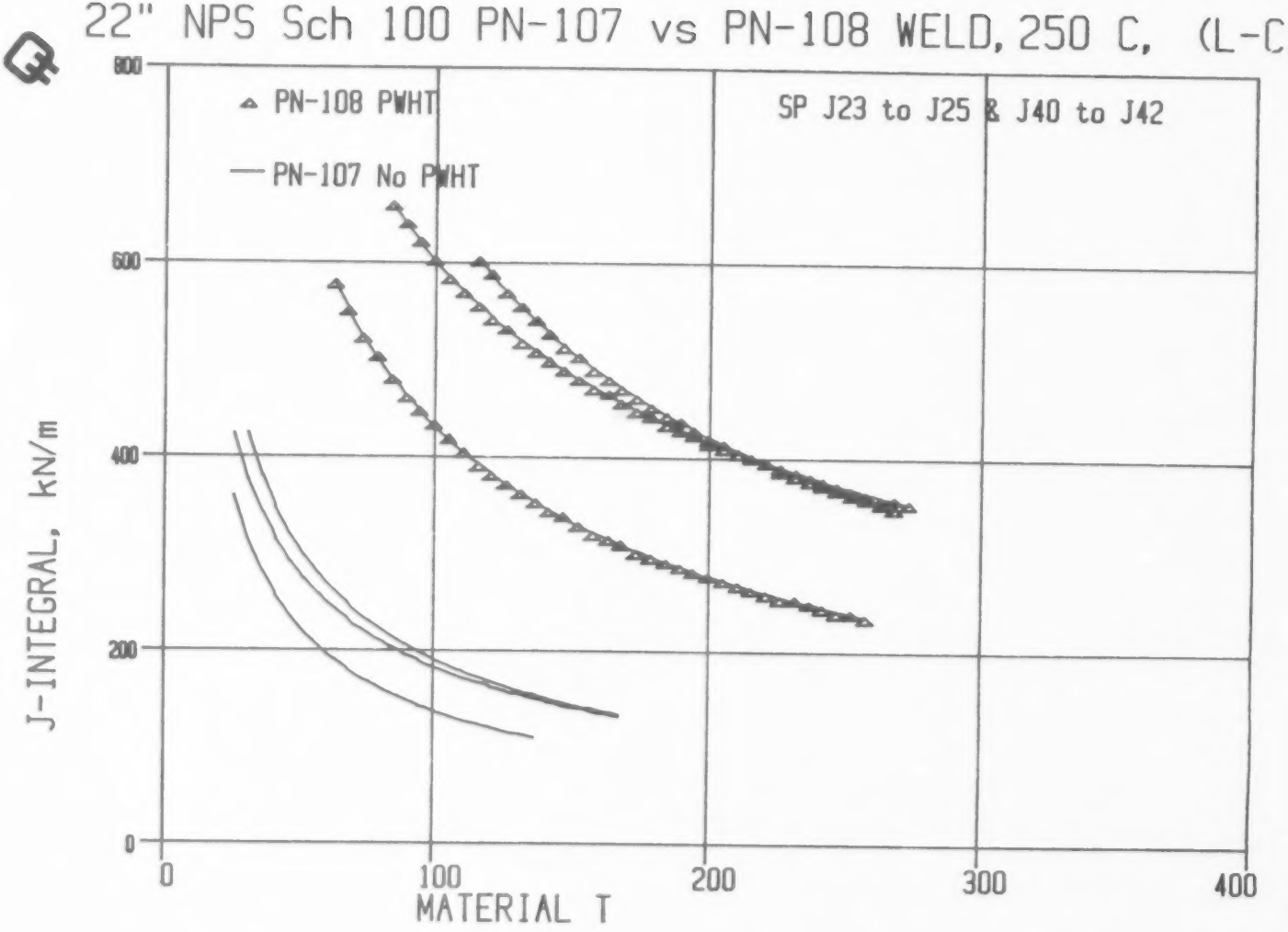

FIGURE 59

COMPARISON OF J-T CURVES FOR PWHT VS NON PWHT WELDS

File JT 40-42
174318-RD

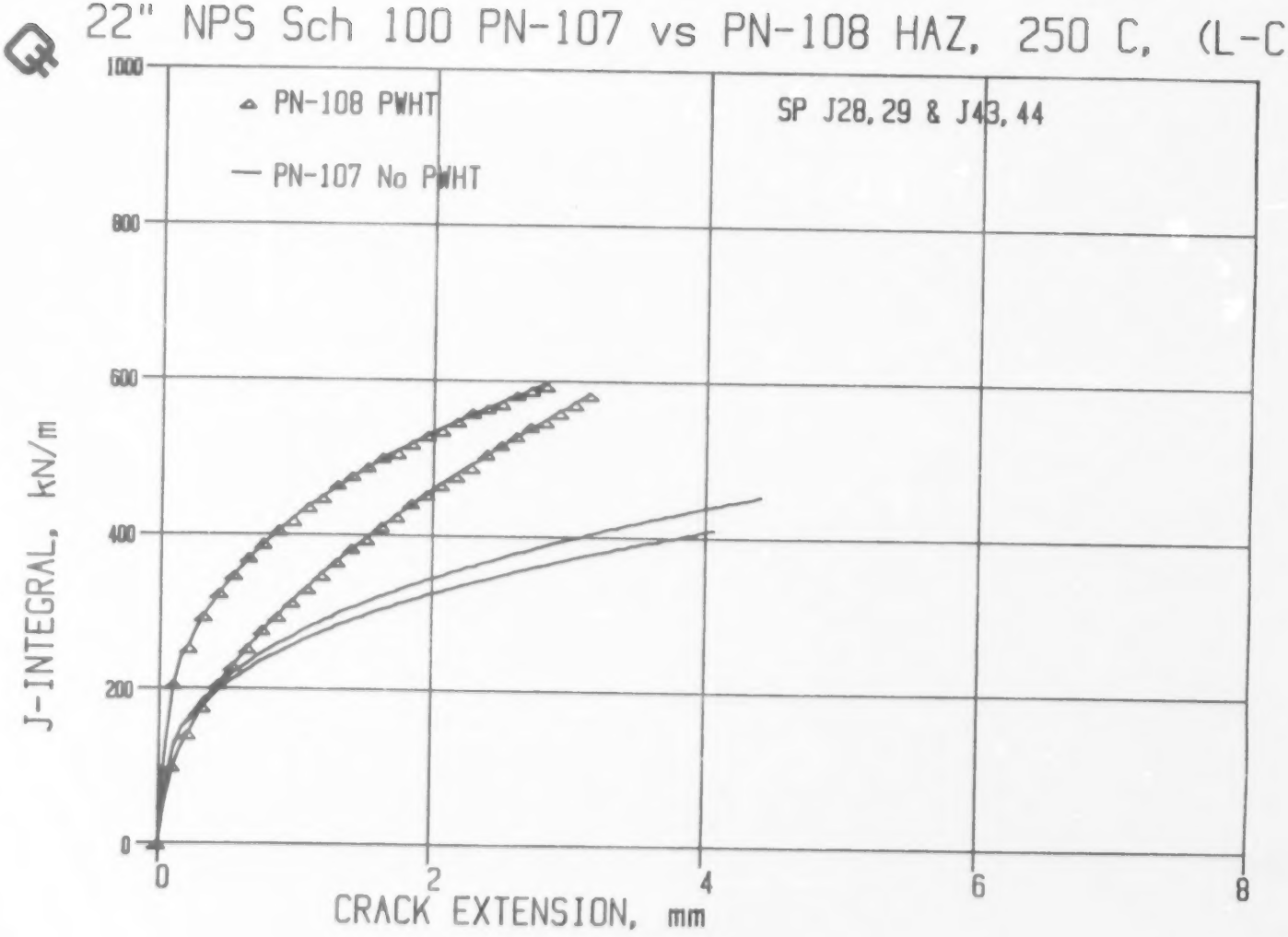

FIGURE 60

COMPARISON OF J-RESISTANCE CURVES FOR PWHT VS NON PWHT HAZ MATERIAL

File J 43-44
174317-RD

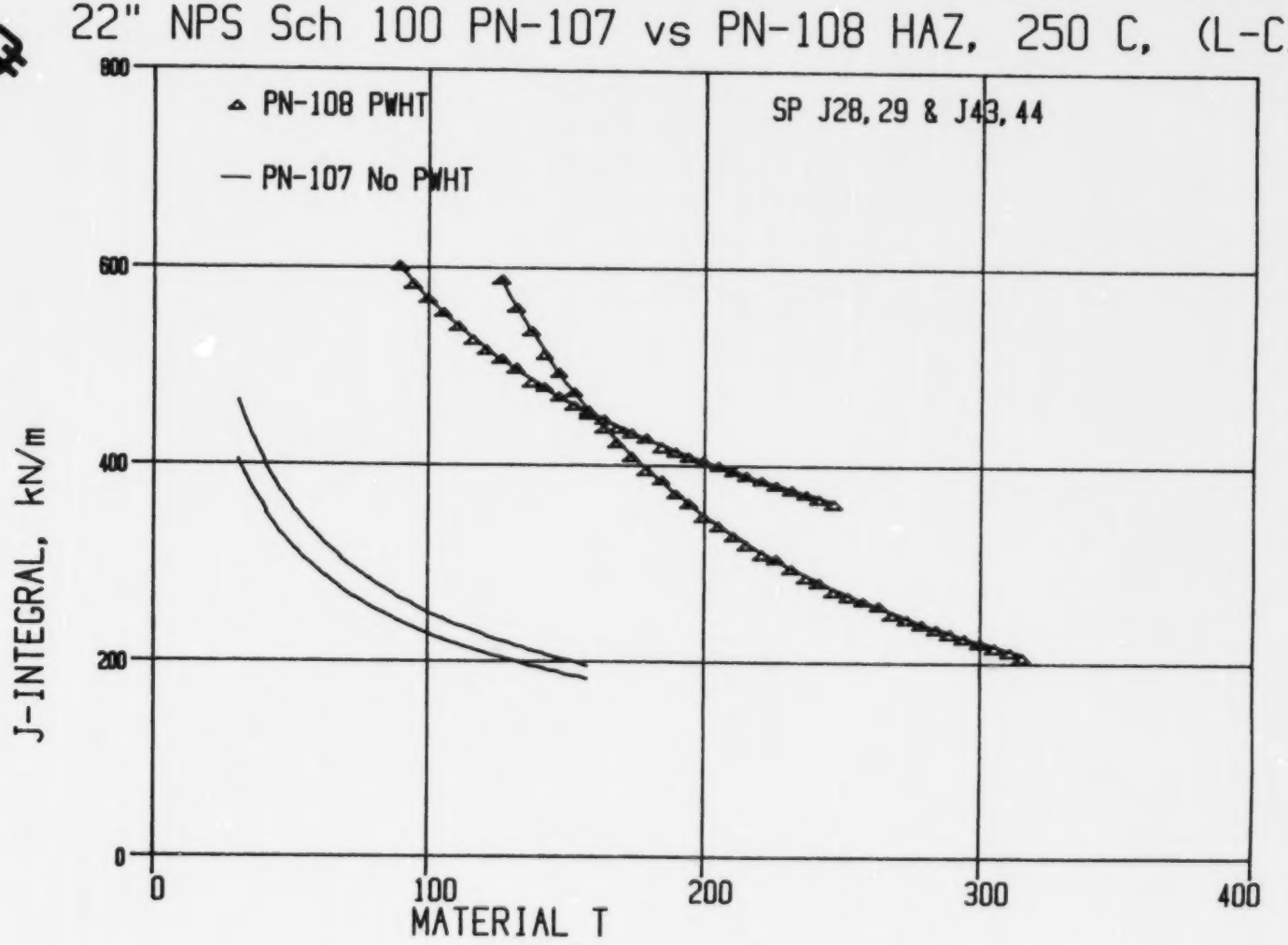

FIGURE 61

COMPARISON OF J-T CURVES FOR PWHT VS NON PWHT HAZ MATERIAL

File JT 43-44
174316-RD

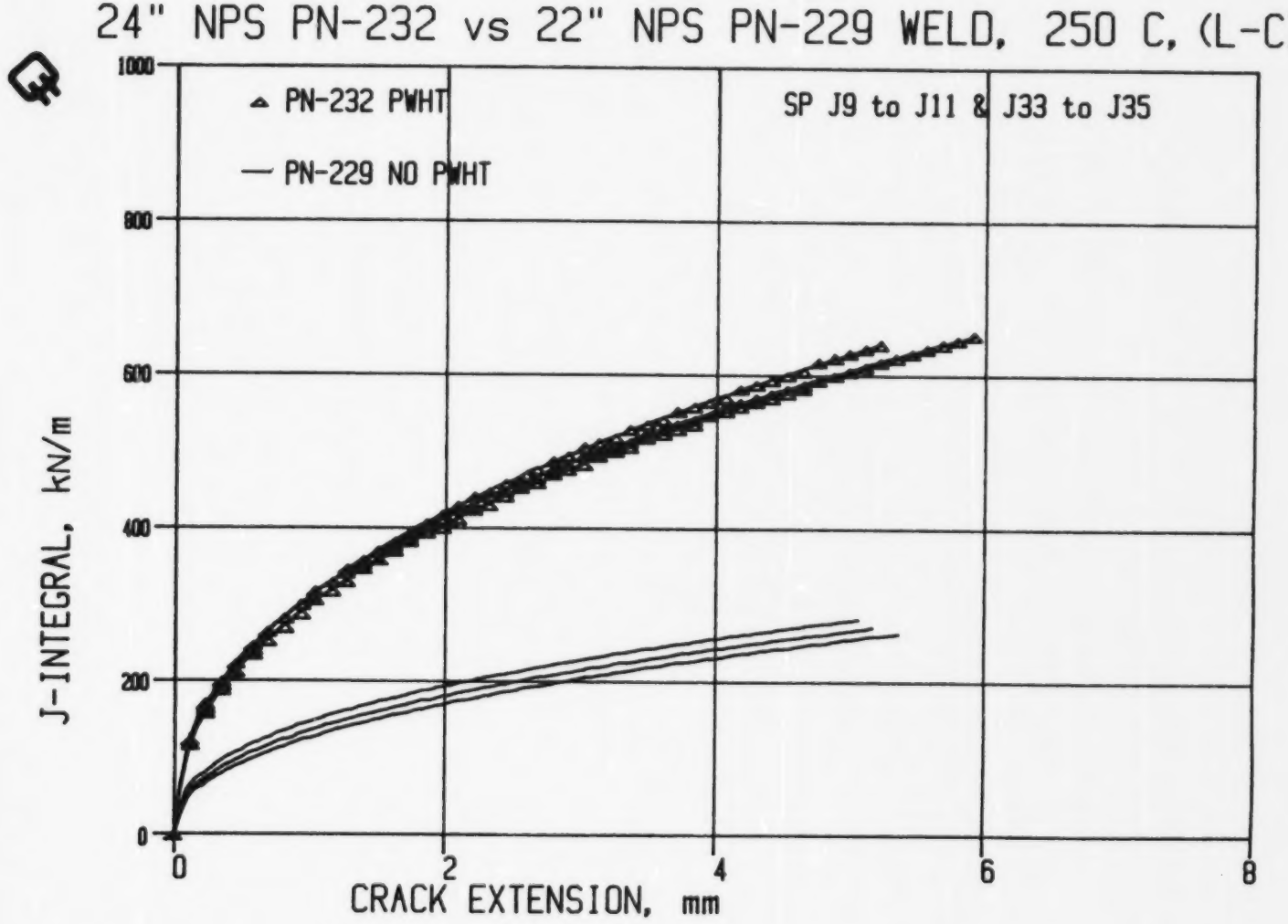

FIGURE 62

COMPARISON OF J-RESISTANCE CURVES FOR PWHT VS NON PWHT WELDS

File J-09-11
174315-RD

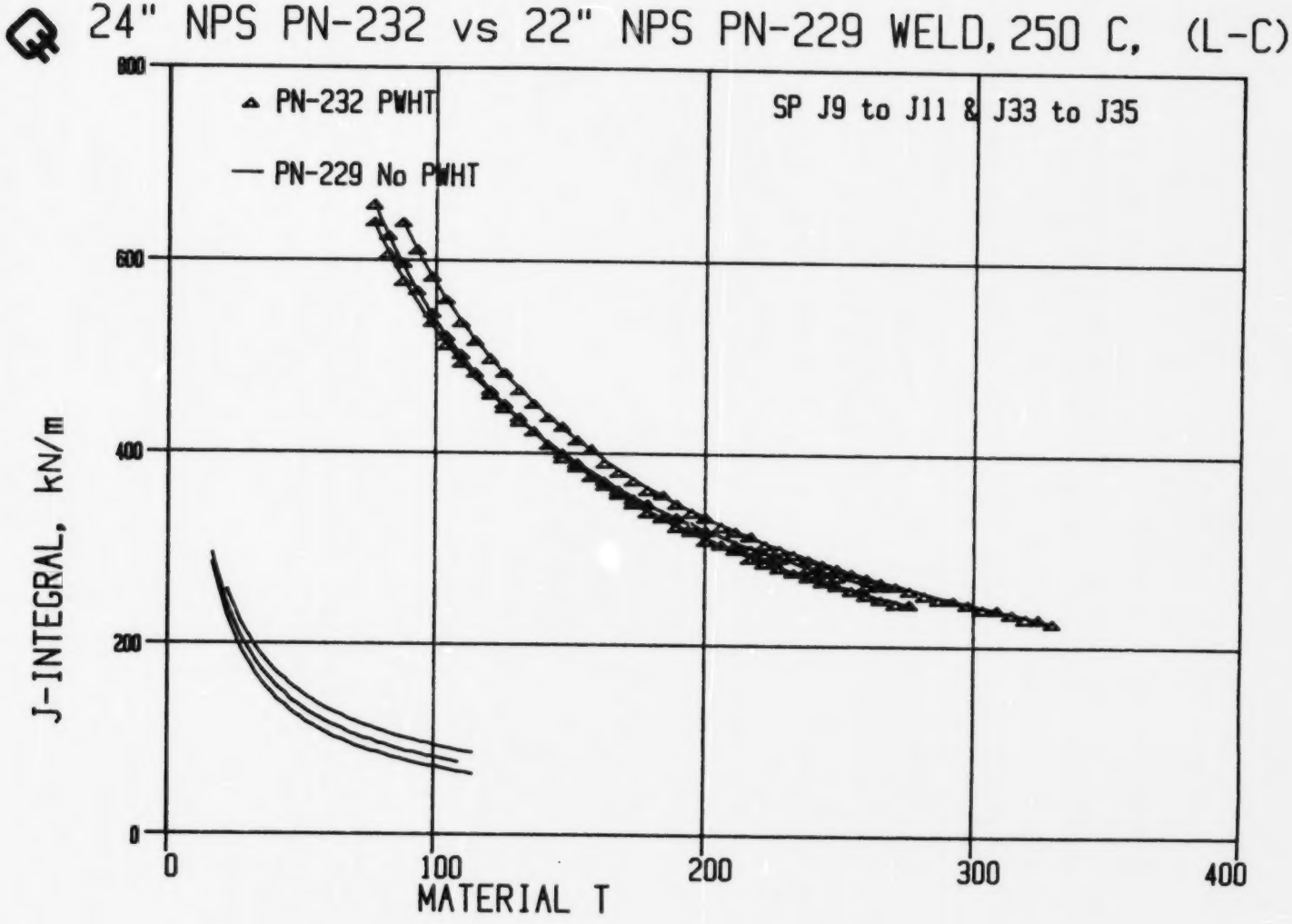

FIGURE 63

COMPARISON OF J-T CURVES FOR PWHT VS NON PWHT WELDS

File JT 09-11
174314-RD

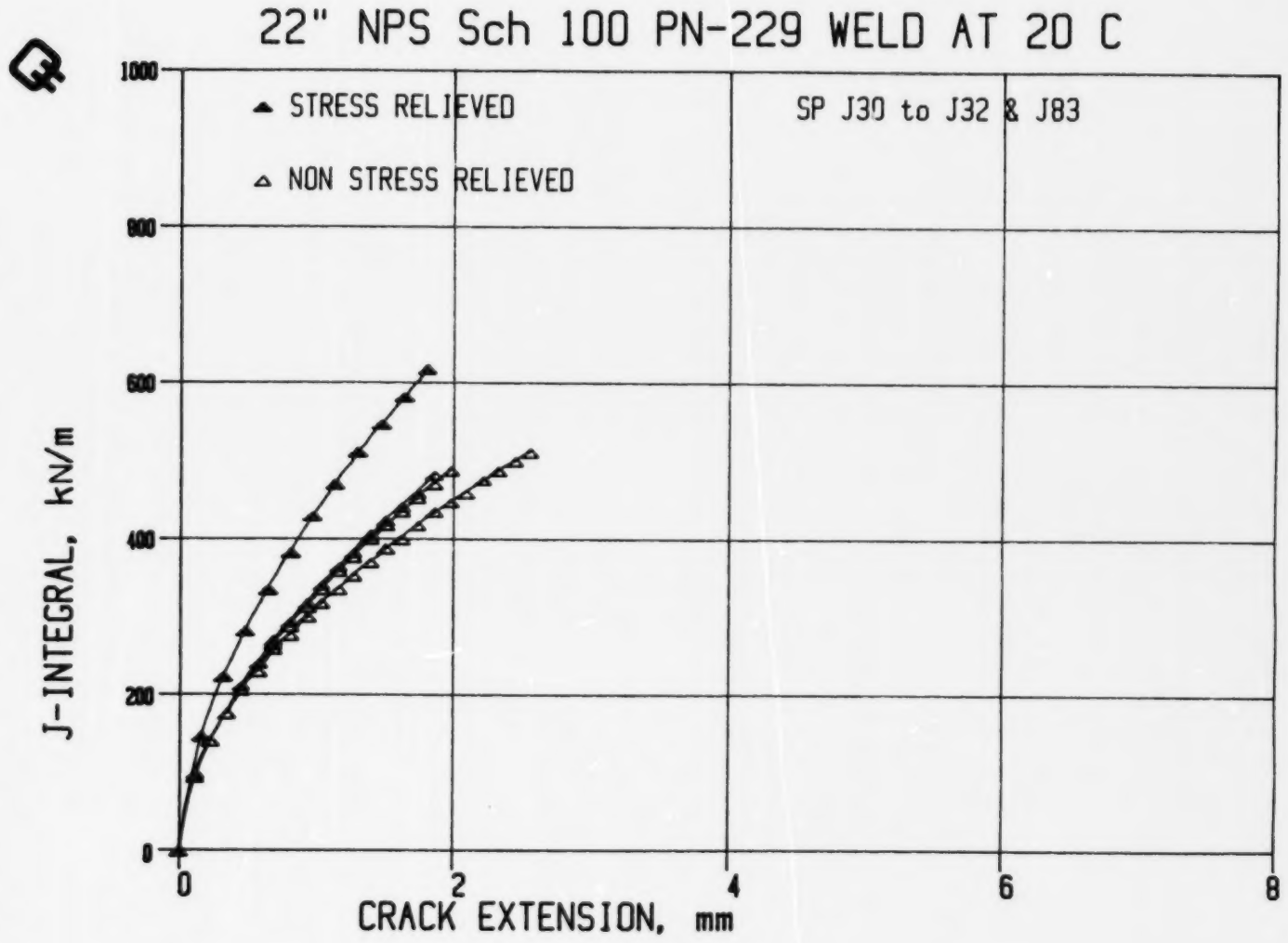

FIGURE 64

EFFECT OF STRESS RELIEVING ON J-RESISTANCE CURVES OF WELDS

File J 83-00
174313-RD

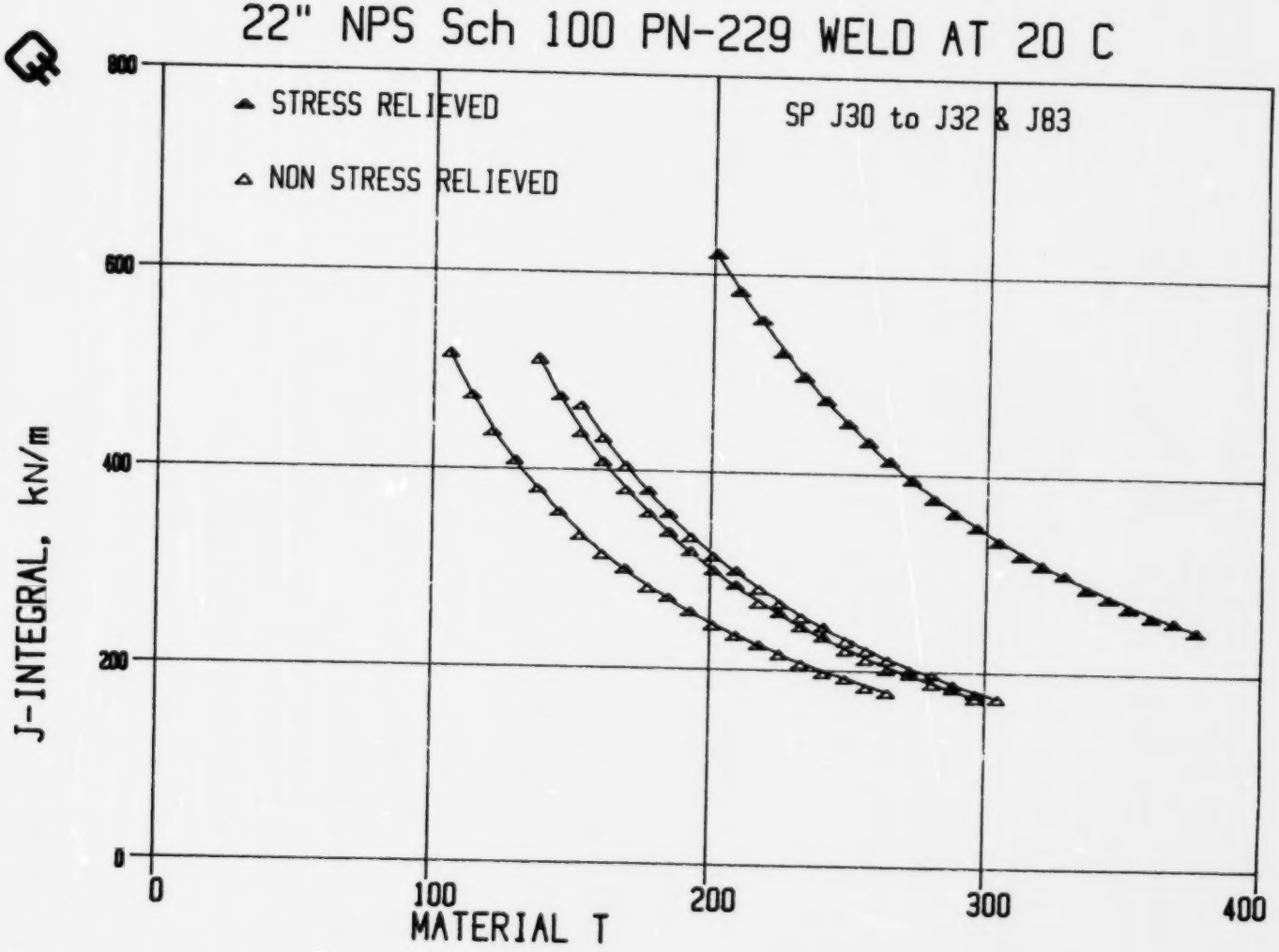

FIGURE 65
EFFECT OF STRESS RELIEVING ON J-T CURVES OF WELDS

File JT 83-00
174312-RD

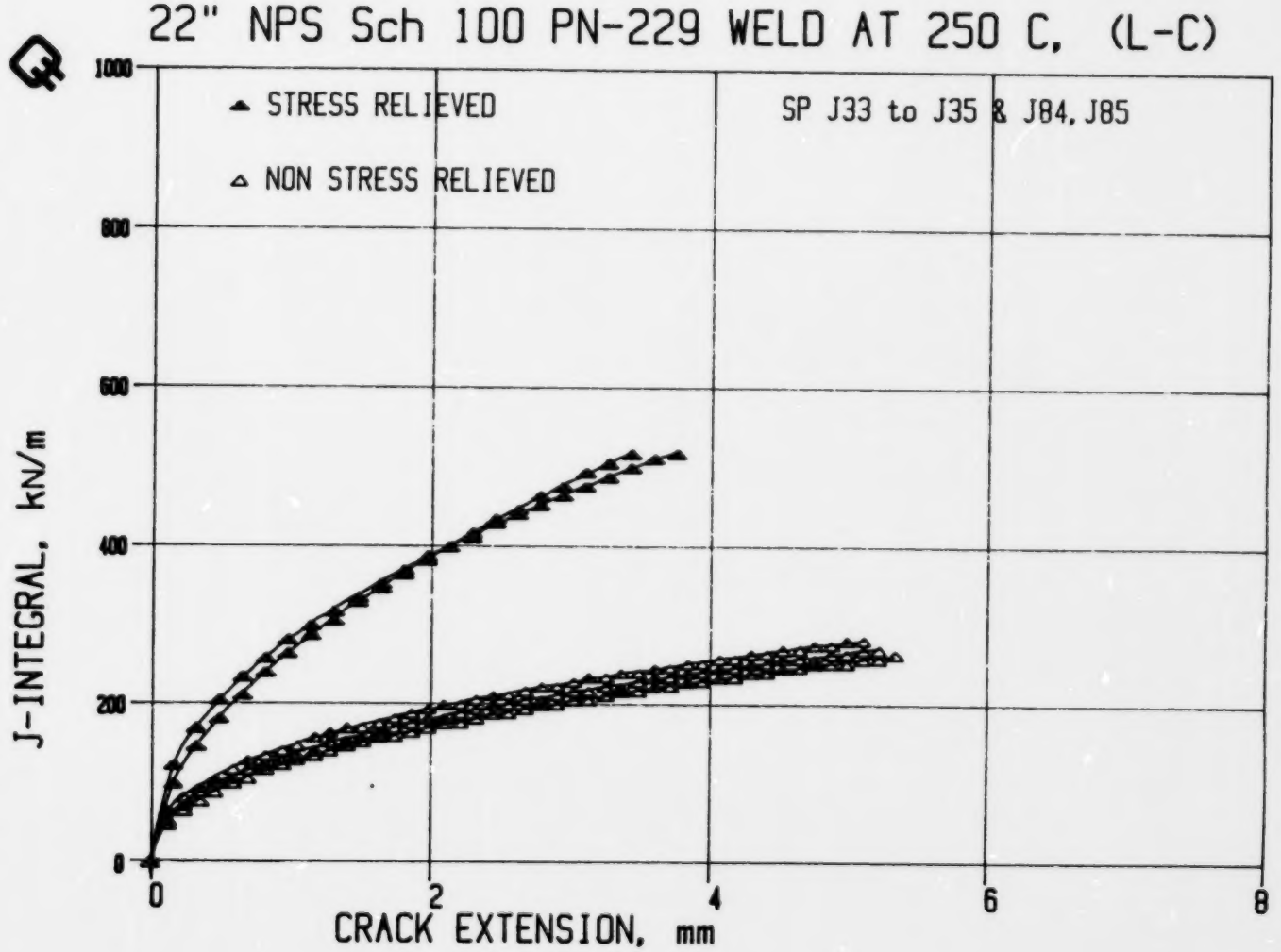

FIGURE 66

EFFECT OF STRESS RELIEVING ON J-RESISTANCE CURVES OF WELDS

File J 84-85
174303-RD

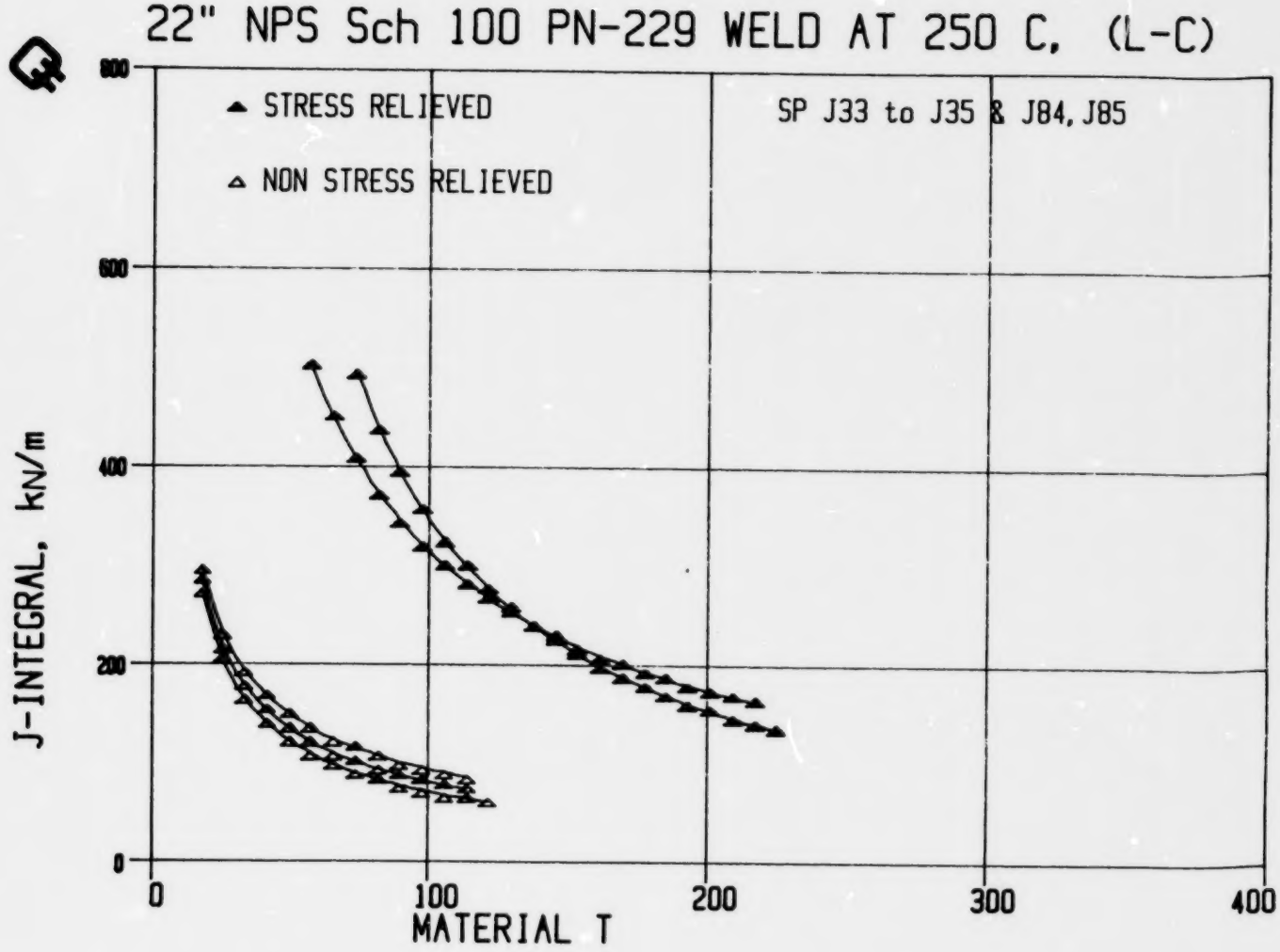

FIGURE 67

EFFECT OF STRESS RELIEVING ON J-T CURVES OF WELDS

File JT 84-85
174302-RD

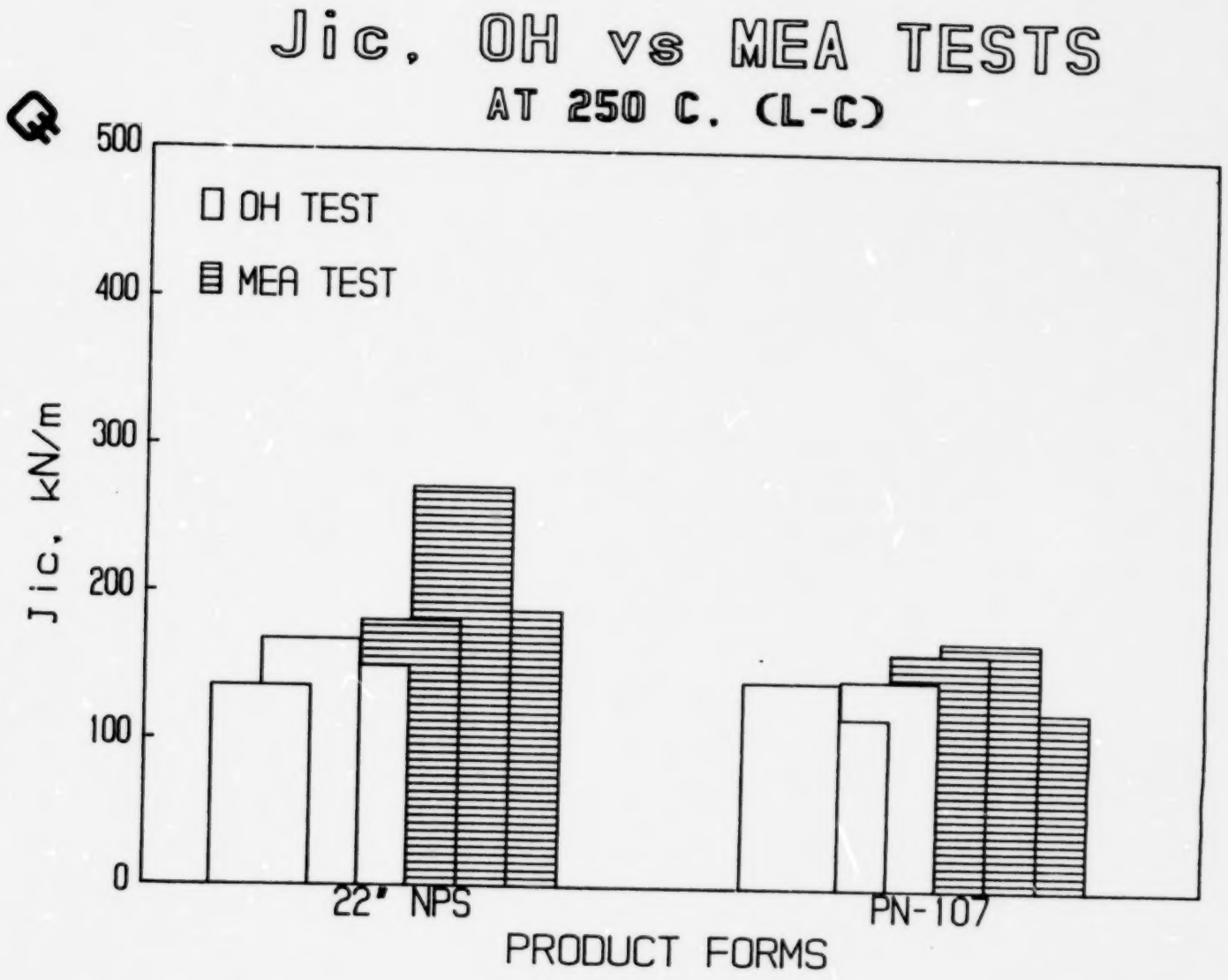

FIGURE 68

COMPARISON OF J_{IC} VALUES BETWEEN OH AND MEA TESTS

File JC MEA
174304-RD

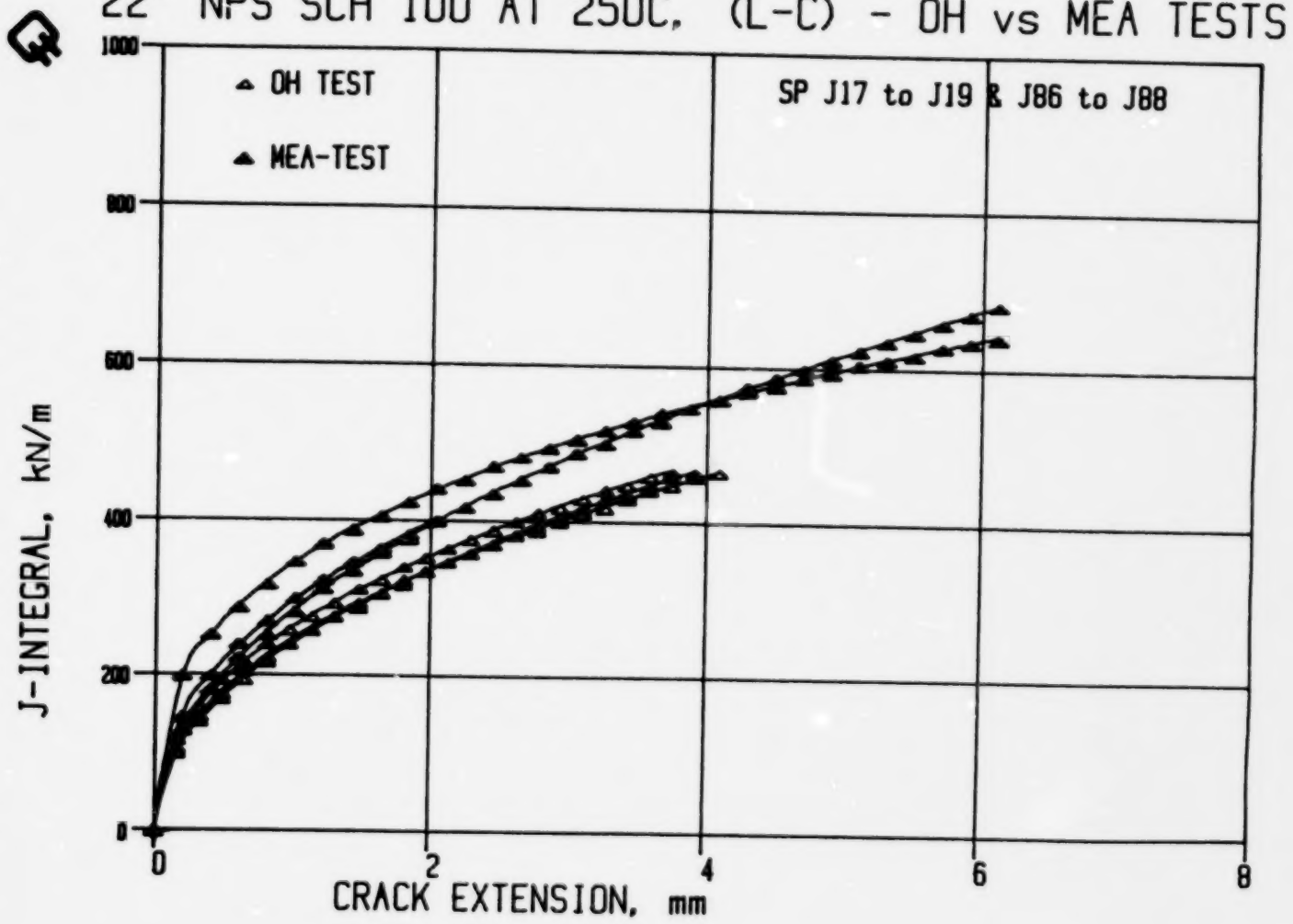

FIGURE 69

COMPARISON OF J-RESISTANCE CURVES BETWEEN OH AND MEA TESTS

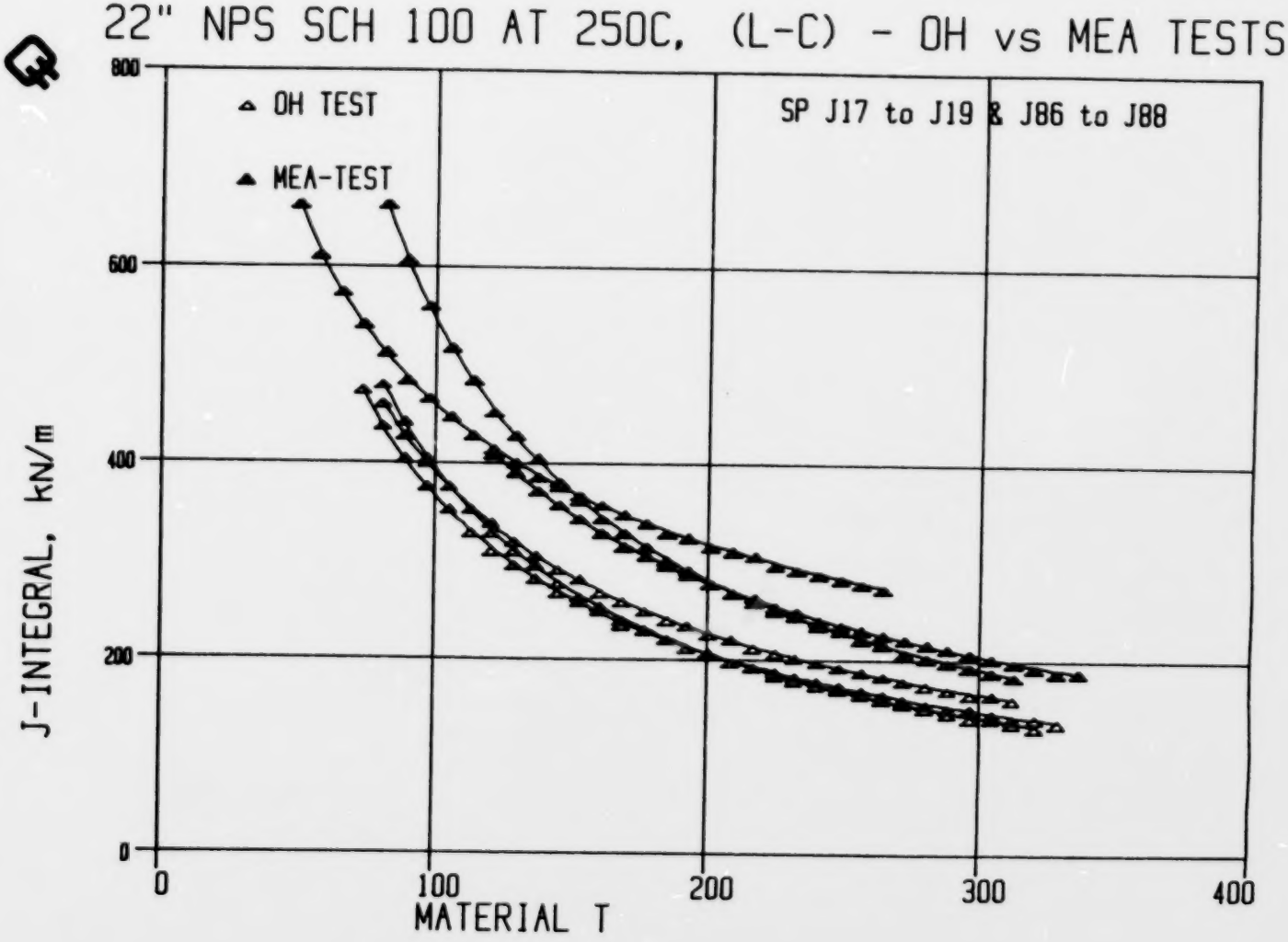

FIGURE 70

COMPARISON OF J-T CURVES BETWEEN OH AND MEA TESTS

File JT 86-88 M
174300-RD

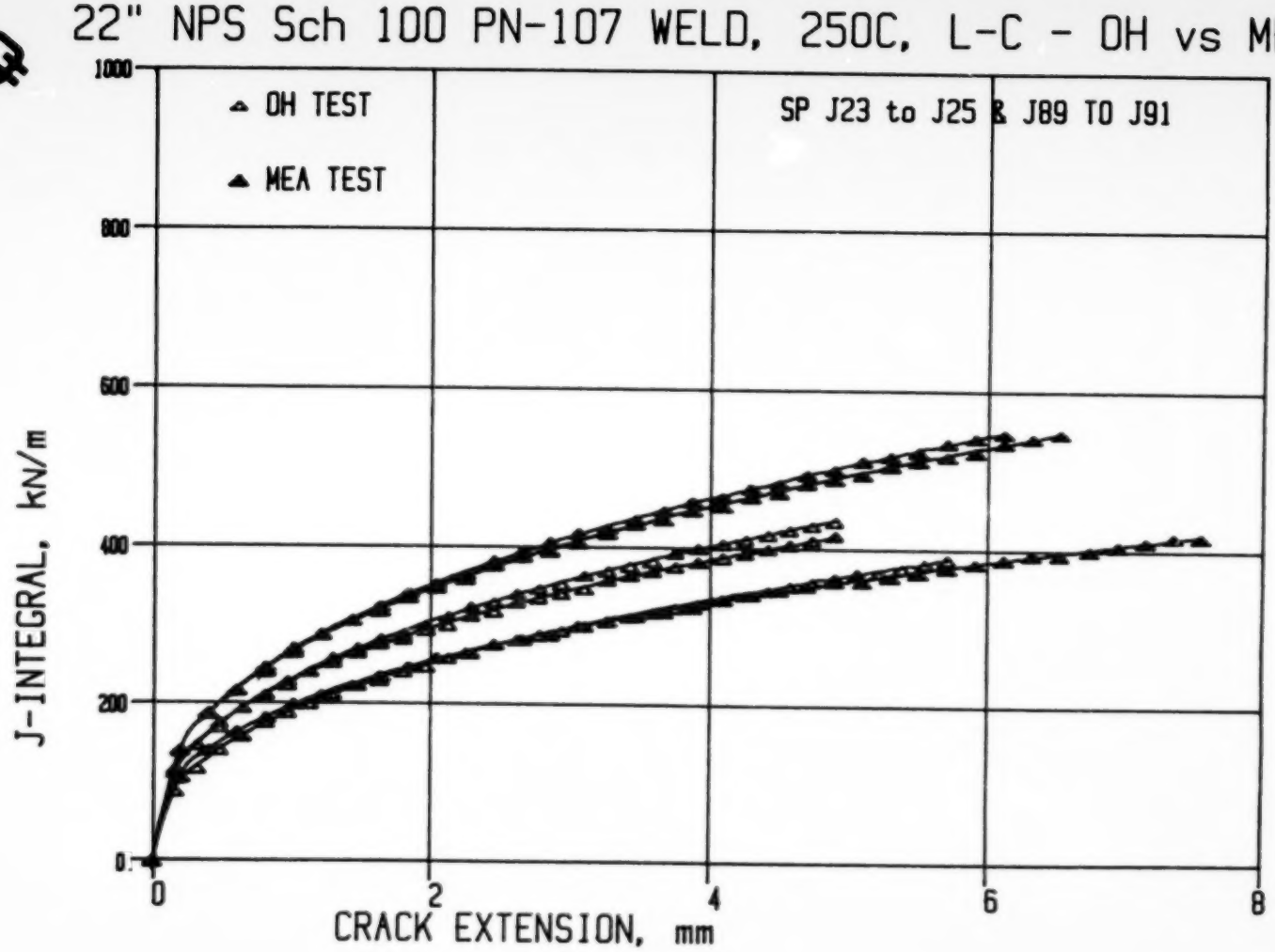

FIGURE 71

COMPARISON OF J-RESISTANCE CURVES BETWEEN OH AND MEA TESTS

File J 89-91 ME
174299-RD

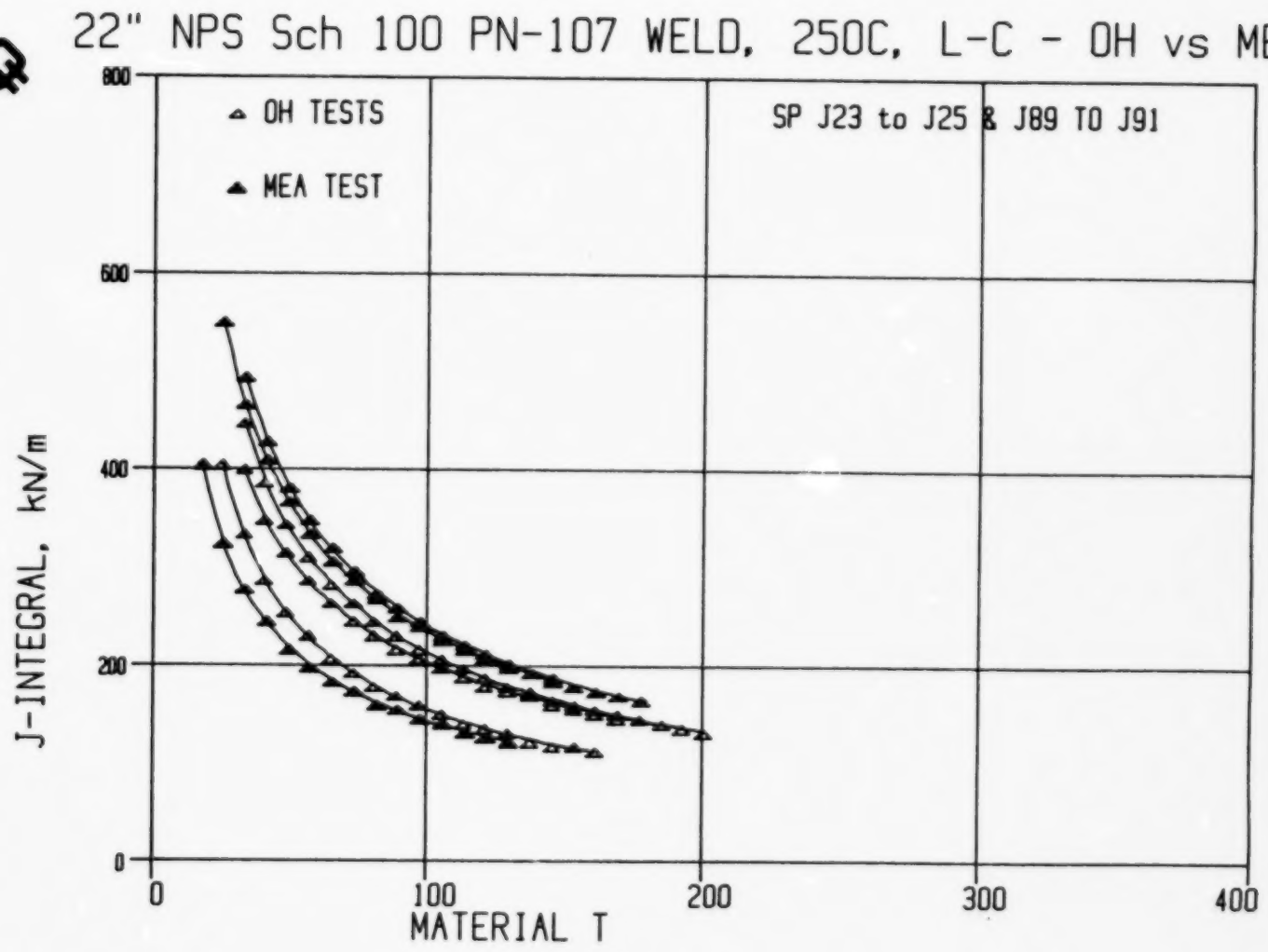

FIGURE 72

COMPARISON OF J-T CURVES BETWEEN OH AND MEA TESTS

File JT 89-91 M
174298-RD

DISTRIBUTION

Mr. M.A. Machacek
Dr. D. Mills
Mr. M.L. Lau
Miss B.L. Kee
—Dr. D.K. Vijay
Mr. M.L. Kozluk (10)
Mr. T.C. Lin
Mr. B.W. Manning
Mrs. N.D. Martin
Dr. J.S. Nathwani
Mr. M.L. Aggarwal
—Dr. G.J. Field
—Dr. D. Sidey
—Dr. M.W. Shanahan
Dr. J. Brown
Dr. J.A. Baron
—Dr. M.A. Clarke
—Dr. E.T.C. Ho
Mr. D.A. Scarth
Mr. M.L. Vanderglas
Mr. O.E. Lepik
—Dr. S. Lawson
—Dr. R. Fleck
—Dr. P. Lichtenberger
Mr. D.W. Carpenter
Dr. B. Mukherjee (10)

Public Reference Centre
Editorial Section (2)
Office Copies (2)
Extra Copies (3)

Design & Construction, H16G1
Director of Research
Design & Development, H14C22
Design & Development, H9C4
Design & Development, H14F22
Design & Development, H14E23
Design & Development, H14E23
Design & Development, H14E25
Design & Development, H14B21
Design & Development, H9D7
Design & Development, H14F24
Design & Development, H10A16
Technical & Training Services, A8H7
Technical & Training Services, A7H8
Metallurgical Research
Metallurgical Research
Metallurgical Research
Metallurgical Research
Metallurgical Research
Metallurgical Research
Metallurgical Research
Metallurgical Research
Metallurgical Research
Metallurgical Research
Metallurgical Research
Metallurgical Research
Metallurgical Research

—Executive Summaries only.